

**T.C.
REPUBLIC OF TURKEY
HACETTEPE UNIVERSITY
INSTITUTE OF HEALTH SCIENCES**

**MODULATION OF GLUCOCORTICOID INDUCED TUMOR
NECROSIS FACTOR RECEPTOR (GITR)-GITR LIGAND
(GITRL) INTERACTION IN BREAST CANCER CELLS UNDER
THE CONTROL OF ATAXIA TELANGIECTASIA MUTATED
(ATM) PROMOTER**

Bengisu ULUATA DAYANÇ

**Tumor Biology and Immunology Program
MASTER OF SCIENCE THESIS**

ANKARA

2017

**T.C.
REPUBLIC OF TURKEY
HACETTEPE UNIVERSITY
INSTITUTE OF HEALTH SCIENCES**

**MODULATION OF GLUCOCORTICOID INDUCED TUMOR
NECROSIS FACTOR RECEPTOR (GITR)-GITR LIGAND
(GITRL) INTERACTION IN BREAST CANCER CELLS UNDER
THE CONTROL OF ATAXIA TELANGIECTASIA MUTATED
(ATM) PROMOTER**

Bengisu ULUATA DAYANÇ

**Tumor Biology and Immunology Program
MASTER OF SCIENCE THESIS**

**ADVISOR OF THE THESIS
Assoc. Prof. Dr. Güneş ESENDAĞLI**

**ANKARA
2017**

APPROVAL PAGE

**MODULATION OF GLUCOCORTICOID INDUCED TUMOR
NECROSIS FACTOR RECEPTOR (GITR)-GITR LIGAND (GITRL)
INTERACTION IN BREAST CANCER CELLS UNDER THE CONTROL OF
ATAXIA TELANGIECTASIA MUTATED (ATM) PROMOTER**


Bengisu Uluata Dayanç

This study has been approved and accepted as a Master dissertation in the program of “Tumor Biology and Immunology” by the examining committee, whose members are listed below, on 21 July 2017.

Chairman of the Committee :	Prof. Dr. A.Lale Doğan Hacettepe University	
Advisor of the Dissertation :	Assoc. Prof. Dr. Güneş Esendağlı Hacettepe University	
Member :	Prof. Dr. Gökhan Özyiğit Hacettepe University	
Member :	Assist. Prof. Dr. Ekim Taşkiran Hacettepe University	
Member :	Assist. Prof. Dr. Serkan İsmail Göktuna İhsan Doğramacı Bilkent University	

This dissertation has been approved by the committee above in conformity to the regulations and by laws of Hacettepe University Graduate Programs.

14 Ağustos 2017


Prof. Dr. Diclehan Orhan
Institute Director

YAYIMLAMA VE FİKRİ MÜLKİYET HAKLARI BEYANI

Enstitü tarafından onaylanan lisansüstü tezimin/raporumun tamamını veya herhangi bir kısmını, basılı (kağıt) ve elektronik formatta arşivleme ve aşağıda verilen koşullarla kullanıma açma iznini Hacettepe Üniversitesine verdiğimi bildiririm. Bu izinle Üniversiteye verilen kullanım hakları dışındaki tüm fikri mülkiyet haklarım bende kalacak, tezimin tamamının ya da bir bölümünün gelecekteki çalışmalarda (makale, kitap, lisans ve patent vb.) kullanım hakları bana ait olacaktır.

Tezin kendi orijinal çalışmam olduğunu, başkalarının haklarını ihlal etmediğimi ve tezimin tek yetkili sahibi olduğumu beyan ve taahhüt ederim. Tezimde yer alan telif hakkı bulunan ve sahiplerinden yazılı izin alınarak kullanılması zorunlu metinlerin yazılı izin alınarak kullandığımı ve istenildiğinde suretlerini Üniversiteye teslim etmeyi taahhüt ederim.

- **Tezimin/Raporumun tamamı dünya çapında erişime açılabilir ve bir kısmı veya tamamının fotokopisi alınabilir.** (Bu seçenekle teziniz arama motorlarında indekslenebilecek, daha sonra tezinizin erişim statüsünün değiştirilmesini talep etmeniz ve kütüphane bu talebinizi yerine getirirse bile, teziniz arama motorlarının önbelleklerinde kalmaya devam edebilecektir).
- **Tezimin/Raporumun 21.07.2020 tarihine kadar erişime açılmasını ve fotokopi alınmasını (İç Kapak, Özet, İçindekiler ve Kaynakça hariç) istemiyorum.** (Bu sürenin sonunda uzatma için başvuruda bulunmadığım takdirde, tezimin/raporumun tamamı her yerden erişime açılabilir, kaynak gösterilmek şartıyla bir kısmı veya tamamının fotokopisi alınabilir).
- **Tezimin/Raporumun.....tarihine kadar erişime açılmasını istemiyorum ancak kaynak gösterilmek şartıyla bir kısmı veya tamamının fotokopisinin alınmasını onaylıyorum.**
- **Serbest Seçenek/Yazarın Seçimi**



16.08.2017

Bengisu ULUATA DAYANÇ

ETHICAL DECLARATION

In this thesis study, I declare that all the information and documents have been obtained in the base of the academic rules and all audio-visual and written information and results have been presented according to the rules of scientific ethics. I did not do any distortion in data set. In case of using other works, related studies have been fully cited in accordance with the scientific standards. I also declare that my thesis study is original except cited references. It was produced by myself in consultation with supervisor Associate Professor Güneş ESENDAĞLI and written according to the rules of thesis writing of Hacettepe University Institute of Health Sciences.



Bengisu ULUATA DAYANÇ



ACKNOWLEDGEMENTS

I would like to thank

My supervisor Assoc. Prof. Dr. Güneş Esendağlı first and foremost for taking a risk and accepting my project as a thesis study, for his unwavering support and patience as well as for showing me that good things will come with passion, patience and curiosity in science throughout my training,

To Prof. Dr. Dicle Güç, Prof. Dr. Lale Doğan, Dr. Hande Canpınar and Assistant Prof. Füsün Özmen for sharing their knowledge, wisdom and experiences with me all through my studies,

To Prof. Dr. Gökhan Özyiğit for his support in radiation treatment experiments,

To Prof. Dr. Metiner Tosun and Assoc. Prof. Dr. Yasemin Eraç for helping me when help is most needed, for sharing their much appreciated research resources and laboratories for the final stages of this project.

To Diğdem Yöyen Ermiş, for helping my experiments as if they were hers and enlightening my dark flow cytometry world,

To Elif Haznedaroğlu and Ece Tavukçuoğlu for reminding me to smile every morning in the laboratory despite everything that goes wrong,

To all of the Basic oncology team for their support and making me feel at home when we were working together,

I would like to dedicate this thesis study to my beloved family Emre Dayanç, Eser and Betül Uluata.

ABSTRACT

Uluata-Dayanç, B. Modulation of Glucocorticoid Induced Tumor Necrosis Factor Receptor (GITR)-GITR Ligand (GITRL) Interaction in Breast Cancer Cells Under the Control of Ataxia Telangiectasia Mutated (ATM) Promoter, Hacettepe University Institute of Health Sciences Tumor Biology and Immunology Program Master of Science Thesis, Ankara, 2017. Treatment response for basal-like breast cancers (BLBC) is limited and this aggressive breast cancer sub-type has poor prognosis and high mortality. Our first aim is to investigate ATM activity in BLBC cell lines with ionizing radiation. Our second aim is to study the viability of BLBC cells by the GITR-GITRL interaction while examining the expression levels of GITR and GITRL with radiation. ATM expression levels in basal-like (MDA-MB-231, HCC38, MDA-MB-468) and luminal (MCF-7, BT-474, SK-BR-3) breast cancer cell lines were analyzed with RT-PCR and found similar. Increase in ATM (S1981) phosphorylation in BLBC cells with ionizing radiation has been demonstrated with Western Blot experiments. HCC38 cells transfected with “pATM-GL3” Luciferase reporter plasmid showed high basal and post-radiation ATM activity. Although there is no difference in ATM mRNA levels, changes in protein levels has been observed, suggesting a post-transcriptional control mechanism. GITR and GITRL expressions in BLBC cells were investigated via RT-PCR and there was no change in expression levels with radiation. While MDA-MB-231 and MDA-MB-468 cell lines show high GITRL expression, HCC38 cell line was GITR positive, with both RT-PCR and flow cytometry. GITR⁺ HCC38 cells were incubated with recombinant GITRL protein at different serum concentrations (1% and 10%) and the change of cancer cells’ viability, proliferation and amount of metabolically active viable cells were investigated with DRAQ7 staining, CFSE assay and MTT assay, respectively. Even though GITR stimulation only has not changed viability and proliferation of HCC38 cells, both ionizing radiation and GITR stimulation had a cumulative effect on cell viability. When cell death was assayed with DRAQ7 staining, a decrease in viability of the cells was observed, which were simultaneously exposed to both 80 ng/ml rGITRL and 5 Gy ionizing radiation. As a result, this study demonstrated that cumulative effect of GITR stimulation and ionizing radiation may affect the viability of breast cancer cells.

Key Words: Basal-like breast cancer, Ataxia Telangiectasia Mutated, GITRL, ionizing radiation

ÖZET

Uluata-Dayanç, B. Meme Kanseri Hücrelerinde Glukokortikoid ile İndüklenen Tümör Nekroz Faktör Reseptör (GITR)- GITR Ligand (GITRL) Etkileşiminin Ataksi-Telenjektazi Mutasyona Uğramış (ATM) Geni Promotor Kontrolü Altında Değerlendirilmesi, Hacettepe Üniversitesi Sağlık Bilimleri Enstitüsü Tümör Biyolojisi ve İmmünolojisi Programı Yüksek Lisans Tezi, Ankara, 2017.

Bazal-benzeri meme kanseri (BBMK) için tedaviye cevap sınırlıdır ve bu agresif meme kanseri türü kötü prognoz ve yüksek mortalite gösterir. İlk amacımız BBMK hücre hatlarında iyonize edici radyasyonun ATM aktivitesine etkisinin incelenmesidir. İkinci amacımız radyasyon ile GITR ve GITRL ifadelerini incelerken, BBMK hücrelerinde GITR-GITRL etkileşimine bağlı canlılığın çalışılmasıdır. Bazal-benzeri (MDA-MB-231, HCC38, MDA-MB-468) ve luminal (MCF-7, BT-474, SK-BR-3) meme kanseri hücre hatlarındaki ATM ifadeleri RT-PCR aracılı incelenmiş ve benzer bulunmuştur. ATM (S1981) fosforilasyonunun BBMK hücrelerinde radyasyon sonucu artışı Western Blot deneyleri aracılı gösterilmiştir. “pATM-GL3” Lusiferaz raporlayıcı plazmidi ile transfekte edilen HCC38 hücreleri bazal seviyede ve radyasyon sonrası yüksek ATM aktivitesi göstermiştir. ATM mRNA düzeylerinde fark olmamasına rağmen protein düzeylerinde farklar gözlemlenmesi post-transkripsiyonel bir kontrol mekanizması olabileceğini önermektedir. BBMK hücrelerinde GITR ve GITRL ifadeleri RT-PCR aracılı incelenmiştir ve radyasyon ile değişmedikleri bulunmuştur. MDA-MB-231 ve MDA-MB-468 hücre hatları yüksek GITRL ifadesi gösterirken, HCC38 hücre hattı RT-PCR ve akım sitometrisi ile GITR pozitif olarak belirlenmiştir. GITR⁺ HCC38 hücreleri rekombinant GITRL proteini ile farklı serum konsantrasyonlarında (1% ve 10%) inkübe edilmiştir ve kanser hücrelerinin canlılığı, proliferasyonları ve metabolik olarak aktif canlı hücreler, sırasıyla DRAQ7 boyaması, CFSE ve MTT testleri aracılı incelenmiştir. Tek başına GITR uyarımı HCC38 hücrelerinin canlılık ve proliferasyonlarını etkilemezken, iyonlaştırıcı radyasyon ve GITR uyarımının hücre canlılığında kümülatif etkisi vardır. DRAQ7 boyaması ile hücre ölümü test edildiğinde, 80 ng/ml rGITRL ve 5 Gy iyonlaştırıcı radyasyona eş zamanlı maruz kalan hücrelerin canlılığında azalma olduğu gözlemlendi. Sonuç olarak, bu çalışma GITR uyarımı ve iyonlaştırıcı radyasyonun kümülatif etkisinin meme kanseri hücrelerinin canlılığını etkileyebileceğini göstermiştir.

Anahtar kelimeler: Bazal benzeri meme kanseri, Ataksi-Telenjektazi Mutasyona Uğramış Geni, GITRL, iyonlaştırıcı radyasyon

CONTENTS

APPROVAL PAGE	iii
YAYIMLAMA VE FİKRİ MÜLKİYET HAKLARI BEYANI	iv
ETHICAL DECLARATION	v
ACKNOWLEDGEMENTS	vi
ABSTRACT	vii
ÖZET	viii
CONTENTS	ix
ABBREVIATIONS LIST	xii
FIGURES	xv
TABLES	xvii
1. INTRODUCTION	1
2. LITERATURE OVERVIEW	3
2.1. Breast cancer	3
2.1.1. Molecular subtypes of breast cancer	4
2.2. Breast Cancer Stem cells	7
2.2.1. CD44 ^{high} /CD24 ^{low/neg} breast cancer stem cells	8
2.3. Radiation therapy in cancer	9
2.3.1. Effect of radiation on breast cancer cells	12
2.3.2. The role of ATM in radiosensitivity	13
2.4. Glucocorticoid-induced tumor necrosis factor receptor (GITR) and its ligand (GITRL)	15
2.4.1. Distribution of GITR and GITRL expression	20
2.4.2. Immunological aspects of GITR-GITRL interaction	21
3. MATERIALS AND METHODS	24
3.1. Materials	24
3.2. Buffers and Solutions	25
3.3. Cell culture	28
3.3.1. Cell counting	29
3.4. Treatment with ionizing radiation	29
3.5. Determination of the amount of viable cells by MTT assay	30
3.6. Western Blot analysis	31

3.6.1. Lysate preparation and protein quantification	31
3.6.2. SDS-PAGE and membrane blotting	32
3.6.3. Antibody incubations and chemiluminescence imaging	34
3.7. Flow cytometry	34
3.7.1. Flow cytometric cell proliferation analysis	35
3.7.2. Analysis of cell viability by flow cytometry	35
3.8. Molecular techniques	36
3.8.1. RNA isolation	36
3.8.2. Removal of DNA from RNA samples	37
3.8.3. Quantitation of RNA	38
3.8.4. Reverse transcription	38
3.8.5. Polymerase chain reaction (PCR)	39
3.8.6. Semi-quantitative real-time PCR	40
3.8.7. Agarose gel electrophoresis	40
3.9. Molecular cloning	41
3.9.1. Cloning of human ATM gene promoter into pGL3-Basic vector	41
3.9.2 MiniPrep Plasmid Isolation	46
3.9.3 Electroporation	47
3.9.4. Luciferase reporter assay	48
3.10. Statistical Analysis	50
4. RESULTS	51
4.1. Analysis of ATM activity in basal-like breast cancer cell lines	51
4.1.1 ATM expression and phosphorylation in basal-like breast cancer cells	51
4.1.2 The change in ATM protein expression in response to X-radiation	52
4.1.3 Cloning of ATM promoter into pGL3-Basic vector	54
4.1.4. Optimization of electroporation for basal-like breast cancer cells	57
4.1.5. Regulation of the ATM promoter activity in response to X-radiation	58
4.2. GITR and GITRL expression in basal-like breast cancer cell lines and the effect of X-radiation	61
4.2.1 GITR and GITRL mRNA levels in basal-like breast cancer cells in response to X-radiation	61

4.2.2. Determination of GITR and GITRL surface protein expression in X-irradiated HCC38 cell line	62
4.2.3 The effect of GITR stimulation and ionizing radiation on HCC38 cells' viability and proliferation	63
5. DISCUSSION	67
6. RESULTS & RECOMMENDATIONS	74
7. REFERENCES	76
8. APPENDICES	
APPENDIX 1: Ethics Committee Approval	
9. CURRICULUM VITAE	



ABBREVIATIONS LIST

ABC	ATP-binding cassette
ABCG2	ATP-binding cassette sub-family G member 2
ATM	Ataxia telangiectasia mutated
ATR	Ataxia telangiectasia and Rad3-related protein
BCA	Bicinchoninic acid
BRCA1	Breast cancer-1
BRCA2	Breast cancer 2
BSA	Bovine serum albumin
cDNA	Complementary DNA
CK	Cytokeratin
CSCs	Cancer stem cells
Ctrl	Control group
DCIS	Ductal carcinoma in situ
DD	Death domain
DDHR	DD homology region
DEPC	Diethyl pyrocarbonate
DMEM	Dulbecco's Modified Eagle's medium
DMF	Dimethylformamide
DR	Decoy receptors
DSB	Double-strand breaks
EBR	External beam radiation
EMT	Epithelial-mesenchymal transition
ER	Estrogen receptor
Erk	Extracellular signal–regulated kinases
ESR1	Estrogen receptor 1
FBS	Fetal bovine serum
GATA3	GATA binding protein 3
HER2/neu	Human epidermal growth factor receptor 2
HR	Homologous recombination
HRM	High resolution melting
ICAM-I	Intracellular adhesion molecule

JNK	Jun N-terminal kinases
LARII	Luciferase Assay Reagent II
LB	Luria-Bertani
LCIS	Lobular carcinoma in situ
Linac	Linear accelerator
MAPK	Mitogen-activated protein kinase
MMP-9	Matrix metalloproteinase-9
MRN	Mre11-Rad50-Nbs1
NFAT	Nuclear factor of activated T cells
NFκB	Nuclear Factor kappa B
NHEJ	Non-homologous end joining
OD	Optical density
PBS	Phosphate-buffered saline
PBS-T	PBS-Tween
pDC	Plasmacytoid dendritic cells
PIC	Protease inhibitor cocktail
PR	Progesterone receptor
PTEN	Phosphatase and tensin homolog
PVDF	Polyvinylidene difluoride
RLU	Relative light unit
RPMI	Roswell Park Memorial Institute
SDS	Sodium dodecyl sulfate
tATM	Total ATM
TBE	Tris-Borate-EDTA
TCR	T cell receptor
TN	Triple-negative
TNFR	Tumor Necrosis factor receptor
TNFRSF18	Tumor Necrosis Factor Receptor Superfamily Member 18
TNFSF18	Tumor Necrosis Factor Superfamily Member 18
TP53	Tumor protein p53
TRAF	TNF receptor-associated factor
TWIST2	Twist family bHLH transcription factor 2

VCAM-I Vascular cell adhesion molecule
ZEB2 Zinc finger E-box-binding homeobox 2



FIGURES

Figure	Page
2.1. Breast anatomical structure and morphological histology depicting luminal or myoepithelial cells which most breast cancer arises from.	3
2.2. Possible outcomes for traditional or CSC targeted cancer therapies.	7
2.3. DNA repair mechanisms in response to radiation. A) Non homologous end-joining NHEJ, B) Homologous Recombination.	11
2.4. ATM-Chk2-Cdc25A DNA damage response pathway.	13
2.5. TNFR ligand family structure.	17
2.6. GITR signaling through SIVA and NF- κ B.	19
2.7. GITRL RNA expression in A) Cancer cell lines, B) Normal human tissues	20
2.8. GITR expression in A) Normal human tissues, B) Cancer cell lines	21
2.9. Outcomes of signaling via GITR and GITRL in different cell types.	22
3.1. Experimental setup for determination of HCC38 cells' viability by MTT or flow cytometric viability assay with/without GITRL and ionizing radiation.	30
3.2. PageRuler™ Prestained Protein Ladder (10 kDA to 250 kDA) as a protein marker (Thermo Scientific, Rockford, USA).	33
3.3. Molecular weights of 50 bp and 1kb DNA ladder.	41
3.4. pGL3-Basic Vector Map (Promega, Madison, Wisconsin, USA).	43
3.5. pCMV6-AC-GFP Vector Map (OriGene, Rockville, Maryland, USA).	48
3.6. pGL3-Promoter Vector Map (Promega, Madison, Wisconsin, USA).	49
3.7. pRL-TK Vector Map (Promega, Madison, Wisconsin, USA).	49
4.1 Basal-like breast cancer cell lines show increased ATM phosphorylation at 5 Gy ionizing radiation.	52
4.2 Total ATM protein levels in basal-like breast cancer cell lines 24h and 48h post-X-irradiation.	54
4.3. ATM promoter region (-860, +53) to be used processed as insert DNA was amplified with PCR.	55

- 4.4. The ampicillin resistant *E. coli* colonies following heat-shock transformation for the cloning of ATM promoter into pGL3-Basic vector. 56
- 4.5. The presence of ATM promoter cloned into the pGL3-Basic vector was initially characterized by digestion with restriction endonuclease *KpnI*. 57
- 4.6. Basal-like breast cancer cell lines transfected with pCMV6-AC-GFP plasmid. 58
- 4.7. ATM promoter activity in HCC38 cell line before and after (A) 3h and (B) 24h X-radiation. 60
- 4.8. GITR and GITRL expression in basal-like breast cancer cell lines and the effect of X-radiation. 61
- 4.9. GITR and GITRL surface protein expression in HCC38 cell line. 62
- 4.10. Viability of HCC38 cells showed no significant alteration in cells treated with rGITRL either in 1% and 10% FBS condition. 64
- 4.11. Amount of viable cells, proliferation and cell death in HCC38 cells exposed to irradiation and rGITRL. 66

TABLES

Table	Page
2.1. Comparison chart of breast cancer subtypes	5
2.2. TNFR and TNFR ligand family members	16
3.1. EBC lysis buffer components and final concentration.	28
3.2. Culture media and subculture ratios for basal-like and luminal breast cancer cell lines	28
3.3. DNase treatment components and their working concentrations	37
3.4. Components and steps of reverse transcription reaction from RNA samples to prepare cDNA.	38
3.5. Forward and Reverse Primers used for PCR reactions.	39
3.6. Components and their final concentration in PCR reactions.	39
3.7. Steps,time and temperatures of a PCR reaction.	40
3.8. Components and working concentrations of ATM PCR product digestion with KpnI restriction endonuclease for cloning.	44
3.9. Components and working concentrations of KpnI digested ATM PCR product digestion with BglIII restriction endonuclease for cloning.	44
3.10. Components and working concentrations of pGL3 Basic vector digestion with KpnI restriction endonuclease for cloning.	44
3.11. Components and working concentrations of KpnI digested pGL3 basic vector digestion with BglIII restriction endonuclease for cloning.	45
3.12. Components for pGL3-Basic and ATM promoter region ligation reaction	45
3.13. Optimal electroporation conditions (Voltage, Pulse width, Pulse number) for MDA-MB-231, HCC-38 and MDA-MB-468 breast cancer cell lines.	48
3.14. Amount of plasmids used in Luciferase assay transfections experimental design.	49
4.1. $2^{-\Delta\Delta Ct}$ values for ATM expression in serum deprivation (1% FBS) and in complete media (10% FBS) conditions, 24 hours after irradiation.	53

- 4.2.** ATM/ β -actin ratios for ATM expression in basal-like and luminal breast cancer cell lines were calculated by using Ct values obtained with relative quantitative real-time RT-PCR. 53
- 4.3.** Δ Ct (GITR or GITRL Ct – β -actin Ct) values for GITR and GITRL expression in control conditions of 24 hours after X-irradiation (5 Gy and 10 Gy) was determined by relative quantitative real-time RT-PCR. 62



1. INTRODUCTION

Breast cancer shows heterogeneity in morphological, molecular signature, dissemination patterns, survival rate and response to medical therapy (5) (1). When this heterogeneity is examined by considering tumor histopathology, clinical prognosis, and response to treatment; all breast cancer sub-types have distinct molecular portraits (6). According to microarray-based gene expression analyses breast cancer is sub-classified as *Luminal A*, *Luminal B*, *Basal-like*, *Normal breast-like*, *Apocrine*, *ErbB2⁺-enriched* and recently discovered *Claudin-Low* types (2). Basal-like sub-type tends to be most aggressive and invasive showing poor response to current therapeutic modalities, owing to not carrying hormone or targeted therapy responsive ER, PR and HER2 receptors. In addition, basal-like breast cancer cell lines show enrichment for resistant cancer stem cells (CSCs) which may be one of the reasons why this cancer type is aggressive and therapy-unresponsive.

Cancer stem cells (CSCs), being a small sub-group of cells in the primary tumor bulk, show unlimited proliferation and differentiation capacities (3). CSCs have strictly regulated and promptly responding DNA damage response pathways (21) as well as show high expression profiles for drug extrusion transporters (20). Although the cancer remission is observed in conventional therapies as a short-term response to treatment, recurrence of the cancer has been inevitable in the long-term, due to chemo- and radio-resistant CSCs. In cancer, resistance to radiation is attributed to highly expressed Ataxia-telangiectasia mutated (ATM) gene, which has a major role in DNA repair and genomic fidelity.

Genomic stability is disrupted by DNA damage, which can be both endogenously developed (single strand breaks, depurinations, oxidative damage) and exogenously originated (ionizing radiation, UV radiation, chemical mutagens). Radiotherapy efficacy is hindered if the cells have well-regulated DNA damage repair proteins, one of the prominent transducer is ataxia telangiectasia mutated (ATM). ATM expression levels are higher in breast CSCs and upon X-radiation, ATM-Chk2-Cdc25A pathway is induced to correct newly created mutations. Upon radiation, Cdk2 protein is converted into multi-phosphorylated “inactive” conformation resulting in S-phase delay so that the cells are given sufficient time to

perform efficient DNA repair. On the other hand, if ATM is mutated or functionally impaired, the cells progress with radioresistant DNA synthesis.

Even though immunotherapy, especially the checkpoint blockade (such as CTLA-4 or PD-1 blocking antibodies) has been regarded as a promising approach, the therapy modality combining immune modulation and radiation in basal-like breast cancer cells has not been entirely elucidated. GITR-GITRL interaction has been well investigated from the immunological aspects (such as T cell regulation). However, GITR can also be found on cancer cells and its interaction with GITRL not only provides cell proliferation via NF-KB pathway induction, but can also directly trigger cell death.

In this study, we carried out analyses for confirming radiation responsiveness of triple-negative breast cancer cell lines (MDA-MB-231, HCC38 and MDA-MB-468). The levels of ATM phosphorylation, mRNA and protein levels of ATM and promoter activity were determined upon exposure to ionizing radiation. For this purpose a reporter plasmid carrying ATM promoter region was constructed. The presence of GITR and GITRL, their expression regulation in response to X-radiation was assessed. In addition, stimulation of GITR expressed on HCC38 cell line was evaluated in terms of proliferation and cell death with or without ionizing radiation on the basal-like breast cancer cells. ATM expression was constitutive at mRNA and protein level in the breast cancer cells and the total protein levels tend to increase upon irradiation. Our results indicate that stimulation of HCC38 GITR⁺ basal-like breast cancer cells with its cognate ligand may have implications to increase radiation sensitivity.

2. LITERATURE OVERVIEW

2.1. Breast cancer

In normal breast tissue, luminal epithelial cells make up a single cell layer which further covers the lumen of channels or lobules. Basal myoepithelial cells create a second cell layer which surrounds luminal cells. This layer is in direct contact with basal membrane (Figure 2.1.).

Origin of breast cancer predominantly based on the cells lining milk ducts and the lobules supplying ducts with milk. Cancers emanating from lobules are known as *lobular carcinomas*, while cancers developing from the ducts are named as *ductal carcinomas*.

Defects regarding cell-cycle checkpoint as well as DNA damage repair system result in breast cancer, which is further classified as *sporadic* or *inherited* (4). If the genes such as BRCA1, PTEN, TP53 aiding in DNA stability maintenance are mutated, the probability of developing breast cancer increases (5).

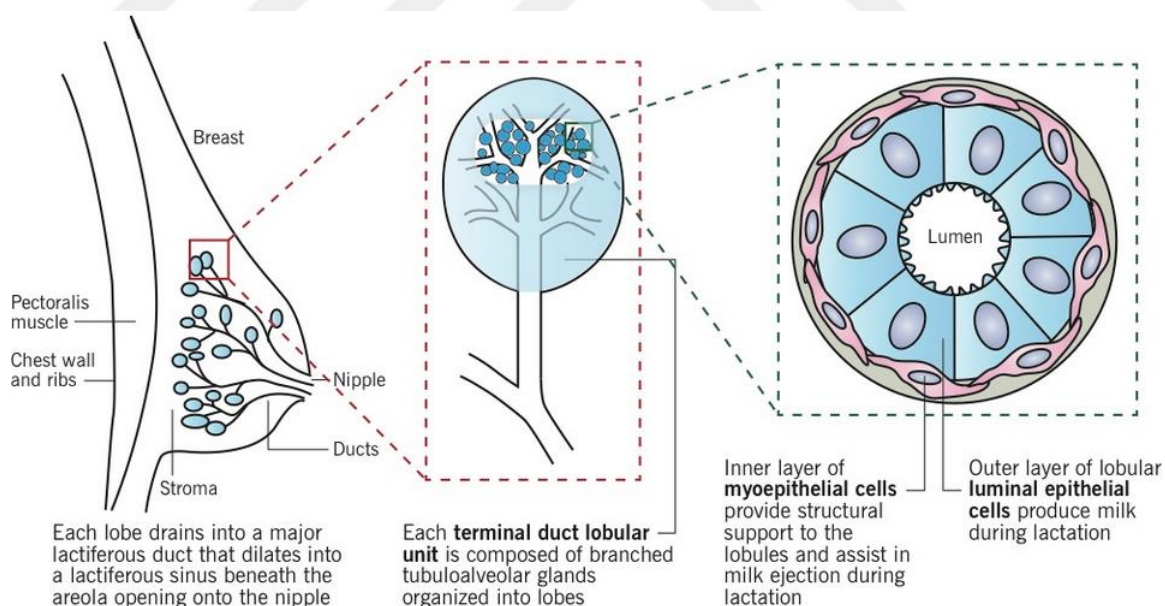


Figure 2.1. Breast anatomical structure and morphological histology depicting luminal or myoepithelial cells which most breast cancer arises from (taken from Clin Obstet Gynecol. 2011 Mar; 54(1):91-5). This Figure is used for “reference and informational purposes” (Authorized Use), as stated in the Copyright rules of the journal.

Breast cancer is the most frequent female cancer in both developed and developing countries (6). Predominance of breast cancer in North America, Europe and Australia surpasses regions of Africa, South and East Asia. According to our national cancer statistics in 2014, 16.646 women (25% of female cancer patients) were diagnosed with breast cancer (7). The stage of cancer at diagnosis differs in regions of Turkey. In Eastern Anatolia, the stage at diagnosis is generally advanced with metastasis (3). In developing countries, five-year survival rate for patients with breast cancer is about 53%, whereas it is reported as 73% in developed countries. The survival difference is not unexpected, since in developed countries patients show awareness for breast cancer, have better access to treatment facilities, early diagnosis due to mammography screening. The mortality rate of breast cancer is 30% (190.000 deaths/ 636.000 cases) in developed countries, whereas this rate is 43% (221.000 deaths/ 514.000 cases) in developing countries (6).

Breast cancer shows heterogeneity in molecular, morphological and clinical aspects (8). As this heterogeneity is investigated by considering tumor histopathology, clinical prognosis, and treatment response; all breast cancer subtypes have distinct molecular portraits (2).

2.1.1. Molecular subtypes of breast cancer

Breast carcinoma *in situ* is divided into two sub-groups known as *ductal carcinoma in situ* (DCIS) and *lobular carcinoma in situ* (LCIS) (9). Ductal carcinoma shows higher prevalence and heterogeneity than LCIS. DCIS is further divided into *solid*, *papillary*, *micropapillary*, *comedo* and *cribiform*, according to its morphological features. A new classification based on molecular markers of *estrogen receptor* (ER), *progesterone receptor* (PR) and *human epidermal growth factor receptor 2* (HER2/*neu*) has gained acceptance, since morphological classification is inadequate. ER, PR and HER2/*neu* status could provide further information regarding tumor response to a particular therapy, such as Trastuzumab for Her2⁺ and aromatase inhibitors or tamoxifen for ER⁺/PR⁺ tumors (10,11). Recently, breast cancer is sub-classified as *Luminal A*, *Luminal B*, *Basal-like*, *Normal breast-like*, *Apocrine*, *ErbB2⁺-enriched* and *Claudin-Low* types, with the use of microarray based gene expression analysis (2) (Table 2.1.). These sub-types actually show disparity for

histological grade, prognosis, survival rate, dissemination patterns and treatment response (1). Approximately 75% of breast cancers show positivity for ER and/or progesterone (PR) receptor (12). Tumor types showing ER positivity typically express genes being unique to luminal epithelial cells, hence named “Luminal”. Luminal group is categorized under two sub-groups called Luminal A and Luminal B (12). While Luminal A tumor cells show ER positivity (ER⁺), they do not carry HER2 (HER2⁻). They are inclined to show tumor grade 1 or grade 2 (1). A portion (28-31%) of breast cancers show luminal A type (2) with low histological grade, highest overall survival rate, low recurrence incidence and plausible response to hormone therapy, owing to their ER positivity (8). Luminal B tumor cells with ER positivity diverge from luminal A type, with or without HER2 positivity (1). Luminal B shows lymph node positivity and larger tumor size with poorer prognosis in comparison to Luminal A.

Table 2.1. Comparison chart of breast cancer subtypes (adopted from “Origins of breast cancer subtypes and therapeutic implications”) adopted from (1)

Breast cancer sub-type	Molecular Signature	Histopathology	Most frequently detected genetic abnormalities	Current Therapies
<i>Luminal A</i>	ER ⁺ , PR ⁺ , HER2 ⁻ GATA3 ⁺	Grade I Invasive lobular	Loss of 16q	Tamoxifen Aromatase inhibitors
<i>Apocrine</i>	ER ^{-/+} , PR ^{-/+} , HER2 ⁺ AR ⁺ , BCL2 ⁻	Grade III	Gain 17q21	Chemotherapy Trastuzumab Lapatinib
<i>Luminal B</i>	ER ^{-/+} , PR ⁺ , HER2 ^{+/+}	Grade III	Gain 17q21	Chemotherapy Trastuzumab Lapatinib
<i>ERBB2 (HER2)</i>	ER ⁻ , PR ⁻ , HER2 ⁺	Grade III	Gain 17q21	Chemotherapy Trastuzumab Lapatinib
<i>Triple negative (Basal-like)</i>	ER ⁻ , PR ⁻ , HER2 ⁻ , High Ki67 expression, CK5 ⁺ and/or CK6 ⁺ CK14 ⁺	Grade III Infiltrating ductal Medullary	Gain 6p21– p25	Chemotherapy Antiangiogenic therapy

HER2-positive tumors show HER2 oncogene amplification or genes related to this pathway with high expression profiles (1). The classification of breast cancer types with low frequency such as normal breast like and/or apocrine breast

carcinoma is still contentious among researchers. Triple-negative breast cancer cells carry neither ER/PR nor HER2; therefore, these cells do not respond to hormone therapy (1). However, in tumors belonging to basal-like sub-type with high expression profile of basal/myoepithelial surface markers (i.e. cytokeratin (CK)5, CK14, CK17 and laminin) (1,12); they do not possess ER, PR and HER2 receptors, hence named as triple-negative (TN) (12). Approximately 15-20% of breast cancers is triple-negative or basal-like. “Claudin-low” type shows low level of claudin gene expression, a protein involved in cell-to-cell adhesion and tight junctions (2). This type is enriched in cells showing tumor initiating cells or cancer stem cell properties (13,14), with epithelial-mesenchymal transition (EMT) signature (15). Clustering analysis on human breast tumors as well as normal breast samples reveals that claudin-low type and basal-like subtypes have shared gene expression patterns (16). They both show low expression profile for ESR1, HER2, GATA3 and luminal keratins 8 and 18 (2). The major discrepancy separating basal-like from claudin-low subtype is that the former shows high expression of cell-to-cell adhesion molecules such as occludin, cingulin, E-cadherin. On the other hand, gene clusters concerning immune response and infiltration show high expression profile in claudin-low subtype. Nonetheless, whether origin of highly expressed CXCL2 and interleukin 6 is claudin-low tumor cells or immune cells in the tumor vicinity are still disputable (2). These cells express vimentin highly (17) and show alteration of cell surface markers towards stem cell-like signature CD44⁺/CD24⁻ phenotype (17).

Basal-like breast cancer cells generally show mutations of tumor suppressor genes BRCA1 and BRCA2 (18,19), which have roles in double-strand DNA repair mechanisms. Such mutations not only increase the propensity to breast cancer, but also raise the sensitivity of tumor cells to ionizing radiation. Despite the fact that chemotherapy and radiotherapy centered treatment modalities as well as usage of estrogen antagonists (such as tamoxifen) and inhibition of signal transduction (such as trastuzumab) aids in clinical and pathological remission of the disease, there is still a high probability for recurrence which may be due to the cancer stem cells.

2.2. Breast Cancer Stem cells

Cancer stem cells (CSCs), being a minute sub-group of cells in primary tumor mass, have unlimited proliferation and differentiation capacities (3). These cells' self-renewal and differentiation properties are provided via pathways like Wnt, TGF- β , STAT, Hippo-YAP/TAZ (3). These must be tightly regulated to preserve stemness of normal stem cells that are critical in physiological processes like embryogenesis and regulation of crypt cells in intestine. However, these pathways are deregulated in cancer (3). CSCs show high expression of ABC transporters such as ABCG2 drug extrusion transporter (20) and have tightly regulated DNA damage response pathways (21); hence, they are resistant to both chemotherapy and radiation. Recurrence of cancer has been attributed to these CSCs in the patients undergone chemotherapy or radiotherapy (21) (Figure 2.2.).

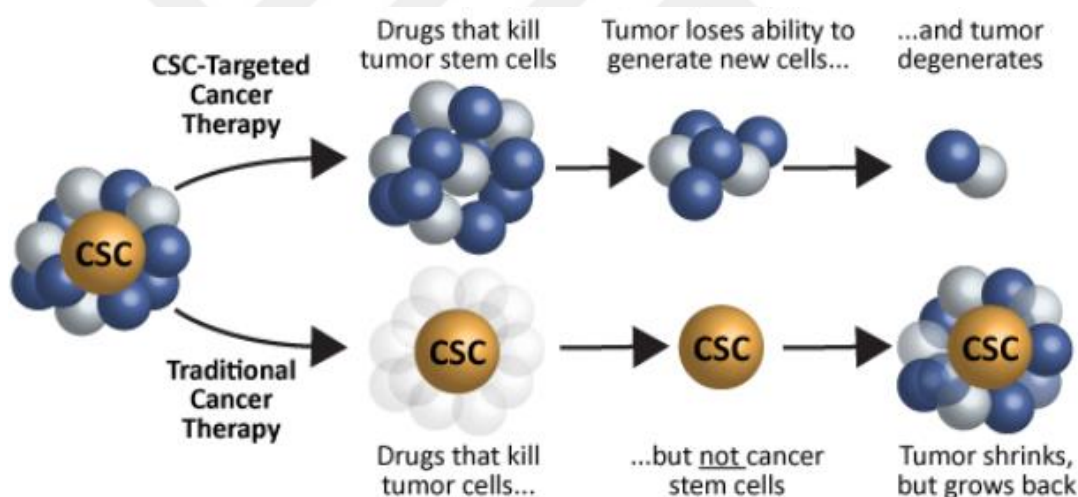


Figure 2.2. Possible outcomes for traditional or CSC targeted cancer therapies (109).

In breast cancer, CSCs (or tumor initiating cells) are regarded to be responsible for resistance against conventional therapy and recurrence of the disease (22). Breast CSCs' surface markers ($CD44^{\text{high}}/CD24^{\text{low/neg}}/ALDH1^+$) are prevalently utilized for identification of these cells (23,24). Breast cancer initiating cells are generally isolated by the help of $ESA^{\text{pos}}/CD44^{\text{high}}/CD24^{\text{low/neg}}/Lineage^{\text{neg}}/ALDH1^{\text{high}}$ cell surface markers (25). Distinct tumor initiating cell sub-populations could be present within the same tumor. These cells are capable of establishing tumors,

promoting tumor growth and providing continuity of tumor when they are inoculated to immunodeficient mice in variable dilutions (25–27). They not only show anchorage-independent growth by creating mammo-spheres *in vitro*, but also they evade *anoikis* (28,29). Salinomycin, which hinders mammo-sphere formation by inhibiting STAT3 activation and resulting in decreasing expression levels for stemness markers (i.e. Nanog and Oct4) in cancer cells, is used to target CSCs (30). Furthermore, CD44^{high}/CD24^{low/neg} breast CSC population is also sensitized to *anoikis* by this antibiotic (30).

In comparison to more differentiated cell types, transcription factors Zinc finger E-box-binding homeobox 2 (ZEB2) and twist family bHLH transcription factor 2 (TWIST2), having roles in epithelial-to-mesenchymal transition (EMT), show higher expression levels in breast CSCs and in CD49f^{high}/EpCAM⁻ mammary stem cells (31,32). EpCAM is widely utilized to detect circulating tumor cells, however this approach is not suitable for isolating CSCs in claudin-low cell lines due to their deficiency in EpCAM (31). A study investigated the transcriptional profiles of 51 breast cancer cell lines in concordance with 145 primary breast tumors (32). They found that 9 cell lines (including MDA-MB-231), previously known as basal-B, actually show the properties of claudin-low type, by having >90% CD44^{high}/CD24^{low/neg} functional CSCs and low expression profile of claudin 3-4-7 cell adhesion molecules (32). Therefore one could conclude that distribution of CD44^{high}/CD24^{low/neg} cell population can be heterogeneous in different cell lines.

2.2.1. CD44^{high}/CD24^{low/neg} breast cancer stem cells

The markers of stemness attributed to breast CSCs are basically CD44, CD24, CD133, ABCG2, ALDH1, EpCAM (23,27). Even though CD44 and CD24 are heterogeneously expressed (CD44^{high}/CD24^{low/neg}, CD44⁻/CD24⁻ and CD44⁻/CD24⁺ cells), most of the studies accept CD44^{high}/CD24^{low/neg} cells as responsible for poor prognosis and aggressiveness in triple-negative breast cancer. Moreover, these cells are able to differentiate into “conventional” tumor cells, as well as initiate metastasis to distant sites such as bones (33) and brain (34).

Wang *et al* (35) showed that a certain percentage of CD44^{high}/CD24^{low/neg} cells of breast CSC phenotype is enriched in MDA-MB-231 (93.25%) and SUM1315

(59.91%) cell lines, whereas MCF-7 and SUM1419 cell lines have low presence of these cells, %0.05 and %2.33 respectively. Sheridan and colleagues also agreed that different breast cancer cell lines have different CD44^{high}/CD24^{low/neg} proportion, by scanning CD44 and CD24 presence in 13 breast cancer cell lines (36). According to their results, MDA-MB-231 cell line is enriched with CD44^{high}/CD24^{low/neg} sub-population (85±5%) and shows the lowest proportion for CD44⁺/CD24⁺ (2%), whereas MDA-MB-468 cell line shows the lowest proportion (3±1%) for CD44^{high}/CD24^{low/neg} and highest proportion for CD44⁺/CD24⁺ (90±6%) (36). On the other hand, HCC38 cell line has 80% CD49f^{high}/EpCAM⁻ mammary stem cells (37). It is proposed that the greater proportion of CD44^{high}/CD24^{low/neg} cells provide these tumors with higher resistance to radiation therapy.

2.3. Radiation therapy in cancer

Radiation therapy is a cytotoxic therapy with a high efficacy for the treatment of solid tumors (38). Local delivery of an optimal dose of radiation is a major concern to minimize dose-dependent toxicity on tumor neighboring healthy cells or tissues. Therefore, host tissue and adjacent tumor tissue should be strictly separated. There is a common misconception that curative success of the radiation therapy depends on the delivery of high radiation doses to the tumor site. Independent of the high dose of radiation delivered, the presence of radioresistant CSCs and tumor-related hypoxia and oncogenic mutations such as EGFR and K-RAS genes may decrease the efficacy of radiotherapy. Radiation modifies tumor microenvironment so that it may facilitate immune cell infiltration and drug penetration into the tumor bulk (38).

Cellular homeostasis is associated with the maintenance of genome stability (39) and cells lose their genomic integrity by radiotherapy. Upon exposure to ionizing radiation, the cells have two options: they either halt their cell cycle to repair mutations, or proceed proliferation process with irreparable mutations accumulating in the cell, risking apoptosis (39,40). Double-strand breaks inflicted by radiotherapy are repaired through either non-homologous end joining (NHEJ) DNA repair mechanism (41,42) or homologous recombination (HR) (Figure 2.3.) (43). The former is more error-prone, because DNA double-strand break ends are directly

ligated, irrespective of homologous sister chromatids (40,41,43,44). Radiotherapy may not be effective if the cells have tightly-regulated DNA damage repair mechanisms such as ataxia telangiectasia mutated - ataxia telangiectasia and Rad3-related protein (ATM-ATR) pathway, γ H2AX, PARP-1, BRCA1 and other damage response proteins (38). By activation of cell cycle checkpoints, ATM and ATR protect the genomic integrity of cells. Even though ATM is activated via DNA double strand breaks and functions through Chk2 activation, ATR is activated by single-stranded DNA damage caused by stalled replication fork and functions through Chk1 (44). On the other hand, high levels of phosphorylated p-ATM, p-Chk1, p-Chk2, PARP1 aids in radioresistance. Inhibition of these damage response proteins leads the cells to be more sensitive to radiation (45). Furthermore, radiosensitivity of cancer cells depends on the cell cycle phase, as cells in late S phase are much resistant to radiation-dependent DNA damage, due to the HR repair mechanism, as far as gamma and X-ray radiation is concerned (38).

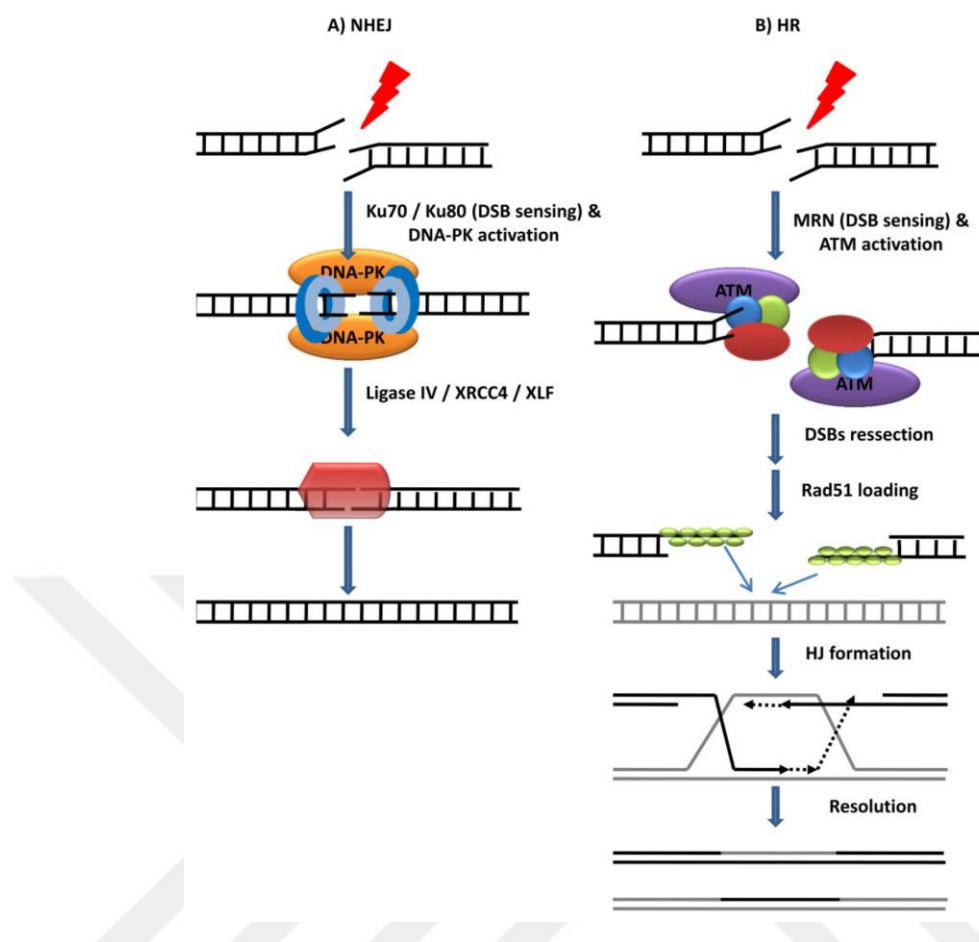


Figure 2.3. DNA repair mechanisms in response to radiation. A) Non homologous end-joining NHEJ, B) Homologous Recombination. (Adopted from: Biochemistry, Genetics and Molecular Biology "Protein Phosphorylation in Human Health", ISBN 978-953-51-0737-8) (110).

Radiation therapy modalities for breast cancer are external beam radiotherapy (EBRT), brachytherapy (BRT) or intraoperative radiation (IORT) (46). EBRT is the most frequently used radiotherapy technique, in which a linear accelerator (Linac) directs radiation with a high energy X-rays to the tumor region (46). Brachytherapy is used after lumpectomy and this method utilizes small pieces of radioactive seeds, which are temporarily inserted into the tumor vicinity with the aid of multiple catheters or balloon-shaped catheters. These seeds emit a certain dose of radiation to the neighboring tissue, in a shorter duration than EBR (46). In the temporary brachytherapy radiation source would be removed after high dose source of radioactive material is applied to the tumor region. On the other hand, in the permanent brachytherapy radioactive seeds are implanted into the tumorigenic region and they emit a continuous dose of radiation.

2.3.1. Effect of radiation on breast cancer cells

Even though germline mutations can enrich genetic diversity, such variations in DNA sequences can be dangerous for somatic cells. Somatic cells have tightly regulated protective mechanisms against genomic changes (21). Genomic stability is challenged by DNA damage, which can be from both endogenous, e.g. single strand breaks, depurinations, oxidative damage, and exogenous, e.g. ionizing radiation, UV radiation, chemical mutagens (39). With the aid of several repair mechanisms specialized for different DNA damage types, the cells manage to protect their genomic integrity (47). Nevertheless, the type of the damage, as well as accumulated mutations can direct the cell to go into programmed cell death (apoptosis). DNA damage-induced apoptosis is more common in normal cells and in tumor cells (48). On the other hand, CSCs have well regulated and prompt DNA damage response pathways (21,49,50). When both CSCs and cancer cells are exposed to ionizing radiation, only a small group of these cells (i.e. cancer stem cells) survive and can reestablish the tumor, whereas abundant number of tumor cells commence to accumulate irreparable mutations and subsequently die (51). Double-strand breaks (DSB) has been regarded as the most cytotoxic DNA damage and would trigger cell cycle checkpoints to decide for cell survival (21). When DSB are inflicted by ionizing radiation or free radicals, CSCs go into rapid cycle arrest, resulting in an S phase delay to resolve the problem (21), whereas most of the cancer cells prefer radioresistant DNA synthesis (52). For DSB, the primary transducer of DNA damage is ATM. Upon activation, this protein phosphorylates the downstream molecules and induces ATM-Chk2-Cdc25A DNA damage response pathway (Figure 2.4.) (52,53).

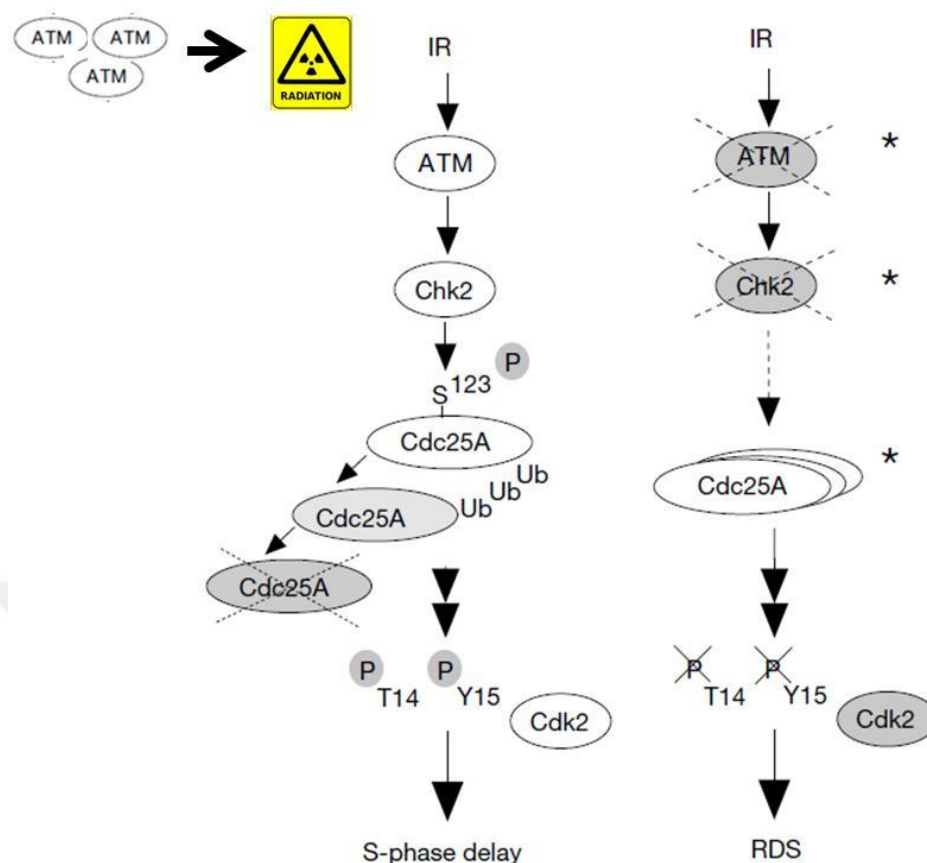


Figure 2.4. ATM-Chk2-Cdc25A DNA damage response pathway (Modified from Falck et al, Nature 2001; 842-47) (52).

2.3.2. The role of ATM in radiosensitivity

ATM belongs to phosphatidylinositol 3-kinase-related kinase family and is a 370 kDa serine-threonine kinase (54). It is found in the cytoplasm as an inactive homodimer or forms heteromultimer. When DNA damage by ionizing radiation occurs, with the assistance of Mre11-Rad50-Nbs1 (MRN) complex, ATM is recruited upon interaction with Nbs1 and converted into its active state by auto-phosphorylation on serine 1981 residue, which further reveals its catalytic kinase domain (59, 60). Furthermore, Rad50 aids DNA unwinding by its ATPase activity (55). Upon activation, ATM phosphorylates Chk2 (Figure 2.4.), then Chk2 phosphorylates Cdc25A, which is further ubiquitinated and destined for degradation via proteasomes (52). ATM activation upon ionizing radiation leaves Cdk2 in a multi-phosphorylated “inactive” state, which results in an S-phase delay, so that the cells are allowed to carry out an efficient DNA repair. On the other hand, if ATM is functionally impaired, the cells proceed with radioresistant DNA synthesis. Many

studies have been focused on direct targeting of the ATM signaling pathway or on important elements downstream of ATM (such as Chk1, Chk2), in order to abolish the CSCs' resistance to radiation (56,57). ATM deficiency could result in pleiotropy accompanied with cerebellar degeneration, immunodeficiency, thymic atrophy, as well as extreme ionizing radiation sensitivity (58,59). Not only radiation but also growth factors regulate ATM pathway (60). Gueven *et al.* showed influence of serum deprivation on ATM promoter activity which varies according to the type of cell line used. When cells are serum deprived, 293T (SV40 immortalized fibroblast cell line) shows an increment, whereas H1299 lung cancer cell line shows a decrement of ATM expression. One of the possible explanations for ATM/Chk2 activation by serum deprivation is that cell proliferation in the absence of serum results in nucleotide pool depletion accompanied with a loss of genomic stability (61). Therefore, DNA damage response pathway is activated. Furthermore, ATM proximal promoter region is regulated with methylation of CpG islands in HCT-116 colorectal tumor cell line, which is accompanied with reduced ATM levels due to epigenetic silencing and higher radiosensitivity (62). When HCT-116 cells are co-cultured with 5-azacytidine, promoter demethylation occurs and ATM expression levels increase resulted in decreased radiation sensitivity. Another study by *Hu et. al.* demonstrated that microRNA 421, whose abundance correlates with N-myc transcription factor in neuroblastoma, interferes with ATM expression by targeting the 3'-untranslated region (3'UTR) of ATM transcripts (63).

There are various and numerous transcription factor binding sites on the ATM promoter, which contribute to its cooperative radiation response with different pathways. The transcription factors SpI, Cre, Ets and API, but not Myb and NFI, have a major effect on the regulation of ATM promoter (60). Another study suggests that E2F-1 transcription factor has a major impact on the transcriptional regulation of ATM (64).

There are contradictory data showing disparate radio-sensitivities of cancer initiating cells and normal cancer cells. In one of such studies, cancer stem cell-rich MDA-MB-231 and MDA-MB-453 cell lines and corresponding non-stem cell rich counterparts were compared in terms of their radio sensitivities (65). These cells were exposed to wide spectrum of radiation, beginning from 1.25 Gy up to 8.75 Gy

and their survival curves and ATM activation was assessed. In contrast to the existing literature that CSCs have high ATM expression accompanied with radioresistance (66), a study reversely asserted that cancer initiating cells show low-level of ATM expression accompanied with poor DNA damage repair capacity which ultimately results in high radiosensitivity (65). Although Ropolo *et al.* reported the importance of cell cycle stratification on determining sensitivity to radiation (67), their study also held ATM expression levels responsible for radiosensitivity, rather than antioxidant levels or cell cycle phases. Many other studies demonstrated that if the majority of cells are in S phase, they are more radioresistant, whereas if they are in late G2 or M phases, they are predisposed to damaging effects of radiation (68).

Ahmed and his colleagues have focused on glioblastoma multiforme, which is among the most aggressive brain cancers. They correlated the inevitable recurrence of this malignancy to the brain cancer stem cells (69). The brain cancer stem cells are more radioresistant compared to “conventional” cancer cells in the tumor bulk. Upregulated expression of ATM, ATR, PARP1 and Chk1 was found in brain cancer initiating cells. Inhibition of either ATR or Chk1 interferes with the G2-M cell cycle checkpoint, which forces cells to show modest radiosensitivity. Radiosensitization emanating from ATM inhibition outweighs and individual inhibition of PARP, ATR or Chk1 separately, because ATM not only has a significant role at cell cycle checkpoint but also has a modulatory effect on DNA damage response, unlike other individual proteins. Nevertheless when PARP and ATR are co-inhibited in brain CSCs, radiosensitivity was enhanced. This study revealed that combined inhibition of DNA damage response proteins may be partially efficient to overcome radioresistance, however not as efficient as inhibition of ATM.

2.4. Glucocorticoid-induced tumor necrosis factor receptor (GITR) and its ligand (GITRL)

Tumor Necrosis Factor Superfamily Member 18 (TNFSF18) and Tumor Necrosis Factor Receptor Superfamily Member 18 (TNFRSF18), namely GITRL and GITR, are members of tumor necrosis factor receptor (TNFR) superfamily (70).

Most of the TNFR family members have a major role in T cell regulation, after initial activation of T cells through T cell receptor (TCR) and CD28-B7 engagement (71). Some members of this superfamily are GITR, 4-1BB (CD137), CD27, HVEM, CD30 and OX40 (CD134), and they all show co-stimulatory effects on T cells. TNFR family is categorized into three groups: i. receptors carrying *death domain* (DD), ii. *decoy receptors* (DR), and iii. *TNF receptor-associated factor* (TRAF)-binding receptors (72–74). DD-carrying TNFRs (i.e. TNFR1, FAS, DR3) could induce canonical caspase pathways by DD-carrying signaling intermediates directly, resulting in apoptosis. Even though TRAF binding receptors (such as TNFR2) are deficient of DDs, they are specialized to recruit TRAF proteins by their special 4-6 amino acid long SXXE motifs (75).

Table 2.2. TNFR and TNFR ligand family members (Drug News Perspect 2002, 15(8):483ISSN0214-0934 Copyright 2002 Tumor Necrosis Factor Family Ligands and Receptors in the Immune System: Targets for Future Pharmaceuticals by Francis Ka-Ming Chan and Michael J. Lenardo)

LIGANDS			RECEPTORS	FUNCTIONS
COMMON OFFICIAL NAME	NAME	OTHER NAMES		
TNF α	TNFSF2		TNFR1/TNFR2	Programmed cell death/cellular proliferation/inflammatory reaction
TNF β	TNFSF1	Lt α	TNFR1/TNFR2/HveA/LT β R	
LT β	TNFSF3		LT β R	Lymphoid organogenesis
Fas-L	TNFSF6	CD95L/Apo1 Ligand	Fas/DcR3	Apoptosis induction
CD40-L	TNFSF5	CD154	CD40	B-cell co-stimulation
TRAIL	TNFSF10	Apo2L	TRAIL-R1/TRAIL-R2/TRAIL-R3/TRAIL-R4/OPG	Apoptosis induction in dendritic cells
APRIL	TNFSF13	TALL-2	TACI/BCMA	T-cell and B-cell proliferation
OX40L	TNFSF4	OX-40	T-cell co-stimulation	
TALL-1	TNFSF13b	BAFF/Blys/THANK/zTNF4	BAFF-R/TACI/BCMA	B-cell development and plasma cell differentiation
TRANCE	TNFSF11	RANKL/OPGL	TRANCE-R	Dendritic cell proliferation/bone development
TWEAK	TNFSF12	Apo3L	TWEAK-R	
VEG1	TNFSF15	TL-1		
4-1BBL	TNFSF9		4-1BB	T-cell co-stimulation
CD27L	TNFSF7	CD70	CD27	
CD30L	TNFSF8		CD30	
GITRL	TNFSF18	AITRL/TL6	GITR	Regulatory T-cell function
LIGHT	TNFSF14		DcR3/HveA/LT β R	
EDA			EDAR/XEDAR	

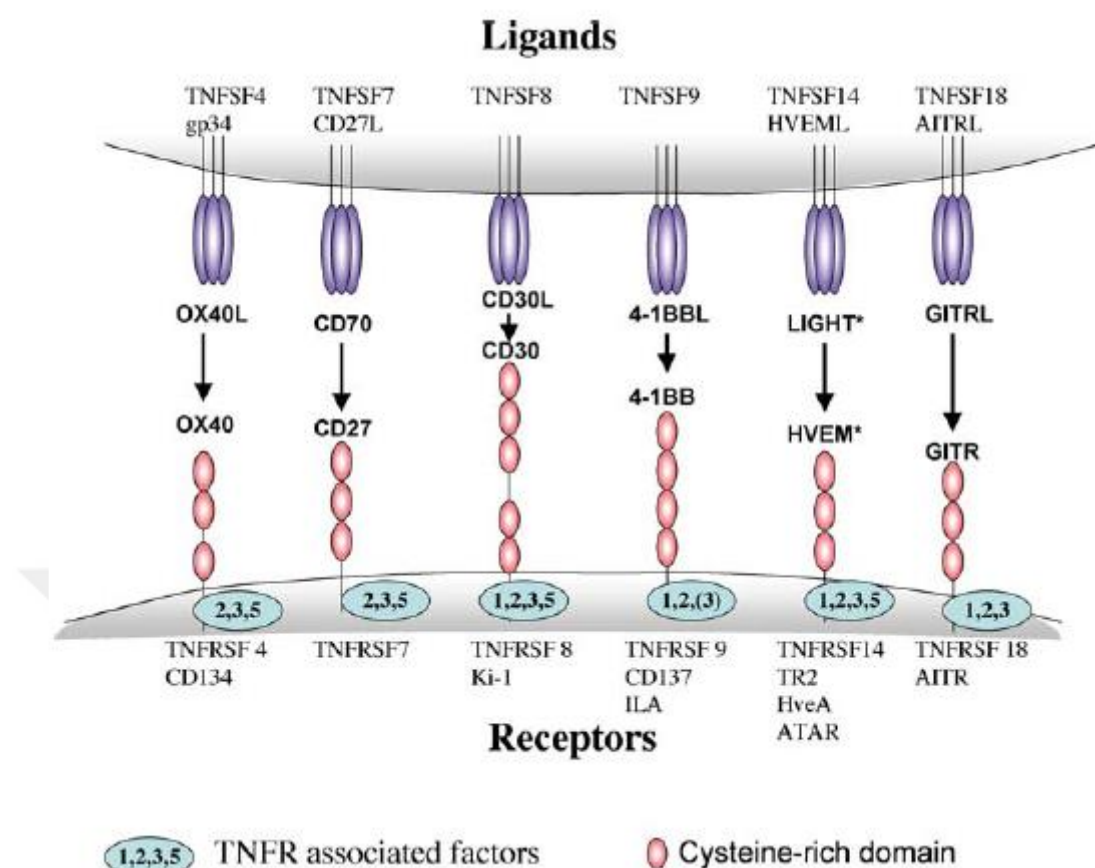


Figure 2.5. TNFR ligand family structure (Adopted from Watts et al, *Annu. Rev Immunol* 2005 23:23-68) (71).

Human GITR (also known as TNFRSF18, AITR, CD357) is designated as h(GITR), is a type I transmembrane protein consisting of 241 amino acids (76). Murine GITR (m(GITR)), which is a 228 amino acid long protein, shows approximately 60% sequence similarity to h(GITR) (77). Human GITR locus is on chromosome 1, on which OX40 and 4-1BB genes assemble together (76). GITR is specifically activated by its ligand GITRL (also known as TNFSF18, AITRL) which is a 177 amino acid transmembrane protein in mouse (76). As receptor h(GITRL) locates on chromosome 1, on which FasL and OX40L genes are clustered together (76,78,79). No binding is observed between h(GITRL) and m(GITR), or vice versa (80). GITR is known to be constitutively expressed on the surface of FoxP3⁺ regulatory T (Treg) cells (81,82). Expression of GITR is regulated through a FoxP3-associated signaling cascade (83). In memory and naïve T cells, GITR expression is limited, but upon T cell activation, GITR expression is upregulated (84). In T cells, GITR expression is influenced by Nuclear Factor kappa B (NF- κ B) (RelA is the

major transducer, with p50 and cRel moderate effects) and nuclear factor of activated T cells (NFAT), mutually (85). Even though NF- κ B upregulates GITR expression, NFAT has a suppressive effect. NFAT and NF- κ B acts reciprocally to decide on the biological outcomes in T cells upon TCR activation. Moreover, interleukin (IL)-15 has a major impact on upregulated GITR levels on CD8⁺ memory T cells in bone marrow, by enhancing T cell survival (86). These results suggest that one of the pathways induced by GITR-GITRL interaction is through NF- κ B.

Signaling through GITR results in positive regulation of Jun N-terminal kinases (JNK), mitogen-activated protein kinase (MAPK), extracellular signal-regulated kinases (Erk) and NF- κ B pathways, enhances cytokine secretion and T cell survival (87). As mentioned previously, GITR belongs to TRAF-binding receptors and recruits TRAF2/5 complex further to activate T cell survival by upregulation of anti-apoptotic protein Bcl-XL (88). All stimulatory TNFR family members recruit TRAF2 in their signaling complex, with affinities for other TRAF molecules. Binding of TRAF2 and TRAF5 results in NF- κ B activation (89), which releases it from the inhibitor protein I κ B α via degradation. This circumstance further upregulates cellular inhibitors of apoptosis (cIAP1 and cIAP2), c-Flip and anti-apoptotic molecule Bcl-XL. Some studies suggest that GITR interacts with TRAF1, yet this engagement could be dispensable, as TRAF1^{-/-} T cells do not show dysregulated NF- κ B pathway upon GITR activation (88). When GITR-GITRL engagement occurs on Treg cells, NF- κ B pathway and JNK becomes activated. JNK phosphorylation can annul suppressive functions of Tregs (90). Besides having a role in cell proliferation, the GITR-GITRL engagement may also result in apoptosis. GITR itself does not carry a death domain (DD), albeit it is suggested that it aids apoptosis via SIVA pathway (91).

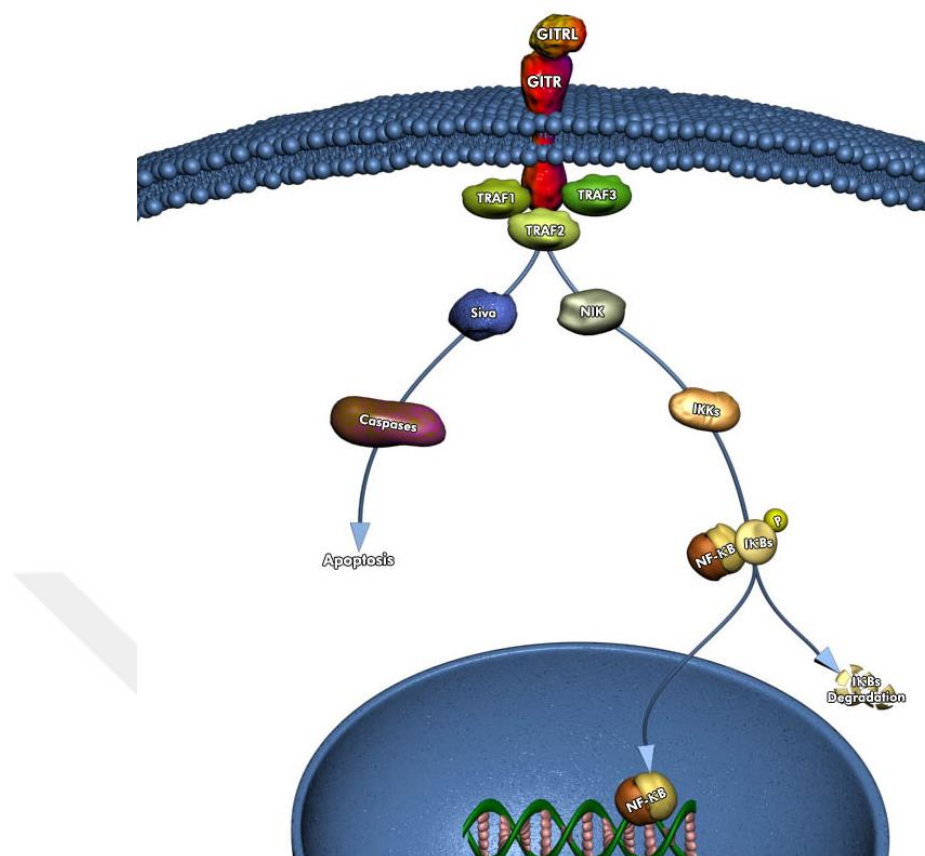


Figure 2.6. GITR signaling through SIVA and NF- κ B (111).

Interaction of pro-apoptotic protein SIVA-I and cytoplasmic tail of GITR has been documented (92). SIVA-I differs from alternative splice form SIVA-II by having a DD (93). To induce apoptosis, SIVA directly binds to anti-apoptotic protein Bcl-XL to inhibit its pro-survival function, rather than activating its own DD. This condition makes cells more sensitive to UV radiation induced apoptosis (92). A wide assortment of DNA damaging agents such as alkylating agents (methyl methanesulfonate) and UV light activate ATR and ATM, however the latter one is activated primarily by irradiation (IR) (94). If cells have upregulated SIVA expression, it is followed by cell shrinkage, caspase activity (initiator caspase 8/9 and effector caspase 3) and translocation of phosphatidylserine onto the cell surface as an early marker of apoptosis (93). Cytochrome c release as well as Bid activation reveals that SIVA pathway triggers mitochondrial-dependent apoptosis pathways (93). Rather than DD homology region (DDHR), C-terminus and N-terminus, which are shared between SIVA-I and SIVA-II, have a significant role in SIVA-related apoptosis (93).

2.4.1. Distribution of GATR and GATRL expression

When GATRL expression in cancer cell lines is compared, TIME and HUVEC TERT2 (endothelial cell lines), EFO-21 (breast cancer cell line) cell lines are enriched with GATRL expression (Figure 2.7A); whereas there is almost no expression in normal human tissues, apart from the minute expression levels seen in esophagus and cerebral cortex (Figure 2.7B).

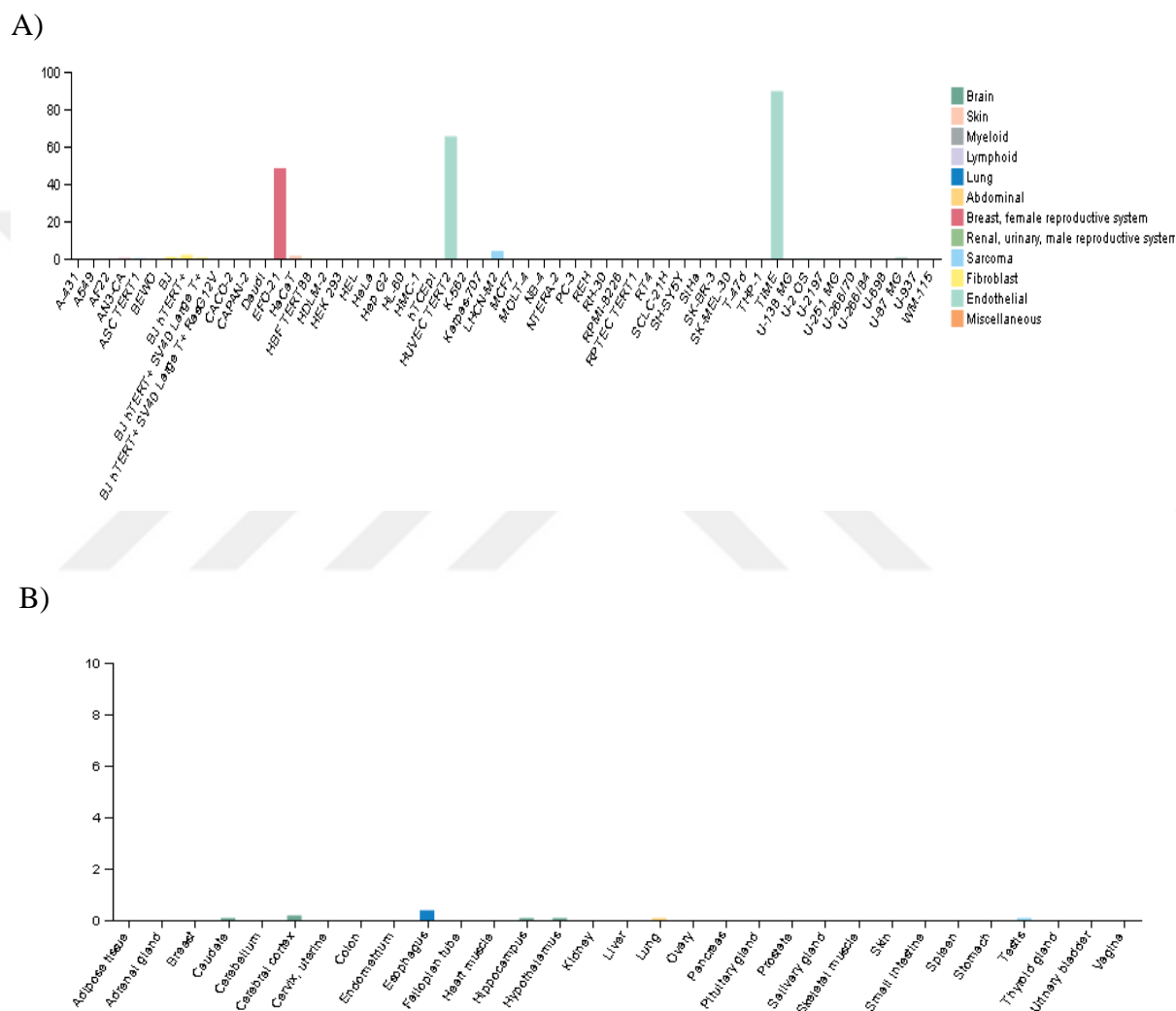


Figure 2.7. GITRL RNA expression in A) Cancer cell lines, B) Normal human tissues (Adopted from Human Protein Atlas) (112).

As far as GATR expression is considered, SCLC-21H and RPMI-8226 cell lines are enriched with GATR (Figure 2.8 B) and there is a high protein level of GATR in female tissues as well as in bone marrow and immune system (Figure 2.8. A).

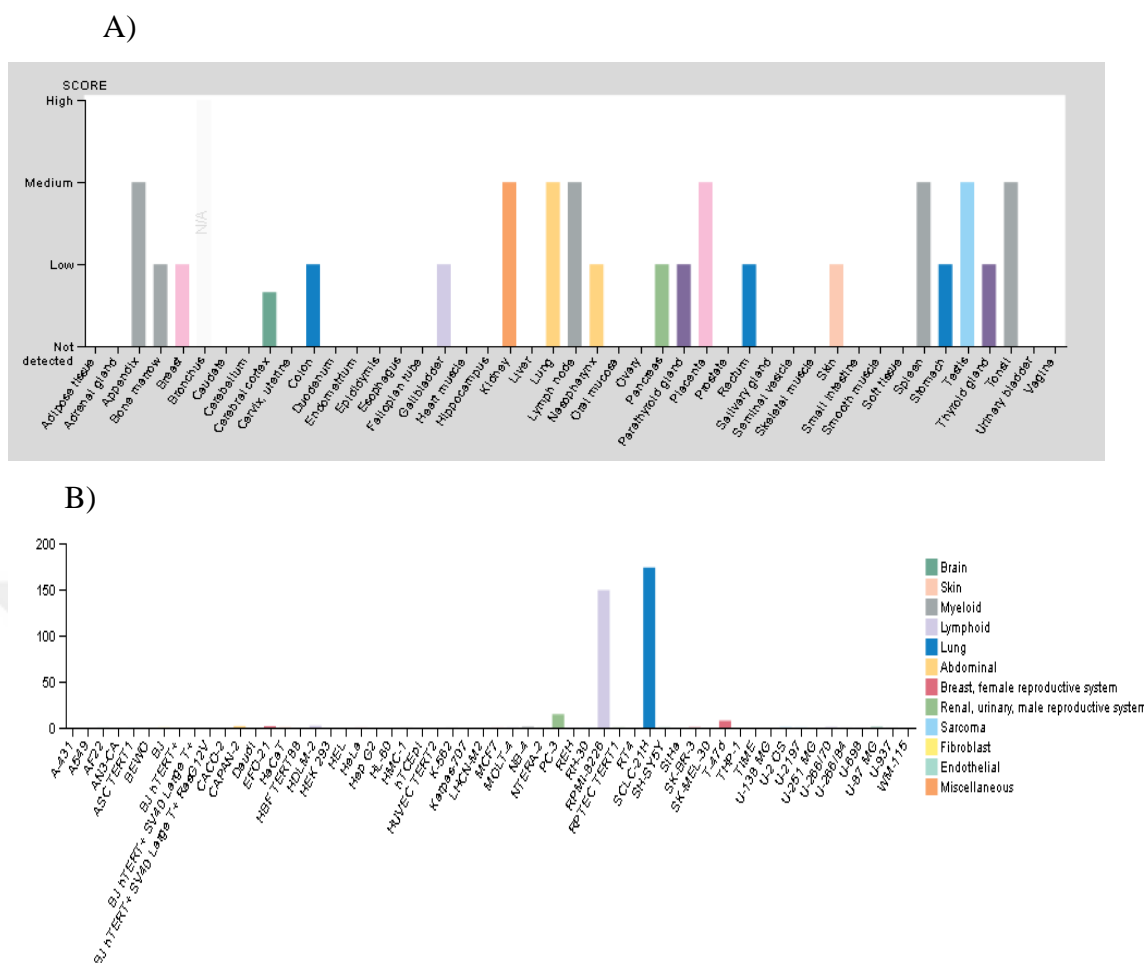


Figure 2.8. GITR expression in A) Normal human tissues, B) Cancer cell lines (Adopted from Human Protein Atlas) (113).

2.4.2. Immunological aspects of GITR-GITRL interaction

Functional consequences of GITR-GITRL interaction among tumor cells and immune cells depend on the cell type. Tumor cells show constitutive expression of GITRL in several cell lines or human colon and rectum tumor tissues, together with repressed expression of costimulatory CD40 and CD54 molecules (95). GITR signaling in tumor cells also results in increased expression of immunosuppressive molecule TGF- β (95). Despite expression at low levels, NK cells have constitutive expression of GITR on their surface, and this expression is enhanced when cells are activated upon simultaneous exposure to IL-2 and IL-15 (95,96). Even though NK cell cytotoxicity is increased with IL-15 pretreatment, tumor cell-expressed GITRL

abrogates NK cell function by impeding IFN- γ release. Therefore, cytotoxicity of NK cells against tumor cells is prevented. Baltz *et al.* (95) demonstrated that IFN- γ release from NK cells can be increased by anti-GITR mAb, since it blocks the GITRL expressed on HCT116 (colon), LX1 (lung), NCCIT (germ cell) tumor cells. Hanabuchi and colleagues reported contradictory results for the effect of GITRL on NK cells. Their study claims that plasmacytoid dendritic cells (pDC) stimulated upon viral infection show high level of GITRL expression (96) and elevated GITRL levels fortify cytotoxicity and IFN- γ production of NK cells. This was observed when type I interferons were present; therefore, the presence of GITRL only is not sufficient to activate NK cells. In addition to GITRL, extra stimuli from IFN- α , IL-2 and NKG2D are required to activate NK cells (96).

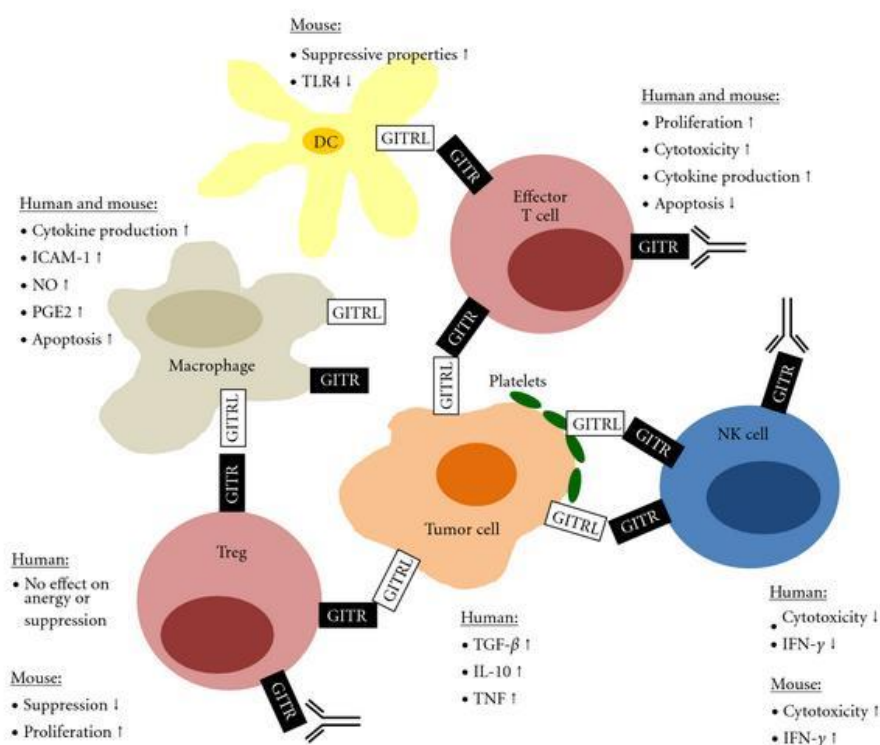


Figure 2.9. Outcomes of signaling via GITR and GITRL in different cell types (114).

Several studies suggest that GITR stimulation with agonist antibodies result in the activation of matrix metalloproteinase-9 (MMP-9) and pro-inflammatory cytokines such as TNF- α (97). Moreover, there are studies showing the function of GITR in leukocyte adhesion and migration (98). By utilizing trans-well migration assays, GITRL-GITR-Fc binding is shown to result in STAT1 phosphorylation

followed by upregulation of intracellular adhesion molecule (ICAM-I) and vascular cell adhesion molecule (VCAM-I). GITR^{-/-} splenocytes show impaired adhesion to endothelium, but this impairment could be reverted by functional GITR-Fc. When GITR-Fc binds to GITRL on endothelial surface, reverse signaling occurs and splenocytes recover their adherence (98). Besides splenocytes, GITRL has been suggested to have an effect on macrophage egress (99). However, whether upregulated VCAM-I and ICAM-I has a role in this egress (99), or altered expression of chemokines and cytokines show ancillary effect for macrophages' mobility is still disputable.

Plasmacytoid dendritic cells (pDCs) has high surface GITRL expression and upon reverse signaling, NF- κ B pathway activates, aiding in immunosuppression through Indoleamine-pyrrole 2,3-dioxygenase (IDO) (100).

When we examine the importance of GITR and GITRL in the context of B cells, even though GITR/L expression increases upon B cell activation, no change in the serum immunoglobulin (Ig) levels or B cell development was noted (101). Nevertheless, it has a major effect on marginal zone B cells and follicular B cell accumulation, but it does not interfere with antibody response of B cells (humoral immunity).

In CD4⁺ and CD8⁺ T cells, GITR engagement with GITRL is indispensable for cell proliferation and survival accompanied with augmented IL-2, IFN- γ and CD25 levels.

3. MATERIALS AND METHODS

This thesis study was performed at Hacettepe University Cancer Institute, Department of Basic Oncology Laboratories and in Ege University, Faculty of Pharmacy, Department of Pharmacology through February 2016 - June 2017. The procedures were submitted to the approval of the Non-interventional Clinical Research Ethics Board at Hacettepe University (Doc. Nr.:16969557-404).

3.1. Materials

The chemicals and biological materials used in this study and their suppliers are listed: DMEM High Glucose, RPMI 1640, Penicillin-Streptomycin solution, Trypsin-EDTA (Biological Industries, Israel); DMEM Low Glucose (Lonza, Basel, Switzerland); L-Glutamine, (200Mm), Fetal Bovine Serum (FBS) (Biowest, Nuaille, France); polyvinylidene difluoride (PVDF) transfer membrane, PageRuler™ Plus Prestained Protein Ladder, Pierce™ ECL Western Blotting Substrate, SuperSignal™ West Femto Maximum Sensitivity Substrate, dNTP mix (25mM), 6x DNA loading dye, DNaseI enzyme, Oligo(dT)₁₈ primer, 5x reaction buffer, Reverse Transcriptase, Ribonuclease inhibitor, 50 bp DNA ladder (Thermo Scientific, Rockford, USA); Halt™ protease inhibitor cocktail (PIC), Pierce RIPA Buffer, Pierce™ BCA Protein Assay Kit (BCA Reagent A, BCA Reagent B), DreamTaq DNA polymerase, 10x DreamTaq Buffer (Thermo Fisher Scientific, USA); Bovine serum albumin (BSA), beta-mercaptoethanol, Sodium dodecyl sulfate (SDS), Trizma Base, Trypan Blue (Sigma-Aldrich, US); T4 DNA ligase, KpnI-High Fidelity and Bgl-II restriction enzymes, CutSmart Buffer and NEBuffer 3.1, NEB® 5-alpha competent *E. coli*-High Efficiency, T4 DNA ligase buffer (10x) (New England BioLabs, Ipswich, Massachusetts, USA); 10x Dulbecco's Calcium-Magnesium free phosphate-buffered saline (DPBS) solution (Gibco, ThermoFisher, Paisley, UK); Western Blotting Buffers and Reagents (Resolver A, Resolver B, APS, TEMED, Stacker A, Stacker B), SsoAdvanced™ Universal SYBR® Green Supermix (Bio-Rad, Hercules, California, USA); anti-polyspecies Beta-actin primary antibody, ATM (D2E2) rabbit mAb #2873 (Cell Signaling Tech, Danvers, Massachusetts, USA); recombinant human GITR Ligand/TNFSF18 (CHO-expressed) Protein, Human GITR/TNFRSF18 APC-conjugated Antibody (Monoclonal Mouse IgG1 Clone # 110416), human GITR

Ligand/TNFSF18 PE-conjugated antibody (Monoclonal Mouse IgG1 Clone # 109101 (R&D Systems, Minneapolis, USA); serological pipettes (Costar, USA); cell strainers (Corning, USA); Mouse anti-human phospho-ATM (S1981) primary antibody (Affymetrix eBioscience, USA); pGL3-Basic vector, pRL-TK vector, pGL3-Promoter vector, Luciferase Assay Reagent II (LAR II), Stop&Glo® Reagent (Promega, Madison, Wisconsin, USA); pCMV6-GFP vector (OriGene, Rockville, Maryland, USA); Cell wash (BD Biochemicals, USA); anti rabbit polyclonal secondary antibody (Dako, Glostrup, Denmark); resuspension buffer R, Buffer E, carboxyfluorescein succinimidyl ester (CFSE) (Invitrogen, Carlsbad, California, USA); primer oligonucleotides (Sentegen Biotech, Ankara, Turkey); Ampicillin (GeneMark, Taichung City, Taiwan); T25 flask (SPL Life Sciences, Korea); T75 flask, 6-well plates (Sarstedt, Nümbrecht, Germany); 15 ml conical centrifuge tubes (Kirgen, Haikou, Hainan, China); 50 ml tubes, 96-well plates flat bottom (Orange Scientific, Belgium); phosphate buffered saline (PBS) tablets (Advansta, California, USA); Glycine crystalline (Merck, Darmstadt, Germany); horse radish peroxidase (HRP) conjugated goat anti-mouse secondary antibody (Dako, Glostrup, Denmark); FACS flow, Bacto-yeast Extract, Bacto-tryptone (BD, San Jose, CA, USA); Bacto-agar (Difco Laboratories, Detroit, Michigan, USA); 10x DNaseI buffer, 1 kb DNA ladder gene ruler (Fermentas, USA); Agarose (BioShop, Burlington, Canada); Ethanol 96% (AppliChem, Germany); DRAQ7 (BioLegend, USA); Ethylenediaminetetraacetic acid (EDTA), Calyculin A, sodium fluoride (NaF), phenylmethylsulfonyl fluoride (PMSF), cell scrapers, glycerol, skimmed milk powder, Ethidium Bromide (EtBr), NaCl, 3-(4,5-dimethylthiazol-2-yl)-2,5-diphenyltetrazolium bromide, DMF/SDS, plastic pasteur pipettes, DNase/RNase-free ddH₂O, Diethyl pyrocarbonate (DEPC), reverse transcriptase enzyme, plastique 2ml syringe, Tween 20, Boric acid

3.2. Buffers and Solutions

Heat-inactivated fetal bovine serum (FBS): FBS was thawed at 4°C, subsequently it was incubated at 56°C water bath for 20 minutes for heat inactivation. Heat-inactivated serum aliquots (approximately 40 ml) were prepared and stored at -20°C.

Complete Roswell Park Memorial Institute (RPMI)-1640 medium: Heat-inactivated FBS (55 ml, 10% final concentration), penicillin-streptomycin (5.5 ml, 1% final concentration) and L-glutamine (5.5 ml, 1% final concentration) were sequentially added into 500 ml RPMI-1640 medium. The complete culture media were kept at 4°C. For serum reduction experiments, FBS final concentration was used as 1%.

Complete Dulbecco's Modified Eagle's medium (DMEM): Heat-inactivated FBS (55 ml, 10% final concentration), 5.5 ml penicillin-streptomycin (1% final concentration) and 5.5 ml L-glutamine (1% final concentration) were sequentially added into 500 ml DMEM (low glucose or high glucose where appropriate). The complete culture media were stored at 4°C. For serum reduction experiments FBS was used at 1% final concentration.

Phosphate-buffered saline (PBS) solution: PBS solution (1x) for cell culture experiments were prepared by dissolving one 10x PBS tablet in 500 ml double-distilled water (ddH₂O). Then the solution was sterilized by autoclaving.

Trypan blue solution: By dissolving 40 mg trypan blue powder in 99.8 ml 1x PBS, 0.4% trypan blue solution was prepared. Then, the solution was filtered through a 0.22 µm sterile filter.

PBS-Tween (PBS-T) buffer: PBS solution (1x) and 500 µL Tween-20 were mixed (v:v 1:1000) to obtain PBS-T buffer for Western-Blot experiments.

Transfer buffer: Tris (7.24 gr, 0.12 M final concentration) and glycine (36 gr, 0.96 M final concentration) was added into 500 ml ddH₂O in order to obtain 5x transfer buffer. Then, by mixing 300 ml ddH₂O, 100 ml methanol and 100 ml 5x transfer buffer (v:v:v 3:1:1), 1x transfer buffer was freshly prepared for each experiment.

Running buffer: Tris (7.5 gr, 0.124 M final concentration), glycine (36 gr, 0.96 M final concentration) and sodium dodecyl sulfate (SDS) (2.5 gr, 0.02 M final concentration) was added into 500 ml ddH₂O to prepare 10x running buffer. Then, by mixing 450 ml ddH₂O with 50 ml 10x running buffer (v:v 9:1), 1x running buffer was freshly prepared.

Western resolver gel: Resolver A solution (3 ml), resolver B solution (3 ml), 30 µL 10% Ammonium Persulfate (APS), 3 µL tetramethylethylenediamine

(TEMED) were mixed to obtain a complete resolver solution for one western resolver gel.

Western stacker gel: Stacker A solution (1 ml), Stacker B solution (1 ml), 10 μ L 10% APS, 2 μ L TEMED were mixed to prepare a stacker solution for one western stacker gel.

Skimmed milk powder in PBS-T: Skimmed milk powder (5 gr) was dissolved in 100 ml PBS-T to acquire a 5% milk PBS-T solution. The mixture was mixed with a magnetic stirrer.

Luria-Bertani (LB) Broth: Bacto-yeast extract (2 gr, 0.5% w/v), Bacto-tryptone (4 gr, 1% w/v) and NaCl (4 gr, 1% w/v) were dissolved in 400 ml ddH₂O and afterwards the mixture was sterilized by autoclaving.

Luria-Bertani (LB) Agar: Bacto-yeast extract (2.5 gr, 0.5% w/v), Bacto-tryptone (5 gr, 1% w/v), NaCl (5 gr, 1% w/v), Bacto agar (7.5 gr, 1.5% w/v) were added into 500 ml ddH₂O and afterwards the mixture was sterilized by autoclaving.

Recombinant GITRL protein: Recombinant human (rh)GITR Ligand/TNFSF18 (CHO-expressed) protein (25 μ g) was commercially obtained in freeze-dried form and reconstituted at 100 μ g/mL in sterile PBS containing 0.1% bovine serum albumin (BSA). Working solution aliquotes (50 μ g/ml) of recombinant GITRL were prepared and stored at -80°C.

Tris-Borate-EDTA (TBE) buffer: TBE buffer (10x) was prepared by mixing Tris (108 gr, 1.1 M final concentration), Boric acid (55 gr, 1.1 M final concentration), EDTA (7.5 gr, 0.03 M final concentration) in 800 ml ddH₂O, then pH was adjusted to 8.

EBC Lysis Buffer for protein extraction: Protease inhibitor cocktail (40 μ L) (PIC), EDTA (4 μ L, 0.005 M final concentration), Calyculin A (0.4 μ L, 0.05 μ M final concentration), NaF (16 μ L, 0.02 M final concentration), PMSF (2 μ L) and RIPA buffer (337,6 μ L) were mixed to obtain lysis buffer enough for preparing one lysate.

Table 3.1. EBC lysis buffer components and final concentration.

Components (for 10 lysis)	Volume	Final concentration
Protease inhibitor cocktail	400 μ L	10% v/v
EDTA (0.5 M)	40 μ L	1% v/v, 5 mM
Calyculin A (50 μ M)	4 μ L	0.1% v/v, 0.05 μ M
NaF (0.5 M)	160 μ L	4% v/v, 20 mM
PMSF	20 μ L	0.5% v/v
RIPA buffer	3376 μ L	

MTT solution: MTT powder was weighed as 5 mg/ml and dissolved in PBS.

Lysis buffer for MTT assay: Dimethylformamide (DMF) (100%) was diluted with ddH₂O to 45%. Sodium dodecyl sulfate (SDS) (23 gr, 0.8 M final concentration) was dissolved in 100 ml 45% DMF.

CFSE: CFSE powder (50 μ g) was dissolved in 18 μ l sterile DMSO, in order to obtain 5mM stock solution and aliquots were stored at -80°C.

3.3. Cell culture

Luminal (MCF-7, BT-474, SK-BR-3) and triple-negative basal-like (MDA-MB-231, HCC-38, MDA-MB-468) breast cancer cell lines were commercially obtained (ATCC, LGC Promochem, Rockville, MD, USA). These cell lines were grown in culture media containing 10% or 1% FBS (for serum reduction experiments), 1% L-glutamine and 1% penicillin-streptomycin. Depending on the cell type, DMEM low- or high-glucose or RPMI-1640 culture media were utilized (Table 3.2.).

Table 3.2. Culture media and subculture ratios for basal-like and luminal breast cancer cell lines

Cell line	Culture media	Sub-cultivation ratio
MDA-MB-231	DMEM	1:10
HCC38	RPMI-1640	1:2
MDA-MB-468	DMEM	1:5
MCF-7	DMEM	1:3
BT-474	DMEM	1:3
SK-BR-3	RPMI-1640	1:2

The cell lines were passaged when they reached approximately to 70-80% confluency. Firstly, the medium was aspirated and the cells were washed with 1x PBS to discard any remaining FBS. Then, the cells were treated with 10x Trypsin-EDTA (300 μ l for T25 flask, 600 μ l for T75 flask) and incubated for 3-4 minutes at 37°C. By gentle tapping, cells were lifted from flasks and they were suspended in 10 ml of appropriate complete culture media. The cells were kept in an incubator (Thermo Scientific, Hera Cell 150i, USA) at 37°C with 5% CO₂ and 96-98% humidity.

3.3.1. Cell counting

Suspended cells (10 μ l) were mixed with 0.4% trypan blue solution (10 μ l), then the mixture was transferred to the Fuchs-Rosenthal Counting Chamber (Hausser Scientific, USA) placing under the coverslip. The mixture was transferred via capillary action. Then, four out of sixteen squares divided by bold grids were chosen under a light microscope; and then, the cells falling inside of these squares were counted. Unstained cells were counted to determine the number of viable cells. The distance between the counting chamber and the coverslip is 0.1 mm, and the size of the chamber is 0.1 mm x 0.1 mm (celeromics, Fuchs-Rosenthal Chamber Formulae, UK). Moreover, the side of each sixteen square corresponds to 1 mm. Correspondingly, total cell count in 1 ml was determined with respect to the formula below (Formula 3.1).

$$\text{Area} = 1 \text{ mm} \times 1 \text{ mm} = 1 \text{ mm}^2$$

$$\text{Volume} = 1 \text{ mm}^2 \times 0.1 \text{ mm} = 0.1 \text{ mm}^3 \quad (3.1)$$

$$\text{Cell concentration} = \frac{\text{Total cell count} \times 10^4}{\text{Number of counted squares}} \times \text{Dilution factor}$$

3.4. Treatment with ionizing radiation

Depending on the experiment, the cells were seeded as 2×10^6 or 4×10^6 per T25 flask, in a culture media containing 10% FBS (complete medium) or 1% FBS (serum reduction). After seeding (24 hours), the cells were exposed to 5 Gy or 10 Gy

ionizing radiation with 6 MV X-ray photons at the Department of Radiation Oncology, Hacettepe University Cancer Institute, by an Elekta Synergy® Platform. Immediately after the radiation, the cells were transferred to the incubator for recovery incubation.

3.5. Determination of the amount of viable cells by MTT assay

HCC38 breast cancer cells were seeded into flat-bottom 96-well plates (6×10^4 or 3×10^4 cells/well) in 100 μ L complete RPMI-1640 media. After 16 hours of incubation at 37°C in 5% CO₂ incubator, media were aspirated from the wells, then control and 5, 20 or 80 ng/ml recombinant GITRL protein (rGITRL) in 100 μ L total volume was distributed into wells. In one experimental setup, the incubation was terminated after 72 hours. In another setup, following the initial 72 hours of incubation the cells were exposed to 5 Gy ionizing radiation; then, culture media with or without 5, 20 or 80 ng/ml rGITRL were refreshed. These cells were left for another round of 72 hours of incubation. The experimental setup is illustrated in Figure 3.1.

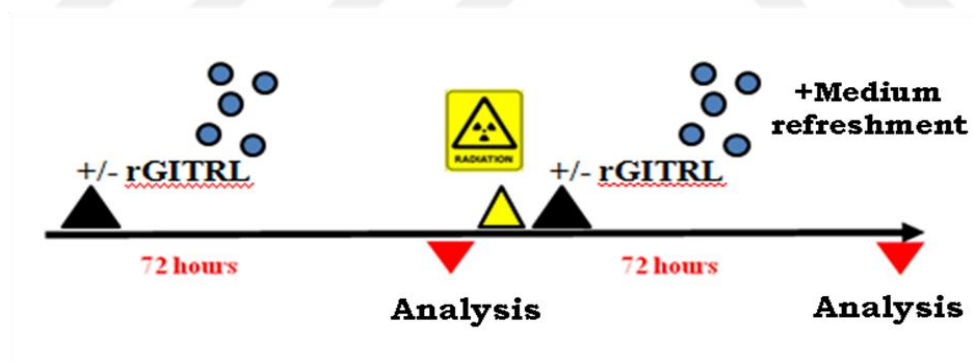


Figure 3.1. Experimental setup for determination of HCC38 cells' viability by MTT or flow cytometric viability assay with/without GITRL and ionizing radiation.

At the end of incubation periods, for measuring the amount of viable cells, 25 μ L MTT (5 mg/ml) was added into the wells. The plates were incubated at 37°C, % 5 CO₂ for 4 hours. At the end of incubation, 80 μ L DMF/SDS lysis solution was added into wells and followed by another incubation period at 37°C, for 12 hours. Optical density (OD) values were measured at 570 nm by spectrophotometric analysis

(Molecular Devices, Spectra Max Plus 384, Sunnyvale, California, USA). Results were calculated as by using the (Formula 3.2.)

Average OD from the sample treated with rGITRL*100/ Average OD from the control sample **(3.2.)**

3.6. Western Blot analysis

3.6.1. Lysate preparation and protein quantification:

Breast cancer cells (2×10^6 and 4×10^6 cells) treated with ionizing radiation (5 Gy and 10 Gy) as well as the control group (no ionizing radiation) was lysed with EBC lysis buffer. Briefly, 1 or 24 or 48 hours after the treatment with ionizing radiation, the flasks were kept on ice for 5 minutes. Then, culture media were aspirated with a pasteur pipette and the cells were washed twice with cold PBS. After PBS removal, 400 μ L lysis buffer was added into each T25 flask and the flasks were shaken on ice for 15 minutes with an orbital shaker (KS 260 Basic, IKA, Germany). The cells were scraped from culture flasks and lysed, with the aid of a cell scraper. Then, the flasks on ice were shaken again for 15 minutes. Scraping was carried out one more time, subsequently the cell lysates were collected into previously cooled 1.5 ml tubes. They were centrifuged (4°C) with a refrigerated centrifuge (Eppendorf Refrigerated Microcentrifuge, Model 5417R) at 12.500 rpm for 15 minutes. Supernatants were collected without disrupting pellets and protein lysates were stored at -80°C until further use.

Protein samples were quantified with colorimetric bicinchoninic acid assay (BCA assay) (Thermo Fisher Scientific, USA). RA reagent (200 μ L) was mixed with RB reagent (4 μ L) in (v:v, 50:1) ratio to prepare a master mix. With respect to protein sample number, a master mix comprising of the RA and RB reagents was prepared. The mixture was thoroughly inverted several times, until color alteration was observed. Standards (2 mg/ml, 1.5 mg/ml, 1 mg/ml, 0.75 mg/ml, 0.5 mg/ml, 0.25 mg/ml, 0.125 mg/ml, 0.025 mg/ml) were prepared in serial dilutions, and mixed with the BCA master mix to acquire a standard curve, in order to find the concentration of unknown proteins. In 96-well plate, 200 μ L RA and RB mixture was distributed to each well. After this, 25 μ L protein lysate sample whose OD value is unknown, as well as albumin standards with known concentration was added into the wells,

sequentially. Previously prepared EBC lysis buffer (25 μ L) and RA and RB mixture (200 μ L) were also added into separate wells for blank reading. The plate was shaken for 30 seconds for proper mixing of protein samples and BCA master mix. Then the plate was kept at 37°C incubator (WTC Binder) for 30 minutes. The absorbance at 562 nm, were measured by spectrophotometry (Molecular Devices, Spectra Max Plus 384, Sunnyvale, California, USA).

3.6.2. SDS-PAGE and membrane blotting

Protein lysates (50 μ g) was separated with sodium dodecyl sulfate polyacrylamide gel electrophoresis (SDS-PAGE). SDS mixture comprises of SDS, β -mercaptoethanol and glycerol. SDS mixture treated lysates were kept at 95°C for 5 minutes for denaturation (Dri-Block® Heaters DB-2D, Techne, Minneapolis, USA). For polyacrylamide gel, resolver solution (Section 3.2.) was prepared and 4500 μ l from the mixture was poured in between vertical electrophoresis glass plates with integrated spacers. Before the stacker gel preparation, for a straight interface between the resolver and stacker gel, ddH₂O was poured onto the interface. After resolver gel was polymerized, stacker solution (Section 3.2.) was prepared and filled to the top. Subsequently, plastic comb was inserted immediately and the gel was left for polymerization. SDS mixture-treated lysates were loaded onto the gel, with the aid of a sample loading guide to locate the wells. Equal amounts of protein were loaded into the wells. For tracing the separation of the bands, for determining approximate size of the proteins and observing the transfer of proteins from the gel onto the PVDF membrane, pre-stained protein ladder (4 μ l) was used as a marker.

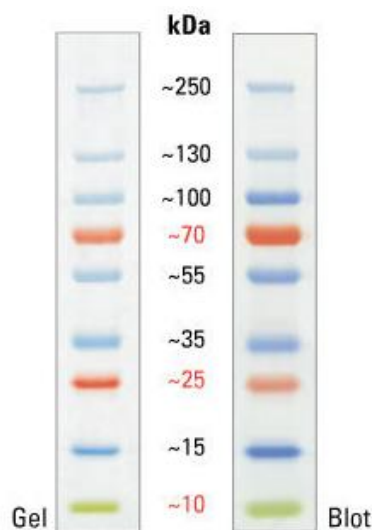


Figure 3.2. PageRuler™ Prestained Protein Ladder (10 kDa to 250 kDa) as a protein marker (Thermo Scientific, Rockford, USA).

The lysates were run at 50 V, for 250 minutes to detect β -actin protein; whereas they were run at 60 V, at 4°C room overnight for detection of ATM proteins. Subsequently, proteins were transferred to polyvinylidene difluoride membrane (PVDF) (Thermo Scientific, USA). When the electrophoresis was completed, the gel was gently separated from the glass plates soaked in ddH₂O.

The membrane was rinsed with methanol, in order to create pores for protein transfer. The PVDF membrane was taken out with a forceps from the methanol. Filter papers, PVDF membrane as well as the gel were shaken orbitally in 1x Transfer buffer (Section 3.2.). For semi-dry transfer, thick filter paper, western gel, PVDF membrane and again thick filter paper were stacked from top to the bottom in the given order. For wet transfer, foam pads, thin filter paper, western gel, PVDF membrane, thin filter paper and foam pads were stacked from anode to cathode in the given order, in gel holder cassettes. Then these cassettes were put into plate electrodes, in the Mini Trans-Blot® Cell system (BioRad, USA), which was completely filled with 1x Transfer buffer. Beta-actin was semi-dry transferred at 25 V for 30 minutes (Thermo Scientific Pierce, fast semi-dry blotter); whereas p-ATM and total ATM were transferred at 340 mA for 135 minutes with a Mini Trans-Blot® Cell system (BioRad, USA). The gel was transferred to the PVDF membrane with wet transfer to observe p-ATM and total ATM proteins.

3.6.3. Antibody incubations and chemiluminescence imaging

Membranes were blocked for one hour with 5% skimmed milk powder or 5% bovine serum albumin (BSA) dissolved in PBS-T buffer. Then, they were rinsed three-times in PBS-T and soaked in primary antibody solution in PBS-T. Purified Mouse anti-human phospho-ATM (S1981 Affymetrix eBioscience) primary antibody was diluted in PBS-T (1/1000). The membrane was kept with this antibody for overnight at 4°C. On the other hand, polyclonal anti- β -actin (D6A8, Cell Signaling) primary antibody was diluted in PBS-T (1/2500) and the membrane was incubated with it overnight at 4°C. Rabbit anti-human ATM mAb (D2E2 Cell Signaling Tech) was diluted in PBS-T (1/1000) and the membrane was treated with the antibody overnight at 4 °C. Antibodies not bound to membrane were removed with three times PBST washing. Ultimately, the membranes were incubated with horse radish peroxidase (HRP)-conjugated goat anti-mouse secondary antibody (1/2500 dilution, 1.5 hour at RT) or anti-rabbit polyclonal secondary antibody (1/2500 dilution, 1 hour at RT) (Dako, Glostrup, Denmark). Antibody binding was observed by preoxidation of ECL substrate (Thermo Scientific, USA). Optical densitometry analysis was carried out via a Kodak Gel Logic 1500 imaging system (Carestream Health, Rochester, New York, USA). Every phosphorylated ATM and total ATM optical density (OD) was normalized to corresponding β -actin values.

3.7. Flow cytometry

Expression of GITR and GITRL on the surface of the breast cancer cells was determined before or after ionizing radiation (5 Gy or 10 Gy). For flow cytometry analysis, breast cancer cells (2×10^6 cells/ flask) were collected with a cell-scraper from cell culture flasks and filtered through 40 μ m cell strainers (Corning, USA). Then, the cells were labeled with PE-conjugated anti-human GITRL antibody (Monoclonal Mouse IgG1, Clone #109101, R&D Systems, Minneapolis, USA) or APC-conjugated human GITR antibody (Monoclonal Mouse IgG1 Clone # 110416, R&D Systems, Minneapolis, USA). After unbound antibodies were removed by washing with cell wash (BD, USA), the samples were analyzed on a FACSAria II cell sorter (Becton-Dickinson, San Jose, CA, USA). The percentage of positively stained cells was evaluated in comparison to proper isotype control antibody staining

(PE or APC conjugated polyclonal mouse IgG1 isotype control). Where appropriate, mean fluorescence intensity (MFI) values were also obtained.

3.7.1. Flow cytometric cell proliferation analysis

After the breast cancer cells (HCC38) were counted with a hemocytometer (Fuchs-Rosenthal counting chamber, Hausser Scientific, Horsham, PA, USA), these cells were suspended in serum-free medium (1×10^6 cells/ml) in a 50 ml tube. Then, the cells were labeled with CFSE (final concentration, $1 \mu\text{M}$). After the sample was vortexed gently, the sample was put into previously heated (37°C) water bath (GFL, Burgwedel, Germany) and incubated for 15 minutes. The tube was filled to the brim with complete RPMI. Subsequently, it was incubated on ice for another 5 minutes. Following centrifugation (4°C) at 1800 rpm for 5 minutes, supernatant was discarded. This washing step was repeated one more time. Then, the cells were resuspended with complete RPMI-1640 and seeded into 6-well culture plates at 5×10^5 cells/well and incubated until they adhered to the culture plates. Next, they were treated with 5, 20 or 80 ng/ml of GITRL protein (R&D Systems, USA) in complete RPMI-1640 containing 1% or 10% FBS. After 72 hours, the cells were exposed to 5 Gy ionizing radiation and incubated for another 72 hours after the culture media containing the same concentrations of rGITRL were refreshed (Figure 3.1). When the incubation period was completed, the cells' proliferation was assessed with the dilution of CFSE intensity. The analyses were performed on a flow cytometer (FACSAria-II, Becton-Dickinson, San Jose, CA, USA). Every cell subpopulation with a decreased CFSE intensity is accepted as a division cycle (Formula 3.3.).

$$\text{Change in proliferation \%} = 100 - \left(\frac{\text{MFI from experimental group} - \text{MFI from control group}}{\text{MFI from control group}} \right) \times 100 \quad (3.3.)$$

3.7.2. Analysis of cell viability by flow cytometry

After the breast cancer cells were cultured in the presence of rGITRL (5, 20 or 80 ng/ml), they were incubated with $150 \mu\text{L}$ trypsin/EDTA for 4 minutes, then 3 ml of complete RPMI-1640 was added onto the cells and collected in flow tubes.

Then, these cells were filtered through cell strainers with 40 μm pores and centrifuged at 1800 rpm for 5 minutes, and supernatant was discarded. Cell Wash solution (100 μL) (BD, USA) was added into each flow tube, and the samples were mixed gently. DRAQ7 (1 μL , 300 $\mu\text{M}/\text{ml}$) cell viability tracer dye was added at room temperature. Then, the samples were incubated in dark for 5 minutes. Viable and dead cells were determined by flow cytometry analysis, where cells stained with DRAQ7 were indicating cell death. Analyses were carried out on a FACSAria II flow cytometer (Becton-Dickinson, San Jose, CA, USA).

3.8. Molecular techniques

3.8.1. RNA isolation

RNA isolation was carried out with QIAamp® RNA Blood Mini Kit (QIAGEN, Maryland, MD, USA). The cell culture medium of 2×10^6 breast cancer cells was discarded from the flasks and the cells were washed with 1x PBS. After PBS removal, 450 μL RLT Buffer containing 4.5 μL beta-mercaptoethanol (1% v/v) was added onto the cells. The flasks were vortexed for 2-3 minutes to detach and lyse the cells. Then, they were collected with a sterile pasteur pipette into 15 ml tubes and 450 μL 70% ethanol was added into the tubes. The resulting mixture (600 μL) was transferred to the QIAamp spin columns. After centrifugation of the columns at 10,000 rpm for 20 seconds (4°C), flow-through was discarded. The same procedure was repeated for the remaining samples until all of the lysate mixture was passed through the spin columns. Then, 700 μL RW1 Wash Buffer was added into the columns and centrifuged at 10,000 rpm for 20 seconds (4°C). Then, 500 μL Buffer-RPE, which was supplemented with absolute ethanol was added and the columns were centrifuged at 10,000 rpm for 20 seconds. This step was repeated by adding 500 μL Buffer-RPE and centrifugation at 13,000 rpm for 4 minutes (4°C). Then, the collection tubes were replaced with new ones and the columns were centrifuged at 13,000 rpm for 1 minutes to dry the filter. Then, the columns were placed on diethyl pyrocarbonate (DEPC) treated 1.5 ml tubes. RNA was eluted with 30 μL DNase/RNase free ddH₂O by pipetting it directly onto the column membranes and centrifuging them at 10,000 rpm for 1 minute. The total RNA samples were stored at -80°C.

3.8.2. Removal of DNA from RNA samples

DNase treatment was carried out with RNA Clean&Concentrator kit (Zymo, Irvine, CA, USA). Briefly, a mixture containing the components (Table 3.3.) was prepared in DEPC-treated 1.5 ml tubes. This mixture was incubated at 37°C water bath for 40 minutes. Two volumes of RNA Binding Buffer were added to the RNA samples and mixed gently. Then, 150 µL absolute ethanol was added to the mixture before it was transferred into the Zymo-Spin™ IC columns. They were centrifuged at 13.000 rpm for 1 minute. Then, the flow-through in the collection tubes was discarded. RNA Prep Buffer (400 µL) was added to the columns and centrifuged at 13.000 rpm for 1 minute. The flow-through in the collection tubes was discarded again. RNA Wash Buffer (800 µL) was added to the columns and centrifuged at 13.000 rpm for 30 seconds. After flow through-was discarded, the previous wash step was repeated with 400 µL RNA Wash Buffer at 13.000 rpm for 30 seconds. Zymo-Spin™ IC columns were centrifuged at 13.000 rpm for 2 minutes for drying the membrane. Then, they were placed on DEPC-treated 1.5 ml tubes, 20 µL RNase/DNase-free ddH₂O was added directly onto the column matrix and after 1 minute incubation, the columns were centrifuged at 11.000rpm for 30 seconds. Eluted RNA samples were stored at -80°C until they were used. Any leftover DNA was checked with β-actin PCR wherein the DNA samples were directly used (Section 3.8.5). This protocol was repeated until all DNA was wiped out.

Table 3.3. DNase treatment components and their working concentrations

Reaction component	Volume	Final concentration
RNA sample (<5ug)	20 µL	
10X DNaseI Buffer	5 µL	1x
RNase free DNase	4.5 µL	
RNase-DNase free ddH₂O	20 µL	
Total volume	50 µL	

3.8.3. Quantitation of RNA

Concentration and quality of isolated RNA were determined via optical density (OD) measurements at 260 nm and 280 nm wavelengths spectrophotometrically (NanoDrop ND-1000, USA). RNA quality was judged with $A_{260/280}$ and $A_{260/230}$ ratios. Accepted range regarding purity was 1.8 to 2.0 for both absorbance ratios.

3.8.4. Reverse transcription

The reverse transcription reaction was performed to convert mRNA to complementary DNA (cDNA). cDNA synthesis was carried out with Fermentas RevertAid First Strand cDNA Synthesis Kit (Fermentas, Lithuania). The reaction was performed on a thermal cycler (Thermo Scientific, Arktik Thermal Cycler, USA). The procedure was done according to the manufacturer's instructions (Table 3.4). Resulting cDNA samples were kept at -20°C .

Table 3.4. Components and steps of reverse transcription reaction from RNA samples to prepare cDNA.

Reaction Component	Volume	Final concentration
Oligo (dT)₁₈ primer (0.5 µg/ µL)	1 µL	0.025 µg/ µL
RNA sample	varies depending on conc.	1 µg
ddH₂O	to 11 µL with RNA	
Incubation	At 65°C for 5 minutes	
5x reaction buffer	4 µL	1x
Ribonuclease inhibitor (20 U/µL)	1 µL	1 U/µL
dNTP mix (10 mM)	2 µL	1 mM
Reverse transcriptase (200 U/ µL)	1 µL	10 U/ µL
Total volume	20 µL	
Incubation	At 42°C for 60 minutes At 70°C for 10 minutes	

3.8.5. Polymerase chain reaction (PCR)

PCRs were performed to amplify GITR, GITRL, ATM and β -actin (as a housekeeping control) transcripts that were converted to cDNA (Section 3.8.4). Forward and reverse primer oligonucleotides specifically designed to bound these transcripts are listed in Table 3.5. dNTP mixture stock (10 mM) was diluted to 2 mM before use. For negative control, ddH₂O instead of cDNA was used in the reaction mixture. The components of PCR are listed in Table 3.6. By mixing components without cDNA, a master mix was prepared and 49 μ l of the mixture was distributed into PCR microtubes. Then, 1 μ l of cDNA was added and mixed by pipetting, gently.

Table 3.5. Forward and Reverse Primers used for PCR reactions.

Gene name	Forward primer	Reverse primer
ATM	5'-CATTGCACTTCCGTCAGCAA	5'-CAAGGCTGCGCTTACACATC
GITRL	5'-AGAGATCATCCTGGAAGCTGTGG	5'-AGCCATACAGGGCTCCTTAGC
GITR	5'-TCCTGCTTGGGACGGGAACGGA	5'-ACACATGCAGTCCCACTCGGA
β -actin	5'-CTGGAACGGTGAAGGTGACA	5'-AAGGGACTTCCTGTAACAATGCA

Table 3.6. Components and their final concentration in PCR reactions.

Components	Volume	Final concentration
DreamTaq Buffer (10x)	5 μ L	1x
dNTP (2 mM)	5 μ L	0.2 mM
ddH₂O	36.8 μ L	
DreamTaq DNA polymerase (5U/ μL)	0.2 μ L	0.02 U/ μ L
Forward-primer (5 μM)	1 μ L	0.1 μ M
Reverse-primer (5 μM)	1 μ L	0.1 μ M
cDNA (1μg)	1 μ L	0.02 μ g/ μ l
Total volume	50 μ L	

PCR tubes were placed in a thermal cycler (Arktik Thermal Cycler, Thermo Scientific, USA) and after 35 cycle amplification by using the conditions listed in Table 3.7 below, PCR reactions were completed. Products were kept at +4°C until electrophoresis.

Table 3.7. Steps,time and temperatures of a PCR reaction.

Step	Time	Temperature
Pre-denaturation	5 minutes	95°C
Denaturation	30 seconds	95°C
Annealing	30 seconds	60°C
Extension	30 seconds	72°C
Final extension	10 minutes	72°C

} 35 cycles

3.8.6. Semi-quantitative real-time PCR

Expression levels of GTR, GTRL and ATM genes were examined by real-time reverse transcriptase PCR (RT-PCR). β -actin gene expression level was used as housekeeping control in order to standardize sample inputs. Data obtained from the samples exposed to ionizing radiation was normalized to that of obtained from control untreated cells. Real-time PCR reactions were performed by using SsoAdvanced™ Universal SYBR® Green Supermix (BioRad, California, USA) on a Bio-Rad® CFX Connect Real-time thermal cycler. The difference between the samples for a specific gene was semi-quantitatively assessed by $2^{-\Delta\Delta C_t}$ method using the (Formula 3.4.).

$$(\text{Ct Exp target gene} - \text{Ct Control target gene}) - (\text{Ct Exp housekeeping gene} - \text{Ct Control housekeeping gene}) \quad (3.4.)$$

In addition, the RT-PCR products were also run on 2% agarose gel electrophoresis (Section 3.8.7) and high resolution melting curve (HRM) analysis were done to verify product purity.

3.8.7. Agarose gel electrophoresis

Agarose (4 gr) was put in an erlenmeyer flask containing 200 ml 1x TBE buffer to prepare 2% agarose gel solution, then the mixture was heated in a microwave oven until brief boil for complete dissolving of agarose. After a partial-cooling period, ethidium bromide (10 mg/ml, 10 μ l) was added into the solution and

mixed, and poured into the gel tray. A comb was placed into the gel to form sample wells. After it was completely solidified, the comb was removed and gel tray was inserted into electrophoresis tank to be covered with 1x TBE buffer. Then, 20 μL of PCR products were mixed with 4 μL 6x DNA loading dye and loaded into the wells created previously by a comb. DNA size marker was loaded into one of the wells. To prepare the DNA size marker (50 bp or 1 kb), 1 μL of 6x loading dye, 1 μL DNA ladder and 4 μL ddH₂O were mixed thoroughly. Electrophoresis was run at 120 V and the bands were observed and photographed under UV light with a Kodak Gel Logic 1500 Molecular Imaging System (Carestream Health, Rochester, NY, USA)

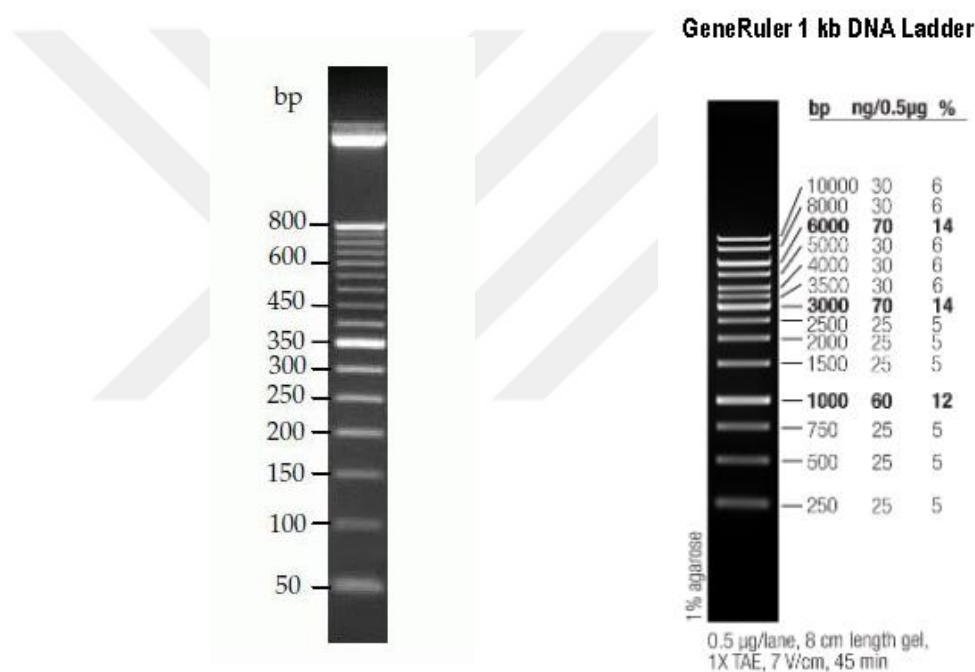


Figure 3.3. Molecular weights of 50 bp and 1kb DNA ladder.

3.9. Molecular cloning

3.9.1. Cloning of human ATM gene promoter into pGL3-Basic vector

ATM promoter sequence was amplified with designed primers, forward 5' GAGTGAGGTACCCGTATTGCGTGGAGGATGGAG 3' and reverse 5' CTCACTAGATCTCAGCGACTTAGCGTTTGCGG 3'. These primers contained regions (underlined) which are recognized and digested by KpnI and BglII restriction

enymes. To amplify ATM promoter region, a polymerase chain reaction (PCR) was set up. PCR conditions were as follows: a pre-denaturation step for 5 minutes at 95°C followed by 38 cycles of denaturation for 30 seconds at 95°C, annealing for 30 seconds at 60°C, and final extension for 10 minutes at 72°C. PCR products were separated on 2% agarose gel electrophoresis and visualized under UV light. PCR products were purified with AbsoGene Gel/PCR purification Kit, before the restriction digestion. Briefly, 6 volumes from Solution A were added to PCR products, to discard primers, dNTPs, polymerase, buffers and any remaining contaminants. Then, samples were mixed by vortexing. Absolute ethanol (200 µl) was added and samples were mixed thoroughly. Then, the mixture was transferred to the spin columns inserted in the collection tubes. Samples were centrifuged at 8000 rpm for 1 minute and flow-through was removed. Solution WA (500 µl) was added into spin columns and samples were centrifuged at 10.000xg for 1 minute. After flow-through was discarded, the spin columns were reinserted into new collection tubes to centrifuge samples at 14.000 rpm for 30 seconds. Afterwards, spin columns were transferred into 1.5 ml tubes and Solution E (35 µl) was added to the middle of spin columns without touching. After 3 minutes incubation at room temperature, samples were centrifuged at 14.000 rpm for 1 minute to obtain purified PCR product. If the DNA was isolated from the agarose gel, DNA band was cut from the agarose gel, under the UV light. Then gel pieces in a tube were weighed and 4 volumes of Solution A was added into them. Gel pieces with Solution A were mixed via pulse-vortexing at least 20 times. They were incubated at 60°C until the gel piece was totally melted. Subsequently, gel modifier (15 µl) was added and samples were mixed at least 20 times, by pulse-vortexing. The mixtures were transferred to the spin columns.

Samples were centrifuged at 10.000xg for 1 minute and flow-through was discarded. Solution WA (500 µl) was added into spin columns and samples were centrifuged at 10.000xg for 1 minute. After flow-through was removed, the spin columns were reinserted into new collection tubes to centrifuge them at 14.000 rpm for 30 seconds. Afterwards, spin columns were transferred into 1.5 ml tubes and Solution E or ddH₂O (35 µl) was added to the middle of spin columns without

touching. After 3 minutes incubation at room temperature, samples were centrifuged at 14,000 rpm for 1 minute to acquire purified DNA.

The restriction digestion and purification steps were performed sequentially as buffers for restriction enzymes (CutSmart Buffer for KpnI-HF and NEBuffer 3.1 for BglII) are not compatible with each other and the enzymes are not suitable for heat inactivation. Then, by using KpnI-HF (New England BioLabs Inc.), both amplified ATM promoter region as well as pGL3-Basic-Luciferase plasmid were digested overnight at 37 °C, on an orbital shaker. Subsequently, KpnI-HF digested products were purified with AbsoGene Gel/PCR purification Kit and digested with BglII enzyme at 37 °C on an orbital shaker overnight. Afterwards, double-digested ATM PCR product (called “*insert DNA*”) and double-digested pGL3-Basic (vector DNA) were purified by using AbsoGene Gel/PCR purification Kit.

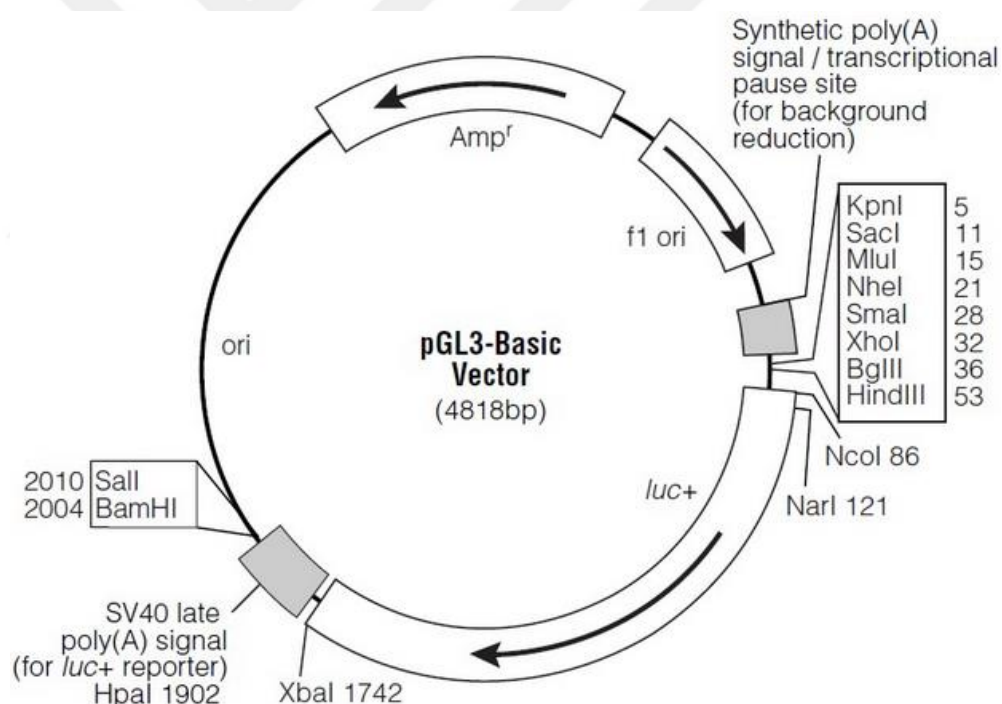


Figure 3.4. pGL3-Basic Vector Map (Promega, Madison, Wisconsin, USA).

Table 3.8. Components and working concentrations of ATM PCR product digestion with KpnI restriction endonuclease for cloning.

Components	Volume	Final concentration
ATM PCR product (insert) (180.6 ng/ μL)	4 μ L	14.448 ng/ μ L
10x restriction enzyme CutSmart® NEBuffer	5 μ L	1x
KpnI-HF restriction enzyme (20.000 units/ml)	1 μ L	0.4 units/ μ L
ddH₂O	40 μ L	
Total volume	50 μ L	

Table 3.9. Components and working concentrations of KpnI digested ATM PCR product digestion with BglII restriction endonuclease for cloning.

Components	Volume	Final concentration
KpnI digested-purified ATM promoter PCR product (insert) (101.6 ng/ μL)	7 μ L	14.224 ng/ μ L
10x restriction enzyme NEBuffer 3.1	5 μ L	1x
BglII restriction enzyme (10.000 units/ml)	1 μ L	0.2 units/ μ L
ddH₂O	37 μ L	
Total volume	50 μ L	

Table 3.10. Components and working concentrations of pGL3 Basic vector digestion with KpnI restriction endonuclease for cloning.

Components	Volume	Final concentration
pGL3-Basic (vector) (435.41 ng/ μL)	1.5 μ L	13.06 ng/ μ L
10x restriction enzyme CutSmart® NEBuffer	5 μ L	1x
KpnI-HF restriction enzyme (20.000 units/ml)	1.5 μ L	0.6 units/ μ L
ddH₂O	42 μ L	
Total volume	50 μ L	

Table 3.11. Components and working concentrations of KpnI digested pGL3 basic vector digestion with BglII restriction endonuclease for cloning.

Components	Volume	Final concentration
KpnI digested-purified pGL3 Basic (vector) (65 ng/ μL)	10 μ L	13 ng/ μ L
10x restriction enzyme NEBuffer 3.1	5 μ L	1x
BglII restriction enzyme (10.000 units/ml)	1.5 μ L	0.3 units/ μ L
ddH₂O	33.5 μ L	
Total volume	50 μ L	

After sequential digestion and purification (with AbsoGene Gel/PCR purification kit), double digested pGL3-Basic vector was purified from the gel to exclude uncut and improperly cut DNA. The gel was cut under UV light and the slice was put in 1.5 ml tubes comprising of 4 volumes of Solution A. By using 2 μ L T4 DNA ligase buffer (1x) and T4 DNA ligase enzyme (20 U/ μ L) (New England BioLabs, Inc.), pGL3-Basic and ATM promoter region were ligated to each other, at 1:3 vector to insert ratio (Table 3.12).

Table 3.12. Components for pGL3-Basic and ATM promoter region ligation reaction

Components	Volume	Final concentration
T4 DNA Ligase Buffer (10x)	2 μ L	1x
Vector DNA (4787 bp), 15.95 ng/ μL	3.1 μ L	Total 50 ng (2.5 ng/ μ L)
Insert DNA (900 bp), 65.5 ng/ μL	0.5 μ L	Total 30 ng (1.64 ng/ μ L)
Nuclease free ddH₂O	13.4 μ L	
T4 DNA Ligase (400 units/ μL)	1 μ L	20U/ μ L
Total volume	20 μ L	

The ligation reaction was incubated at room temperature for 15 minutes. Heat inactivation was carried out at 65°C for 10 minutes. The resulting recombinant plasmid products were heat-shock transformed into chemically competent *E. Coli* (NEB® 5- α Competent *E. coli* (New England BioLabs, Ipswich, Massachusetts, USA). For transformation, frozen competent *E. coli* cell stock was thawed on ice for 10 minutes. Then, plasmid DNA (1 pg- 100 ng) was gently added onto the cells. The

plasmid DNA and competent bacteria mixture was flicked gently 4 to 5 times. Then, the mixture was incubated on ice for 30 minutes. Cells were heat-shock transformed at 42°C for 30 seconds in a dry-block and placed on ice for 5 minutes. SOC medium (950 µl) was added onto the mixture and the tube was shaken at 37°C for 60 minutes for bacterial growth. For transformant selection, LB agar plates supplemented with Ampicillin (100 µg/ml) were warmed to 37°C before spreading the transformed bacteria. Following an overnight incubation at 37°C, transformed colonies were picked with a sterile loop and inoculated to 15 ml falcon tubes containing 3ml ampicillin (100 µg/ml) enriched LB broths. After 16-18 hours of incubation at 37°C, plasmids were isolated from cells via MiniPrep (Wizard® Plus Minipreps DNA Purification Sys, Promega) as described in Section 3.9.2. Afterwards, isolated plasmids were re-cut with KpnI restriction enzyme and digests were resolved with agarose gel electrophoresis and visualized under UV light.

3.9.2 MiniPrep Plasmid Isolation

Plasmid isolation from the transformed bacteria was carried out with Wizard® Plus Minipreps DNA Purification System (Promega, Madison, Wisconsin, USA). Briefly, 3 ml of bacteria culture was transferred into 1.5ml tubes. Samples were centrifuged at 10,000g for 2 minutes. After supernatant was removed, same procedure was repeated for the remaining sample, until all bacteria were pelleted. The tubes were drained for any remaining broth from the bacteria pellet. Then, 200 µL Resuspension Solution was added into all samples and by gentle pipetting, the pellets were resuspended. Cell Lysis Solution (200 µL) was added and the tubes were inverted 4 or 5 times until turbidity disappeared. Neutralization Solution (200 µL) was added and the tubes were inverted 4 times. Lysates were centrifuged at 10,000g for 5-10 minutes. Wizard® Minicolumns were inserted into new 1.5 ml tubes. Syringe barrels (2 ml) without pistons were assembled to the openings of Minicolumns. Resin solution (1 ml) was pipetted into each syringe barrel-Mini column assembly. Then, the lysates were added onto the resin. By inserting the pistons, the resin-lysate mixtures were pushed through the Minicolumn membranes. When all of the samples were completely passed through the Minicolumns, the barrel and piston were removed gently. Then, new barrels and Minicolumns were

reassembled and 2 ml Wash Solution (supplemented with ethanol) was added into each barrel. The Wash Solution was pushed through the Minicolumns. After the syringes were discarded, the Minicolumns were placed on 1.5 ml tubes. To dry the Minicolumn membranes, they were centrifuged at 10.000g for 2 minutes. Then, they were transferred to 1.5 ml tubes and 50 μ L DNase&RNase-free ddH₂O was added onto the Minicolumns and incubated for at least 1 minute. Following centrifugation at 10.000xg for 20 seconds, plasmid DNA was eluted. The plasmid DNA was quantified and kept at -20°C.

3.9.3 Electroporation

Electroporation studies were performed at Ege University, Medical Faculty Department of Pharmacology. Neon® Transfection Device (Thermo Fisher Scientific, Waltham, Massachusetts, USA) and Neon™ Transfection System 10 μ L Kit was used in these experiments.

The culture media were aspirated from the breast cancer cell culture plates and the cells were washed with 1x PBS. The cells were detached from the culture plates with Trypsin/EDTA. After cell counting, they were centrifuged at 1000 rpm for 5 minutes at room temperature. Following the supernatant removal with an aspirator, PBS (4 ml) was added onto the cells, mixed gently and centrifuged for washing. After PBS supernatant was discarded, the cell pellet was dissolved in *Resuspension Buffer R* (Invitrogen, Carlsbad, California, USA). Electroporation was performed with 10 μ L Neon® Tips and for every electroporation reaction 10 μ L *Resuspension Buffer R* was used. Firstly, for every electroporation reaction 500 ng of plasmid was transferred to a 1.5 ml tube, subsequently the cells that were suspended in the resuspension buffer was added on the top of the plasmid solution. Then, tubes were flipped to mix. Neon® Tube was filled with 3ml *Buffer E* and electroporation was performed in Neon® Tips specialized with gold plated electrode. Optimization experiments for MDA-MB-231, HCC38 and MDA-MB-468 were carried out in 24-well plates. To clarify, 1×10^5 cells/well were transfected with pCMV6-AC-GFP plasmid (0.5 μ g) (OriGene, Rockville, Maryland, USA) using 10 μ l Neon® Tips. Following the electroporation, the cells were kept in complete media with 20% FBS and L-glutamine without antibiotics for 24 hours in an 37°C incubator. Transfection

efficiency was measured by counting pCMV6-GFP plasmid transfected cells under fluorescence microscope (IX71, Olympus) compared to untransfected cells.

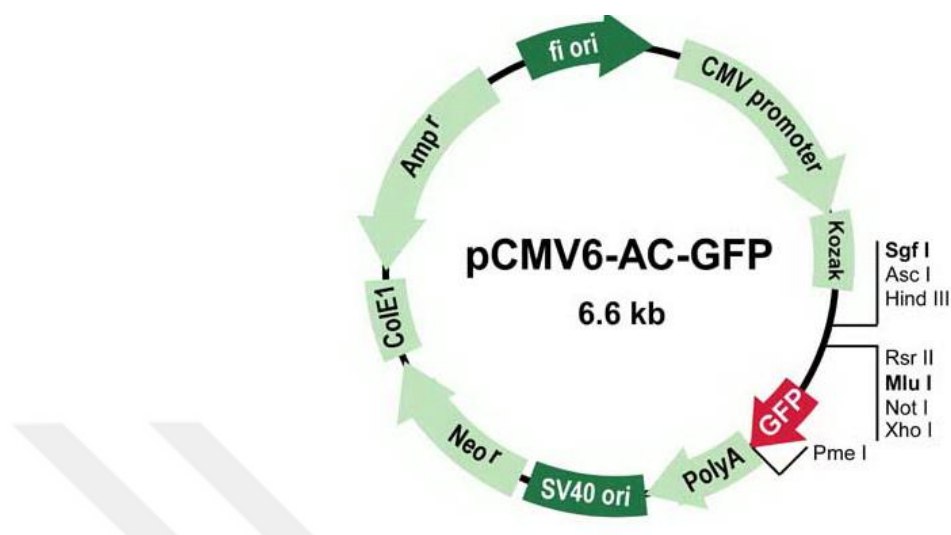


Figure 3.5. pCMV6-AC-GFP Vector Map (OriGene, Rockville, Maryland, USA).

Table 3.13. Optimal electroporation conditions (Voltage, Pulse width, Pulse number) for MDA-MB-231, HCC-38 and MDA-MB-468 breast cancer cell lines.

Cell line	Voltage (V)	Pulse width (ms)	Pulse number
MDA-MB-231	1100 V	20 ms	3 pulses
HCC-38	1100 V	20 ms	2 pulses
MDA-MB-468	1300 V or 1400 V	20 ms or 20 ms	3 pulses or 2 pulses

3.9.4. Luciferase reporter assay

Breast cancer cells were co-transfected with pATM-GL3 reporter and pRL-TK-Renilla control plasmid; pGL3 Basic and pRL-TK control plasmid; pGL3 Promoter and pRL-TK-Renilla vectors simultaneously and separately (Figure 3.4, 3.6 and 3.7). pRL-TK-Renilla vector has been used to quantify the success of gene transfer and expression whereas pGL3-Promoter vector contains a promiscuous promoter that serves as a positive control.

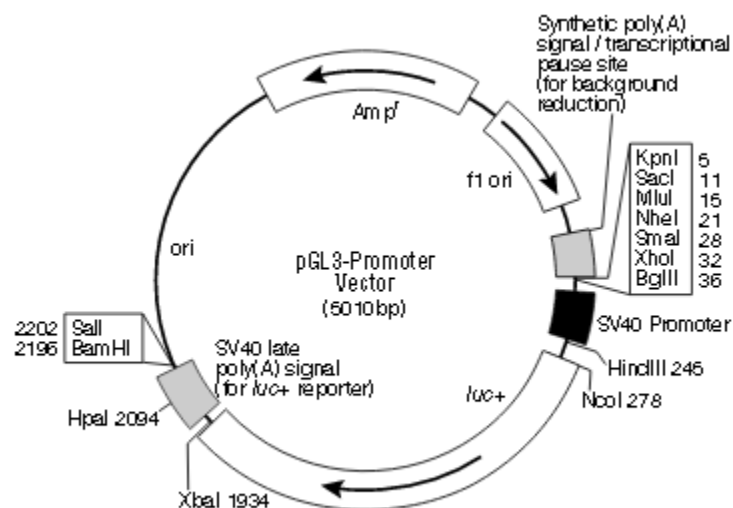


Figure 3.6. pGL3-Promoter Vector Map (Promega, Madison, Wisconsin, USA).

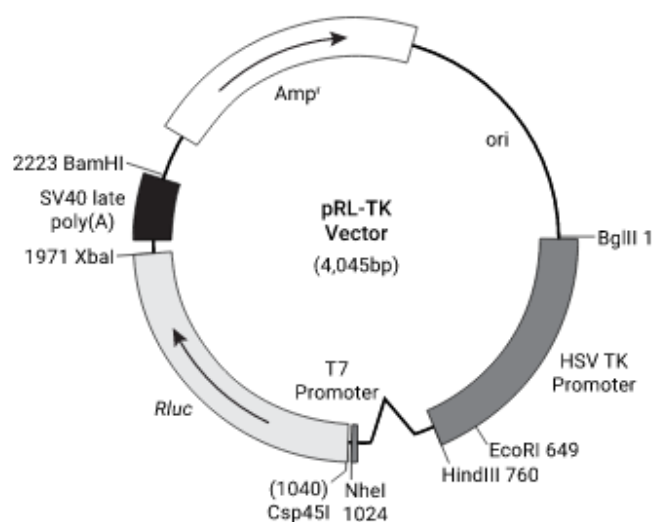


Figure 3.7. pRL-TK Vector Map (Promega, Madison, Wisconsin, USA).

Table 3.14. Amount of plasmids used in Luciferase assay transfections experimental design.

Co-transfection	Control plasmid (25 ng)	Reporter plasmid (475 ng)
1	pRL-TK	pGL3 Basic (empty vector)
2	pRL-TK	pAMT-GL3
3	pRL-TK	pGL3 promoter

After transfection (24 h), the cells were exposed to 5 Gy ionizing radiation. The cells that were not exposed to radiation were used as a control group. Then, protein lysates were collected by treating cells with 100 μ L, 1x Passive Lysis Buffer (PLB) per well of 24-well culture plates. Luciferase assay was measured with Dual-Luciferase® Reporter Assay System (Promega, Madison, Wisconsin, USA). Firefly luciferase signal was measured with the addition of 100 μ L Luciferase Assay Reagent II (LARII). After luminescence was measured, the reaction was ceased with 100 μ L Stop & Glo® Reagent and Renilla Luciferase measurement was carried out concomitantly (Thermo Scientific Varioskan® Flash,) and for every sample firefly luciferase activity was normalized to Renilla Luciferase activity. Results were reported as relative light unit (RLU) (Formula 3.5).

$$\text{Relative light unit (RLU)} = \frac{\text{RLU from Firefly luciferase}}{\text{RLU from Renilla luciferase}} \quad (3.5)$$

3.10. Statistical Analysis

All data were obtained from at least three independent experiments. Student's paired or unpaired t-test or ANOVA and Chi-square tests were used to show the statistical differences. When P values were found as ≤ 0.05 , the differences were accepted as statistically significant. Throughout these statistical analysis, standard deviation (SD) or standard error of the mean (SEM) were used.

4. RESULTS

4.1. Analysis of ATM activity in basal-like breast cancer cell lines

4.1.1 ATM expression and phosphorylation in basal-like breast cancer cells

In the basal-like breast cancer cell lines (MDA-MB-231, HCC-38, and MDA-MB-468), ATM levels and induction of ATM phosphorylation in response to 5 Gy and 10 Gy ionizing radiation were analyzed. All breast cancer cell lines had a minimal basal p-ATM level; nevertheless, showed a distinctive increase in active p-ATM (S1981) levels when analyzed 1-hour after the treatment with ionizing radiation (Figure 4.1A and C). The 5 Gy ionizing radiation was enough to induce a prominent ATM phosphorylation upon whereas, for MDA-MB-231 cell line, 10 Gy was much effective to induce a significant increase in ATM phosphorylation (Figure 4.1A and C). A trend of increase in pATM/ β -actin densitometric ratios, right along with the increased radiation dose was observed (Figure 4.1C). Since 5 Gy irradiation was active in inducing p-ATM, this radiation dose was selected to be used in further experiments.

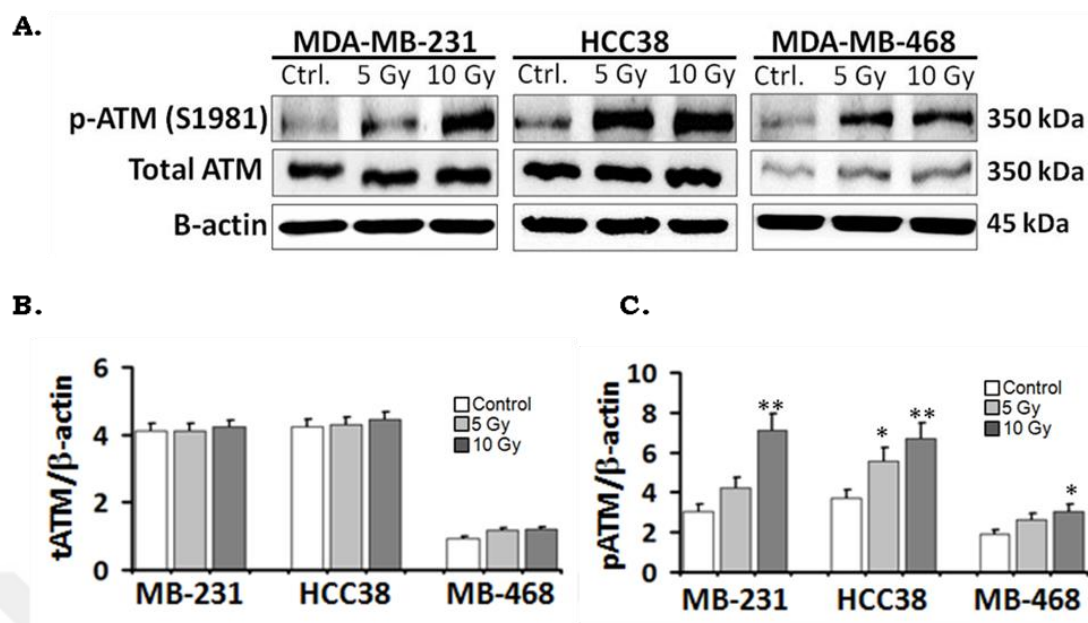


Figure 4.1 Basal-like breast cancer cell lines show increased ATM phosphorylation at 5 Gy ionizing radiation. **A)** MDA-MB-231, HCC38, and MDA-MB-468 breast cancer cell lines were exposed to 5 Gy and 10 Gy ionizing radiation, control group (Ctrl.) received no ionizing radiation. Cell lysates were prepared 1 hour after ionizing radiation and analyses were performed with Western Blot. Bands are representative of three independent experiments from cells treated on separate days. The expression levels of **(A)** total ATM (tATM) and **(B)** phospho-ATM (p-ATM, S1981) was semi-quantitatively analyzed by calculating the ratio of their optical density (OD) values relative to that of β -actin. (* $P \leq 0.05$, ** $P \leq 0.01$; MB-231, MDA-MB-231; MB-468, MDA-MB-468)

When total ATM levels were examined, all basal-like breast cancer cell lines show no qualitatively significant change with ionizing radiation. MDA-MB-231 and HCC38 cell lines which are of “the basal type B” showed higher levels of total ATM protein than that of “basal type A” MDA-MB-468 (Figure 4.1A and B).

4.1.2 The change in ATM protein expression in response to X-radiation

In order to determine if ATM expression was affected long after the ionizing radiation treatment in basal-like breast cancer cells, both mRNA and protein expression levels were evaluated 24 and/or 48 hours after 5 Gy X-irradiation. Since ATM expression regulation has been reported to depend on the presence of serum, the cells were also maintained in culture media with reduced serum (1%). When the

mRNA levels of ATM were analyzed, no significant change between the control and the 5 Gy irradiated cells was observed (Table 4.1). For MDA-MB-231 cells, a slight reduction was evidenced both in complete and reduced serum culture conditions. Non-significant fluctuations were observed in ATM mRNA levels in other cell lines. Therefore, X-irradiation only had a slight influence on ATM expression in the basal-like breast cancer cell lines studied. Furthermore, there was no discrepancy regarding ATM expression levels in normal serum culture conditions, when basal-like breast cancer cell lines (MDA-MB-231, HCC38, and MDA-MB-468) and luminal type breast cancer cell lines (MCF-7, BT-474, and SK-BR-3) were compared (Table 4.2).

Table 4.1. $2^{-\Delta\Delta C_t}$ values for ATM expression in serum deprivation (1% FBS) and in complete media (10% FBS) conditions, 24 hours after irradiation. (MB231, MDA-MB-231; MB-468, MDA-MB-468). Analyses were performed with relative quantitative real-time RT-PCR.

Serum concentration in culture	MDA-MB-231		HCC38		MDA-MB-468	
	10%	1%	10%	1%	10%	1%
Control	1	1	1	1	1	1
5 Gy	0.872212	0.6598	1.62160	0.82359	0.82	2.54
10 Gy	0.985532		1.39448		1.23	

Table 4.2. ATM/ β -actin ratios for ATM expression in basal-like and luminal breast cancer cell lines were calculated by using Ct values obtained with relative quantitative real-time RT-PCR. (MB231, MDA-MB-231; MB-468, MDA-MB-468).

	<u>ATM/β-actin</u>
MB-231	1,80082
HCC38	1,74275
MB-468	1,82829
MCF-7	1,65742
BT-474	1,77514
SK-BR-3	1,66749

ATM protein levels were assayed 24 and 48 hours post-ionizing radiation. All breast cancer cell lines showed various extents of increase in ATM levels especially 48h post-ionizing radiation. MDA-MB-231 cell line showed the most notable increase in ATM levels, whereas HCC38 and MDA-MB-468 cell lines showed minimal increment for ATM protein.

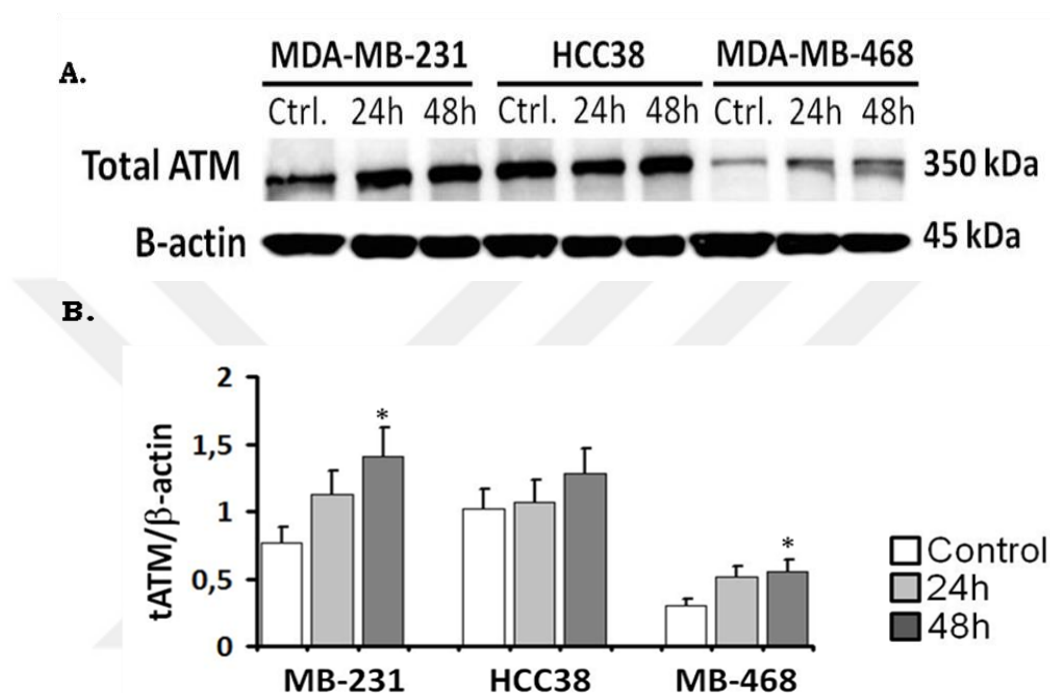


Figure 4.2 Total ATM protein levels in basal-like breast cancer cell lines 24h and 48h post-X-irradiation. MDA-MB-231, HCC38 and MDA-MB-468 breast cancer cell lines were exposed to 5 Gy ionizing radiation, control group (Ctrl.) received no ionizing radiation. Cell lysates were prepared 24 and 48 hours after ionizing radiation and analyses were performed with Western Blot. **A)** Bands are representative of three independent experiments from cells treated on separate days. **B)** The expression levels of total ATM were semi-quantitatively analyzed by calculating the ratio of their optical density (OD) values relative to that of β -actin. (* $P \leq 0.05$, ** $P \leq 0.01$; MB-231, MDA-MB-231; MB-468, MDA-MB-468)

4.1.3 Cloning of ATM promoter into pGL3-Basic vector

The primer oligonucleotides designed to amplify DNA insert for cloning of ATM gene promoter region and to carry restriction sites for *KpnI* and *BglII* endonucleases were successfully used in the PCRs. Following optimization of the reactions, ATM promoter bands localized between 750 bp and 1000 bp, which was consistent with the expected 913 bp ATM amplicon size, were obtained (Figure 4.3.).

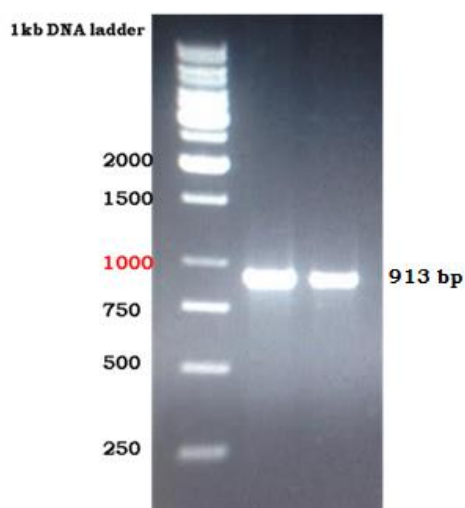


Figure 4.3. ATM promoter region (-860, +53) to be used processed as insert DNA was amplified with PCR. In agarose gel electrophoresis, DNA ladder (1kb) was run in the first lane whereas ATM PCR products can be seen in the other two lanes.

Following sequential endonuclease digestion and purification steps of amplified ATM promoter region (insert DNA) and pGL3-Basic vector, ligation reaction and heat-shock transformation into competent bacteria were performed. The ampicillin resistant colonies emerged on LB agar plates (Figure 4.4). Although the negative control (comprised of ddH₂O instead of insert DNA) had background colony formation (which includes uncut and self-ligated plasmids) (Figure 4.4A), the plates containing ATM promoter insert ligation reaction displayed numerous colonies (Figure 4.4 B).

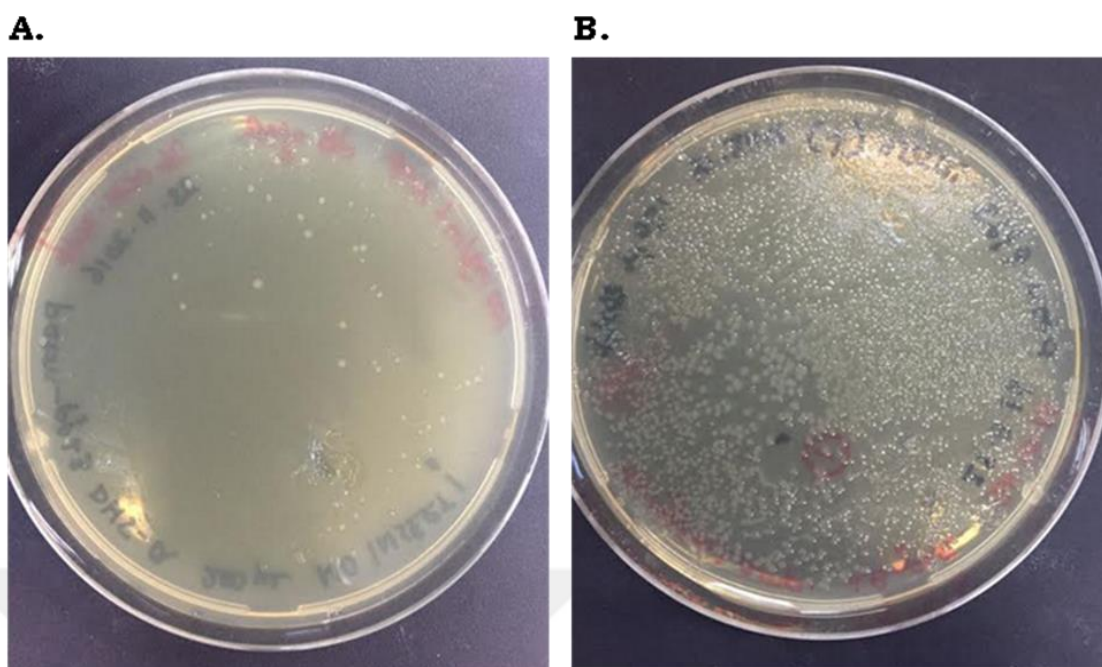


Figure 4.4. The ampicillin resistant *E. coli* colonies following heat-shock transformation for the cloning of ATM promoter into pGL3-Basic vector. Following ligation reaction between the vector and ATM promoter insert DNA at 1:3 ratio (for the negative control dH₂O was used instead of insert DNA), heat-shock transformation into competent DH5- α *E. coli* strain was done and the bacteria were spread onto LB agar plates supplemented with ampicillin. Colony formation was observed approximately after 18 hours. A) The negative control plate showed minimal number of colonies as a background, B) The agar plate had numerous colonies potentially containing pGL3-Basic vector ligated to the insert DNA.

After the colony formation, 7 colonies were chosen from different plates to isolate plasmids. Then, plasmid DNA was digested with *KpnI* restriction enzyme in order to verify whether or not the insert region was cloned successfully. Insertion of 913 bp ATM promoter sequence into 4818 bp pGL3-Basic vector results in 5731 bp long recombinant construct. Upon single digestion with *KpnI*, 6 out of 7 colonies were potentially positive for the insert (Figure 4.5). The pGL3-basic vector that was carrying the ATM promoter sequence was named as “pATM-GL3”.

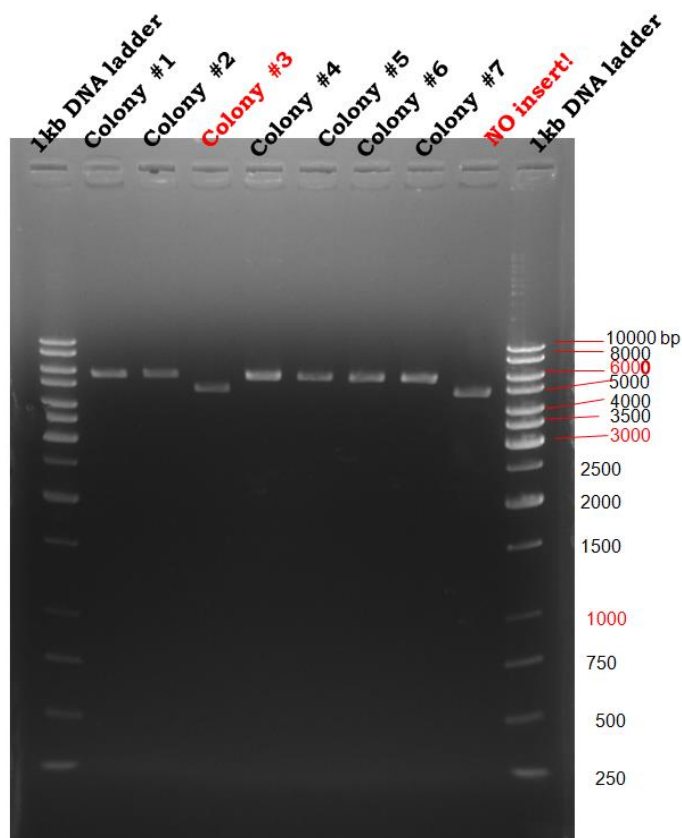


Figure 4.5. The presence of ATM promoter cloned into the pGL3-Basic vector was initially characterized by digestion with restriction endonuclease *KpnI*. Following the digestion reaction, the products were run on agarose gel. The first lane and last lane show 1kb DNA ladder, the other lanes show the plasmids isolated from different colonies. Please note that the digested plasmid in the 9th lane the pGL3-Basic vector was run as a control whereas the plasmid from “colony #3” (lane 4) is a background isolated from the plate with bacteria transformed ATM promoter insert ligation reaction.

4.1.4. Optimization of electroporation for basal-like breast cancer cells

Before MDA-MB-231, HCC38 and MDA-MB-468 cell lines were transfected with pATM-GL3, optimal electroporation conditions were determined with pCMV6-AC-GFP reporter plasmid. After a wide assortment of trials, 1100 V, 20 ms, 3 pulses; 1100 V, 20 ms, 2 pulses; 1300 V, 20 ms, 3 pulses (or 1400 V, 20 ms, 2 pulses) were chosen as optimal transfection parameters for MDA-MB-231, HCC38 and MDA-MB-468, respectively (Figure 4.6A, B, C).

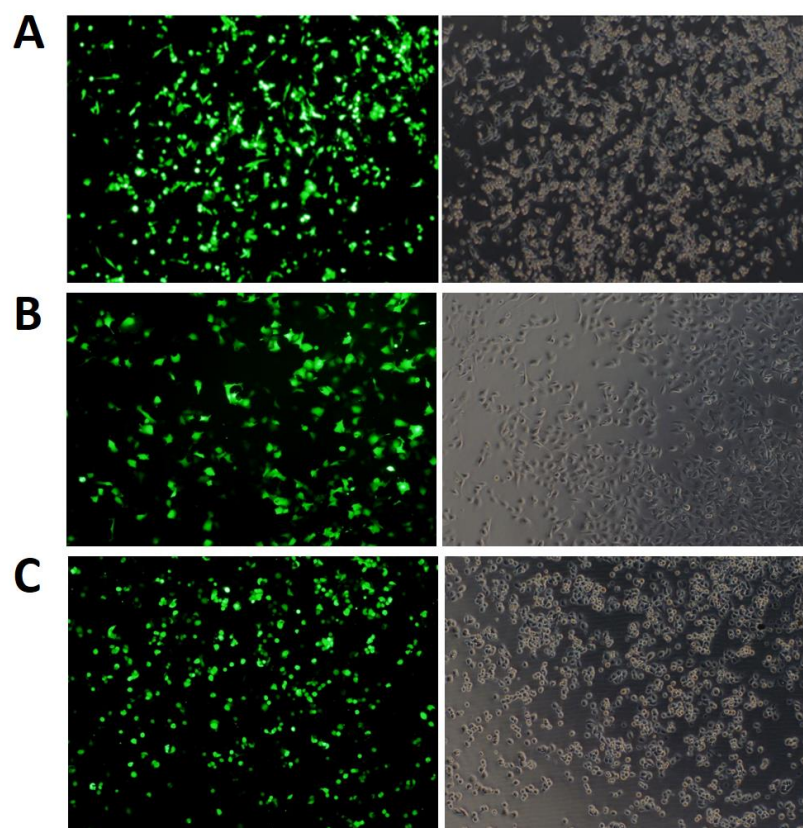


Figure 4.6. Basal-like breast cancer cell lines transfected with pCMV6-AC-GFP plasmid. Neon® Transfection Device (Thermo Fisher Scientific, Waltham, Massachusetts, USA) and Neon™ Transfection System 10 μ L Kit was used for electroporation. The gene transfer efficiency into (A) MDA-MB-231, (B) HCC38 and (C) MDA-MB-468 cells was determined by GFP fluorescence microscopy.

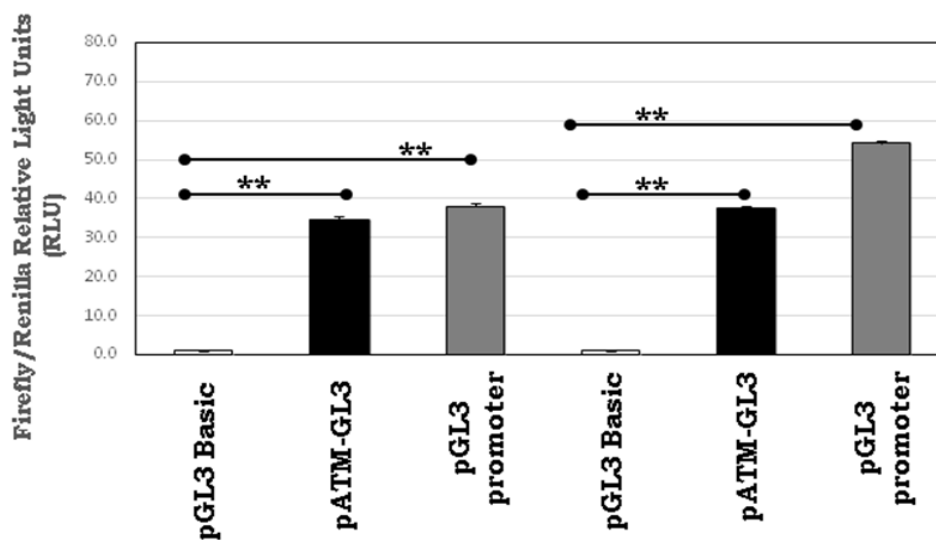
4.1.5. Regulation of the ATM promoter activity in response to X-radiation

To further test the role of X-radiation in induction of ATM expression, the minimal ATM promoter region (-860, +53) pATM-GL3 firefly luciferase reporter construct was transfected into HCC38 cell line as a representative basal-like breast cancer cell line. In order to normalize the reporter activity and to minimize the assay heterogeneity due to different transfection efficiencies, co-transfections were performed by using a constitutive reporter construct harboring renilla luciferase gene (pRL-TK). Relative light unit (RLU) values were calculated by taking the ratio of firefly luciferase activity to renilla luciferase activity. Signals derived from the pGL3-Basic without a specific promoter was used as negative control. pGL3-

Promoter vector carrying firefly luciferase gene under the control of CMV promoter was transfected as positive control. RLU values revealing ATM promoter activity were determined in the absence or presence of X-radiation (5 Gy). Early response and late response of ATM promoter to X-radiation exposure was observed measuring RLUs 3 hours and 24 hours after irradiation, respectively.

In general, the negative control experiments with promoterless pGL-3-basic vector showed only minimal reporter activity. In the absence of irradiation, ATM promoter activity of obtained from pATM-GL3 was very high and compatible that of the positive control pGL3-Promoter vector (RLU from HCC38 transfected with pATM-GL3 vs pGL-3-Promoter, mean range 34.46-34.16 vs 38.01-42.57), (Figure 4.7A). Three hours after irradiation, the ATM promoter activity tended to display a minimal increase. Intriguingly, RLUs from pGL3-Promoter positive control showed a distinctive increase (control RLU, 38.01; 3h post-irradiation 54.26, an increase about 42%) (Figure 4.7A). At 24h post-irradiation, positive control promoter activity was still significantly enhanced (by ~66%); on the other hand, ATM promoter activity was abrogated when compared to non-irradiated control HCC3 cells basal ATM promoter activity (Figure 4.7B). There was no significant change in negative control upon irradiation (Figure 4.7).

A)



B)

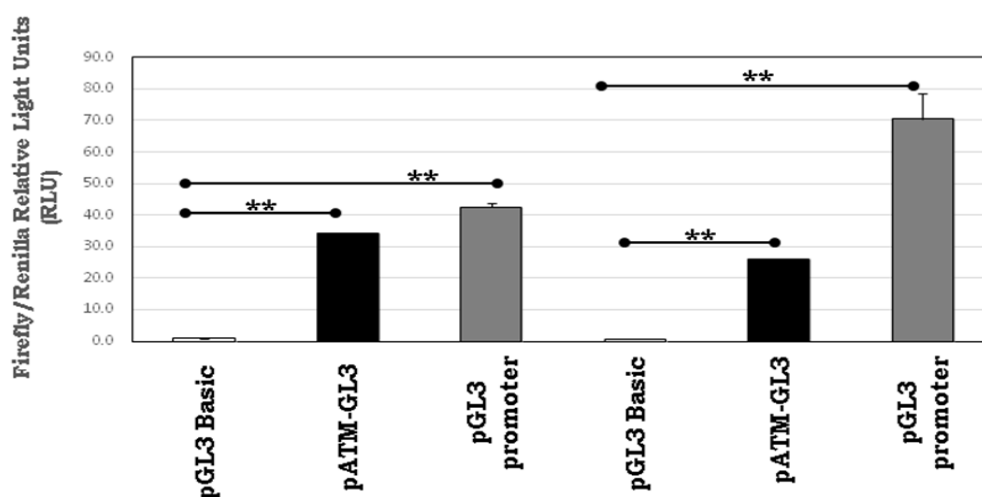


Figure 4.7. ATM promoter activity in HCC38 cell line before and after (A) 3h and (B) 24h X-radiation. HCC38 basal-like breast cancer cell line was co-transfected with pRL-TK (as an internal transfection normalization control) and pGL3-Basic (negative control), or pATM-GL3 or pGL3-Promoter (positive control) plasmids. After 24 hours of transfection, the cells were exposed to 5 Gy ionizing radiation or remained untreated for 3 or 24 hours. RLU values derived from the Firefly luciferase:Renilla luciferase signals were used to determine promoter activities. (* $P \leq 0.05$, ** $P \leq 0.01$).

4.2. GITR and GITRL expression in basal-like breast cancer cell lines and the effect of X-radiation

4.2.1 GITR and GITRL mRNA levels in basal-like breast cancer cells in response to X-radiation

The presence of GITR and GITRL expression was investigated in basal-like breast cancer cell lines before and after 5 Gy or 10 Gy irradiation. Under control conditions (no irradiation), GITRL gene expression was observed in MDA-MB-231 and MDA-MB-468, but not in HCC38 cell line. In contrast, GITR expression was only observed in HCC38 cell line, however it was not detected in MDA-MB-231 and MDA-MB-468 cell lines (Figure 4.8.). Twenty-four hours after ionizing radiation, no significant change in the level of GITR and GITRL was observed in any of cell lines (Table 4.3). Regardless to X-radiation treatments, GITR expression was highest in HCC38 cell line (as also noted from lower C_t values), whereas GITRL expression was relatively higher in MDA-MB-231 and MDA-MB-468 cell lines than in HCC38 (Table 4.3).

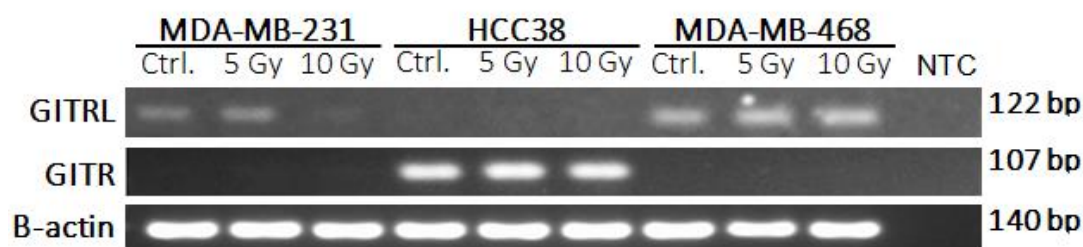


Figure 4.8. GITR and GITRL expression in basal-like breast cancer cell lines and the effect of X-radiation. MDA-MB-231, HCC38, and MDA-MB-468 breast cancer cell lines were exposed to 5 Gy or 10 Gy ionizing radiation whereas control group (Ctrl.) received no radiation. Total RNA isolation was performed 24 hours after ionizing radiation and the presence of GITR and GITRL mRNA was determined with RT-PCR. Amplified PCR products were segregated on 2% agarose gel electrophoresis. The size of GITRL, GITR and β -actin genes is 122 bp, 107 bp and 140 bp, respectively.

Table 4.3. Δ Ct (GITR or GITRL Ct – β -actin Ct) values for GITR and GITRL expression in control conditions of 24 hours after X-irradiation (5 Gy and 10 Gy) was determined by relative quantitative real-time RT-PCR.

	MB-231	HCC38	MB-468	
Control	17,79066	20,44352	16,45381	GITRL
5 Gy	17,468502	20,7351	16,04083	
10 Gy	17,330207	20,37822	17,64066	
Control	20,462156	7,908706	21,90885	GITR
5 Gy	19,098094	7,649386	21,23848	
10 Gy	18,289356	8,114909	20,17608	

4.2.2. Determination of GITR and GITRL surface protein expression in X-irradiated HCC38 cell line

Since HCC38 was the only cell line studied to have GITR gene expression, surface protein levels of this receptor and its ligand was further examined by flow cytometry. A large percentage of HCC38 was GITR⁺. However, the surface GITR levels tend to decrease in response to irradiation, especially at 10 Gy (Figure 4.9 A and B). There was almost no detectable GITRL surface protein and exposure to radiation did not induce its expression (Figure 4.9 A).

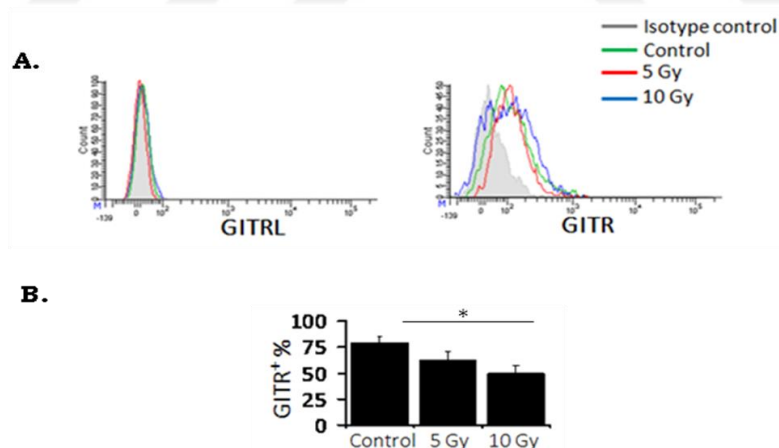


Figure 4.9. GITR and GITRL surface protein expression in HCC38 cell line. The expression of GITR and GITRL on the surface of HCC38 was determined before or 48h after ionizing radiation (5 Gy or 10 Gy) by flow cytometry. **A)** Representative histograms out of 3 independent experiments are given. **B)** The percentages of GITR⁺ in control or irradiated HCC38 cells are plotted. (* $P \leq 0.05$, ** $P \leq 0.01$).

4.2.3 The effect of GITR stimulation and ionizing radiation on HCC38 cells' viability and proliferation

To examine the effect of GITR stimulation on HCC38 viability and proliferation, these cells were treated with increasing amounts (5, 20, 80, and/or 160 ng/ml) of soluble recombinant GITRL protein (rGITRL) protein. Following an initial 3 days of incubation the media containing the rGITRL were refreshed the cells were incubated for another 3 days. For the experiments with irradiation, following the initial 3 days of incubation, the cells were irradiated (5 Gy) and the media containing the rGITRL were refreshed. Then, the cells were incubated for another 3 days. At the end of 6-day-long incubation period the cell viability (DRAQ7 staining), proliferation (CFSE assay) and total amount of viable cells (MTT assay) was assessed.

Initially, a possible negative effect of serum reduction together with GITR induction on the HCC38 cells' viability was tested. The even at the highest concentration of rGITRL (80 ng/ml), in the complete medium or in the serum deprivation conditions the cell viability was not significantly hampered (Figure 4.10).

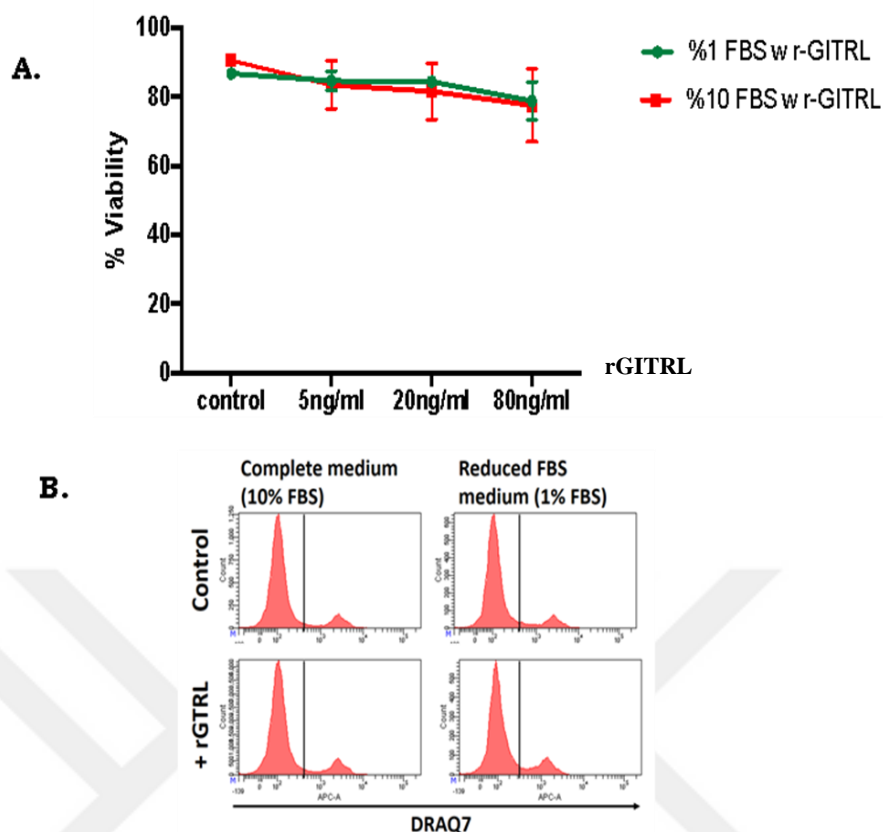
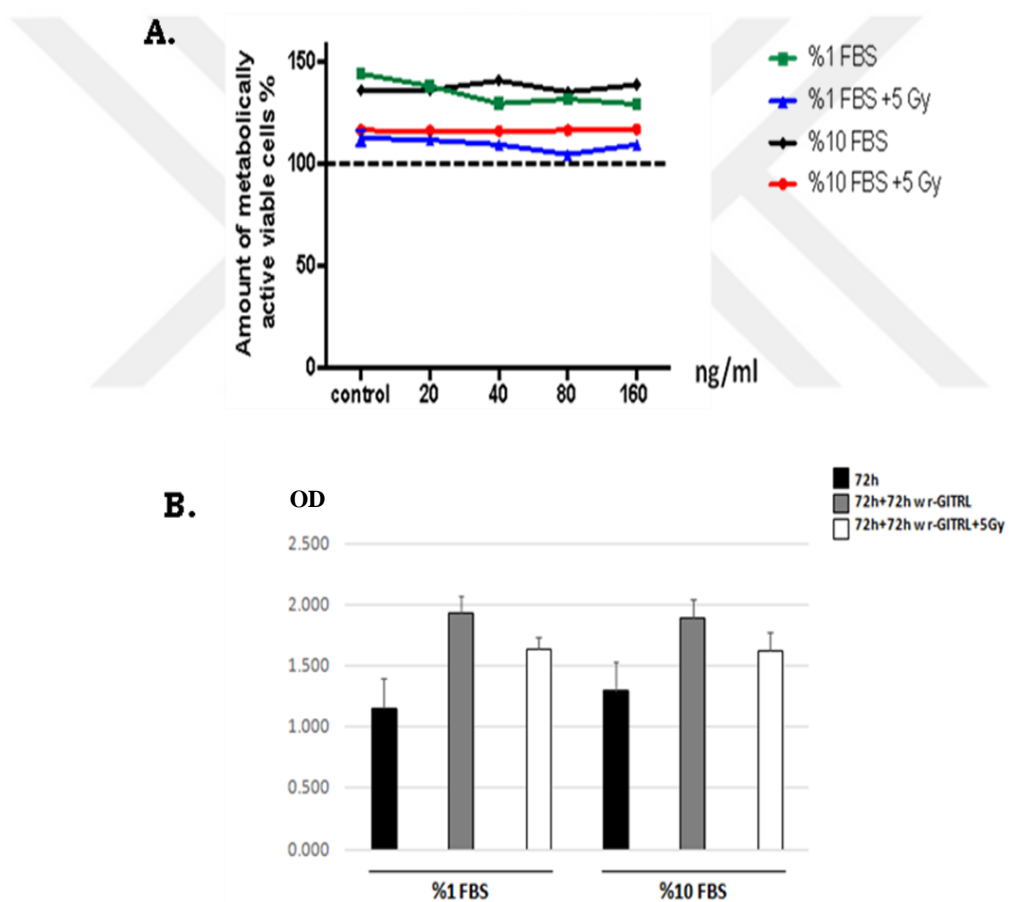


Figure 4.10. Viability of HCC38 cells showed no significant alteration in cells treated with rGITRL either in 1% and 10% FBS condition. A) HCC38 cells were treated 5, 20, or 80 ng/ml rGITRL was cultured for 6 days; where, following an initial 3 days of incubation the media containing the rGITRL were refreshed the cells were incubated for another 3 days. At the end of 6-day-long incubation period the cell viability was assessed by DRAQ7 staining and read on flow cytometry. B) Representative flow cytometry histograms of control and 80 ng/ml rGITRL-treated HCC38 cells are shown.

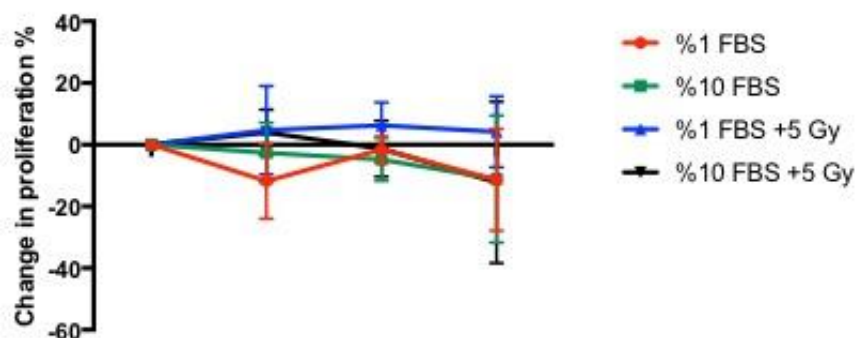
Next, HCC38 cells treated with increasing concentrations of rGITRL protein in complete medium or in FBS-reduced medium were exposed to 5 Gy ionizing radiation. MTT results showed that there is a significant difference regarding the amount of viable cells between the cells treated with ionizing radiation and the control cells (Figure 4.11A). Independent from the rGITRL dose applied and culture media conditions, HCC38 cells treated with radiation had contained compatible amounts of viable cells to that of control (no rGITRL added) cells (Figure 4.11A).

MTT assay is based on measurement of metabolic activity in mitochondria and has been used as an indirect test to gather information on both cell viability and

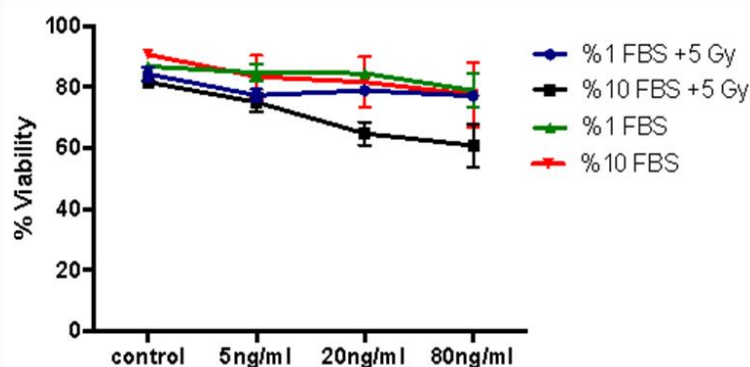
proliferation of the cells (i.e. total amount of metabolically active cells). Therefore, for being more explicit, the proliferation activity of HCC38 cells under different conditions was also separately analyzed. There was no difference between control and rGITRL and/or X-irradiated cells proliferation (Figure 4.11 C). On the other hand, when cell death was also separately assayed, a trend of viability attenuation in the cells exposed to both rGITRL and 5 Gy ionizing radiation was observed (Figure 4.11 D). Especially, at 80 ng/ml rGITRL concentration the cumulative effect of GITR stimulation with ionizing radiation reached to a level of statistical significance (Figure 4.11 D and E).



C.



D.



E.

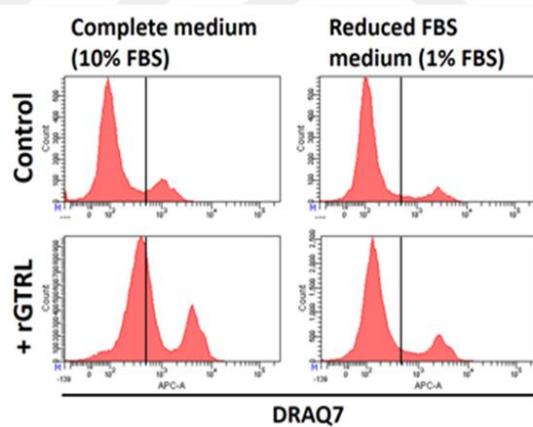


Figure 4.11. Amount of viable cells, proliferation and cell death in HCC38 cells exposed to irradiation and rGITRL. HCC38 cells were treated with increasing amounts (5, 20, 80, and/or 160 ng/ml) of rGITRL. Following an initial 3 days of incubation, the cells were irradiated (5 Gy) and the media containing the rGITRL were refreshed. Then, the cells were incubated for another 3 days. At the end of 6-day-long incubation period (A) total amount of metabolically active viable cells (MTT assay), (B) OD results (MTT assay) (C) cell proliferation (CFSE assay), and (D) cell viability (DRAQ7 staining) was assessed. (E) Representative flow cytometry histograms of control and 80 ng/ml rGITRL-treated HCC38 cells are shown. (* $P \leq 0.05$).

5. DISCUSSION

In this study, we performed analyses in order to verify radiation responsiveness of triple-negative breast cancer cell lines named MDA-MB-231, HCC38 and MDA-MB-468. While mRNA levels of ATM was determined both in luminal and basal-like breast cancer cell lines, change in ATM phosphorylation, protein levels of ATM and promoter activity were determined in basal-like breast cancer cell lines, upon radiation exposure. For this aim, a reporter plasmid with ATM promoter region was designed. In basal-like breast cancer cell lines, GITR and GITRL expression changes upon X-radiation (5 Gy and 10 Gy) was investigated. Furthermore, GITR⁺ HCC38 cells were treated with recombinant GITRL protein, in order to examine its effect with/without ionizing radiation. ATM expression was constitutive both in luminal and basal-like breast cancer cell lines and total protein levels were inclined to increase, upon radiation. Our results revealed that HCC38 GITR⁺ cancer cells' stimulation with its correspondent ligand may increase radiation sensitivity.

Although immunotherapy, especially the removal of checkpoint inhibition is a novel therapeutic modality, immune modulation and radiation therapy against triple negative breast cancer cells is yet to be extensively studied. GITR-GITRL interaction has been well elucidated from immunological aspects, we know that this interaction result in direct apoptotic effect for immune cells (92). There are several trials targeting GITR molecule in inoperable Stage III or Stage IV malignant melanoma and other solid tumor malignancies (102).

In this thesis study, our first aim was to study the cytotoxic effect of radiation on typical triple negative breast cancer cell lines (MDA-MB-231, HCC38 and MDA-MB-468) and to investigate change in ATM activity with 6 MV X-ray photons. Our second aim was to examine whether or not these cells regulate GITR and GITRL, in the absence and presence of X-radiation. We further investigated any possible cumulative effect of GITR stimulation and ionizing radiation on basal-like breast cancer cells (HCC38) to correlate to any immune modulatory effect.

Genomic stability is challenged by DNA damage, which can be from either endogenous or exogenous origins. In literature, it has been shown that UV radiation, chemical mutagens or ionizing radiation creates DNA strand breaks which trigger

ATM activity. Dose and duration of the extrinsic stimuli (i.e. X-radiation) varies among different cell types on different experimental setups, mostly exploring easily achievable radiation doses in radiation therapy. Hence, we applied 2 different doses (5 Gy and 10 Gy) of X-radiation for DNA damage induction for basal-like breast cancer cell lines in our study, with lowest possible cytotoxicity due to radiation (sub-optimal radiation dose for cytotoxicity). We observed distinct ATM phosphorylation at S1981 in all cell lines (MDA-MB-231, HCC38 and MDA-MB-468) with 5 Gy dose, we have chosen this dose in subsequent experimental setups, rather than 10 Gy. Kim et. al showed that notable ATM activation was provided in MDA-MB-231 cells irradiated with 8.75 Gy (65). Our results are in agreement with this study, we found that 10 Gy of radiation results in higher phosphorylated ATM levels in MDA-MB-231 cells, than cells irradiated with 5 Gy. Another study investigated that while 6 Gy was enough to induce ATM phosphorylation in MCF-7 CD44⁺/CD24⁻ cells, this radiation dose climbs to 8 Gy in order to induce ATM phosphorylation in MDA-MB-231 cancer stem cells (50). Since there is no consensus on the treatment modality for ATM phosphorylation, we have chosen two different radiation doses. We did not show any prominent change of total ATM levels in our analyses, indicating activation, rather than a direct transcriptional upregulation of the ATM protein.

MDA-MB-231 and HCC38 cell lines belong to the Basal B sub-type, but MDA-MB-468 cell line is categorized as Basal A sub-type of triple negative breast cancers, which is classified closer to the Luminal type, than Basal subtype B. Intriguingly, we observed lower ATM levels in MDA-MB-468 cell line, which might be attributed to possible proportion of cancer stem cell phenotype in this cell line. In one of the studies (35), a high percentage of CD44^{high}/CD24^{low/neg} cells of breast CSC phenotype was shown to be enriched in MDA-MB-231 (93.25%) cell lines (35). Sheridan and colleagues also agreed that MDA-MB-231 cell line comprised of high proportion CD44^{high}/CD24^{low/neg} CSC sub-population (85±5%), while containing lowest proportion for CD44⁺/CD24⁺ (2%) (36). On the contrary, MDA-MB-468 cell line shows the highest proportion for CD44⁺/CD24⁺ (90±6%), while showing the lowest proportion (3±1%) for CD44^{high}/CD24^{low/neg} CSCs. HCC38 cell line is enriched with (80%) CD49f^{high}/EpCAM⁻ mammary stem cells. It is proposed that the greater proportion of CD44^{high}/CD24^{low/neg} (CSC) cells provide these tumors with

higher ATM expression and higher resistance to radiation therapy. Our results are in agreement with this hypothesis. Despite the fact that CSCs percentage is low in MDA-MB-468 cell line, there is still ATM phosphorylation upon ionizing radiation, suggesting mammary stem cells also activating their ATM proteins via phosphorylation upon radiation.

De novo expression of ATM in these cell lines should also be considered with ionizing radiation, as persistence of DNA damage response could only be supported with further synthesis of ATM protein in the long term. Therefore, we further investigated whether or not ATM mRNA expression levels differ in basal-like breast cancer cell lines. Since regulation of ATM expression has been reported to depend on the presence of serum, proposing that cell lines cultured with extremely low serum (0.05% FCS- serum deprivation) for 72 hours, show higher ATM expression (60). Fang *et al.*(103) demonstrated that irradiated fresh skin biopsies show average three-fold increase in ATM levels with serum-starvation. Although their serum-starvation conditions are achievable to induce increased ATM expression *in vitro*, it is not practical for *in vivo* models. Therefore, rather than risking cell death, in our experimental setup, we treated cell lines with 1% FBS containing medium (serum deprivation) for 48 hours, which shows minimum impact on cell viability. We did not observe any disparity regarding ATM expression levels, when the cells are maintained in reduced serum levels (1%). Moreover, when luminal type breast cancer cell lines (MCF-7, BT-474 and SK-BR-3) and basal-like breast cancer cell lines (MDA-MB-231, HCC38 and MDA-MB-468) were compared, ATM expression levels were almost same, hence there is no intrinsic variability on relative ATM levels among different subclasses of breast cancer cell lines.

Low ATM protein levels were observed in MDA-MB-468 cell line, and as all tested cell lines expressed close relative ATM transcript levels, we hypothesize that ATM transcripts may be subjected to a post-transcriptional regulation in MDA-MB-468 cell line, although we have not tested this hypothesis further. In addition to breast cancer, diminished ATM protein levels (in spite of higher mRNA transcripts) was also showed in glioblastoma, colorectal cancer and gastric cancers (104), however the molecular mechanism is still disputable. Chen and colleagues suggested that high tumor protein D52 (TPD52) levels interfere with ATM protein levels, so it

is a negative regulator for ATM protein. By utilizing GST pull-down assay, they showed that there is a physical interaction between ATM residues (1-245 and 772-1102) with TPD52 residues (111-131), which results in reduced ATM protein levels, without influencing ATM mRNA levels and stability. MDA-MB-468 is one of the breast cancer cell lines expressing TPD52 highly (105), which may result in down-regulation of ATM protein levels, without affecting transcript levels, therefore may explain our observation. Other studies showed that TPD52 protein levels were high in SK-BR-3 and AU-565 cell lines, BT-474, MCF-7 and MDA-MB-468 cell lines were also positive for TPD52 protein, however they have not tested other cell lines we used (i.e. MDA-MB 231 or HCC38), to make a meaningful comparison of post-transcriptional regulation.

In addition, we should take into consideration that ATM expression is not only restricted to cancer stem cells, however its expression in CSCs surpasses the expression levels in normal cancer cells. Therefore we should expect breast cancer cell lines with high proportion of CSCs (such as MDA-MB-231 and HCC38) to have a higher ATM expression than cell lines with lower proportion of CSCs (such as MDA-MB-468), this might explain the observed high ATM expression in basal-like breast cancer cell lines. If we could have a chance to compare cancer stem cells or cancer cells with normal-immortalized breast epithelial cells, maybe we could observe different ATM expression levels. This shows the pitfall in our experimental design.

We investigated temporal changes in ATM protein levels for 24 and 48 hours post-ionizing radiation treatment. Starting at 24 hours, but prominent on the 48th hour, ATM protein levels increased, in comparison to control (untreated) cells. Cells may prefer to activate available homodimer or heteromultimer ATM proteins via phosphorylation, rather than inducing *de novo* transcription, when they were exposed to irradiation. One may hypothesize that, after 48 hours, cells may prefer to elongate their DNA damage response, by increasing ATM protein levels in their protein pool with transcriptional regulation.

In our study ATM promoter region (-860 to +53) was cloned into the pGL3-Basic luciferase reporter construct forming pATM-GL3 reporter plasmid, in order to further test the role of X-radiation on induction of ATM transcription. This allows

direct transcriptional monitoring of ATM promoter region with radiation. Subsequently, HCC38 cells were transfected with pATM-GL3, basal activity of the ATM promoter is monitored without treatment. We found that basal ATM promoter activity in these cells is fairly high, even in the absence of ionizing radiation. This observation could be attributed to two possible reasons: i) Expression levels of transcription factors that has consensus binding sequences in the putative ATM promoter (AP-1, NF-Y, CBF-A, NFκB) might be intrinsically high in HCC38 or ATM promoter sequence may contain tandem sequences for these trans-acting factors. This could be tested with further western blot experiments supported with sequencing. It has been well known that there are assorted transcription factor binding sites on the ATM promoter. If HCC38 cell line is enriched with transcription factors named SpI, Cre, Ets and E2F1, this could enhance luciferase expression of ATM promoter. ii. it has been known that HCC38 cell line is enriched with breast cancer stem cells (80% CD49^{high}/EpCAM⁻ mammary stem cells), and these CSCs highly express ATM to preserve genomic fidelity in case of DNA damage. This could be the most reasonable explanation for high luciferase signal for the basal levels of ATM promoter activity in transfected HCC38 cells. Moreover, we know that total ATM protein levels in HCC38 cells are high even in the absence of irradiation, so this might explain the observed high basal luciferase activity. Three hours after irradiation, the ATM promoter activity inclined to show minimal increase. 24 hours after irradiation, the ATM promoter activity predisposed to show decrease, this can be attributed to the reduced metabolic activity of the cell.

Ionizing radiation exposure on living cells have two possible outcomes for a cell destiny: i.it creates DNA damage as a direct effect or ii. Radiolysis of cellular water results in the generation of chemical reactive species (reactive oxygen (ROS) and nitrogen (RNS) species) that can further damage the cellular components (106). Therefore, observing changes in amount of metabolically active cells in our findings would be expected. Upon irradiation JNK was shown to localize into mitochondria and by phosphorylating Bcl-x1, it initiates apoptosis through mitochondria-mediated intrinsic pathway. However, JNK is targeted by a MAPK phosphatase (MKP1) after irradiation, therefore radiation-induced apoptosis is halted in cells (107). Although cells increase their metabolic activity, they could stay in a quiescent state. Any

possible hypothesis suggesting this mechanism as an explanation for not observing a difference in cell proliferation assays after irradiation.

It is noteworthy that RLUs from pGL3-Promoter vector showed a distinctive increase upon ionizing radiation. At 24h post-irradiation, positive control promoter activity continued to increase significantly (by app. 66%). Activator protein-1 (AP-1) and specificity protein-1 (Sp1) are the well known transcription factors showing strong binding affinity to the SV40 promoter region (108). Two hexameric GC boxes (GGGCGG consensus sequences), binding sites for Sp1 transcription factor, localized on SV40 promoter region. TFCP2 recognizes certain sites within SV40 late promoter region. TEA domain family member 1 (TEAD) and transcription factor AP-2a (TFAP2A) bind to DNA from CCCCAGGC consensus sequences in the SV40 promoter region. It would be better to further check HCC38 cell line for AP-1 and Sp1 transcription factor levels, upon ionizing radiation. In overall, we showed that ATM pathway was induced with 5 Gy and after 48 hours of irradiation there was an increase of total ATM levels.

We further analyzed GITR and GITRL expression levels in basal-like breast cancer cell lines, with ionizing radiation. Intriguingly, cell lines with high GITR levels showed low GITRL expression (HCC38), whereas cell lines with high GITRL expression showed low GITR levels (MDA-MB-231 and MDA-MB-468). This observation directs our hypothesis to whether or not GITR-GITRL pair expressed mutually exclusive on the surface of the tumor cell, due to possible apoptotic pathways. Then, we considered if GITR⁺ HCC38 cell line is treated with soluble recombinant GITRL protein, this might trigger possible apoptotic pathways mentioned previously. Upon X-irradiation, we observed minimal changes for GITR and GITRL mRNA levels. Nonetheless, GITR surface expression on HCC38 cells was reduced to 50%, with 10 Gy irradiation dose. Since 10 Gy influenced the cell viability, we decided to treat cells with 5 Gy in our subsequent experiments. When HCC38 cells were only treated with r-GITRL, in both 1% and 10% FBS condition we did not observe any change of variability, right along with the increased GITRL doses. HCC38 cells treated with both X-radiation and r-GITRL showed reduced metabolic activity levels as expected. This decrement in metabolic activity did not alter with the increasing r-GITRL dose. When cells are serum deprived for 6 days,

cellular quiescence was observed and their viability did not influenced from various doses of recombinant GITRL. On the other hand, HCC38 cells exposed to irradiation and treated with 80 ng/ml recombinant GITRL protein, were inclined to trigger apoptotic pathways.

In conclusion, since ATM promoter activity is high in basal-like breast cancer cell lines, this created a good gene regulation sequence. We have preliminary data showing that ATM protein stability may increase with irradiation. Furthermore, we observed that GTR and GITRL expressions were mutually exclusive in basal-like breast cancer cell lines (MDA-MB-231, HCC38, MDA-MB-468). We did not observe any direct effect of recombinant GITRL stimulation on GTR⁺ HCC38 cells. However, this data give an idea that both rGITRL and irradiation can show additive effect on HCC38 cells.

6. RESULTS & RECOMMENDATIONS

In this study:

Basal-like breast cancer cell lines (MDA-MB-231, HCC38 and MDA-MB-468) showed increased ATM (S1981) phosphorylation at 5 Gy ionizing radiation. HCC38 and MDA-MB-468 cell lines showed phosphorylated ATM at 5 Gy, whereas MDA-MB-231 showed p-ATM levels with 10 Gy X-radiation. All cell lines were verified as radiation- responsive.

Total-ATM levels did not show any disparity after 1hr and 24hr of X-radiation. After 48 hours of irradiation, their levels in MDA-MB-231 and HCC38 cell lines increased, to a certain extent.

ATM expression levels in serum deprivation (1% FBS) and in complete media (10% FBS) conditions were compared and no significant change was observed.

ATM expression levels were compared between basal-like breast cancer cells and luminal type (MCF-7, BT-474, SK-BR-3) and there was no difference of expression patterns.

ATM promoter region was cloned into pGL3-Basic vector with KpnI and BglII restriction enzymes. Then, pATM-GL3 vector was re-digested with KpnI endonuclease to verify whether or not the insert region was cloned.

With the aid of pCMV6-AC-GFP plasmid, optimal transfection conditions were determined for MDA-MB-231, HCC38 and MDA-MB-468 cell lines. 1100V, 20ms, 3 pulses; 1100V, 20ms, 2 pulses and 1300V, 20ms, 3 pulses were chosen as optimal transfection parameters for MDA-MB-231, HCC38 and MDA-MB-468, sequentially.

In Luciferase experiments, while HCC38 transfected with pATM-GL3 and pGL3-Promoter vectors showed higher ATM promoter activity even in the absence of irradiation; our negative control pGL3-Basic showed no reporter activity, as expected.

pGL3 promoter vector showed a distinctive promoter activity, after 24 hours of irradiation.

The presence of GITR and GITRL and their expression regulation in response to X-radiation did not alter.

After 48 hours of irradiation, GITR surface protein levels reduced with 10 Gy ionizing radiation.

HCC38 GITR⁺ cell lines were stimulated with recombinant GITRL protein did not show any difference of cell viability and proliferation. But, cells treated with both X-radiation and r-GITRL showed a predisposition for apoptosis.

Mitochondrial membrane potential assays can be performed in further studies.

Luciferase experiments with pATM-GL3 construct can be performed in other basal-like breast cancer cell lines and luminal breast cancer cell lines.

Annexin or TUNEL assay can be utilized for cell death measurement, as alternative assays.

In *in vivo* tissues expression levels of ATM, GITR and GITRL can be analyzed.

In animal models, radio-genetic studies combining ATM promoter region with GITRL gene induction and X-radiation analysis can be carried out.

REFERENCES

1. Sims AH, Howell A, Howell SJ, Clarke RB. Origins of breast cancer subtypes and therapeutic implications. *Nat Clin Pract Oncol*. 2007;4(9):516–25.
2. Prat A, Perou CM. Deconstructing the molecular portraits of breast cancer. *Mol Oncol*. 2011;5(1):5–23.
3. Ajani JA, Song S, Hochster HS, Steinberg IB, Rochlitz C, Diamandis EP. Cancer stem cells: the promise and the potential. *Semin Oncol*. 2015;42(2):Suppl 1:S3-17.
4. Davis JD, Lin Jennifer Davis S-YD, Lin S-Y, Araujo A. DNA damage and breast cancer. *World J Clin Oncol*. 2011;2(9):329-338.
5. Walsh T, Casadei S, Coats KH, Swisher E, Stray SM, Higgins J, et al. Spectrum of Mutations in BRCA1, BRCA2, CHEK2, and TP53 in Families at High Risk of Breast Cancer. *JAMA*. 2006;295(12):1379-1388.
6. Tuncer AM, Özgül N, Olcayto E, Gültekin M. Cancer Control in Turkey. Ankara:Republic of Turkey Ministry of Health Cancer Control Department;2010.
7. 2014 Yılı Türkiye Kanser İstatistikleri [Internet]. 2014[cited 2017 May 1]. Available from: <http://kanser.gov.tr/daire-faaliyetleri/kanser-istatistikleri/2106-2014-y%C4%B1%C4%B1-t%C3%BCrkiye-kanser-istatistikleri.html>
8. Rivenbark AG, O'Connor SM, Coleman WB, Campbell PJ, Dausman J, Gray JW, et al. Molecular and Cellular Heterogeneity in Breast Cancer. *Am J Pathol*. 2013;183(4):1113–24.
9. Malhotra GK, Zhao X, Band H, Band V. Histological, molecular and functional subtypes of breast cancers. *Cancer Biol Ther*. 2010;10(10):955–60.
10. Payne SJL, Bowen RL, Jones JL, Wells CA. Predictive markers in breast cancer - the present. *Histopathology*. 2007;52(1):82–90.
11. Rakha EA, Reis-Filho JS, Ellis IO. Combinatorial biomarker expression in breast cancer. *Breast Cancer Res Treat*. 2010;120(2):293–308.
12. Yersal O, Barutca S. Biological subtypes of breast cancer: Prognostic and therapeutic implications. *World J Clin Oncol*. 2014;5(3):412–24.
13. Hennessy BT, Gonzalez-Angulo A-M, Stemke-Hale K, Gilcrease MZ, Krishnamurthy S, Lee J-S, et al. Characterization of a Naturally Occurring Breast Cancer Subset Enriched in Epithelial-to-Mesenchymal Transition and Stem Cell Characteristics. *Cancer Res*. 2009;69(10):4116-4124.
14. Creighton CJ, Li X, Landis M, Dixon JM, Neumeister VM, Sjolund A, et al. Residual breast cancers after conventional therapy display mesenchymal as well as tumor-initiating features. *Proc Natl Acad Sci U S A*. 2009;106(33):13820–5.
15. Taube JH, Herschkowitz JI, Komurov K, Zhou AY, Gupta S, Yang J, et al. Core epithelial-to-mesenchymal transition interactome gene-expression

- signature is associated with claudin-low and metaplastic breast cancer subtypes. *Proc Natl Acad Sci U S A*. 2010;107(35):15449–54.
16. Parker JS, Mullins M, Cheang MCU, Leung S, Voduc D, Vickery T, et al. Supervised risk predictor of breast cancer based on intrinsic subtypes. *J Clin Oncol*. 2009;27(8):1160–7.
 17. Prat A, Parker JS, Karginova O, Fan C, Livasy C, Herschkowitz JI, et al. Phenotypic and molecular characterization of the claudin-low intrinsic subtype of breast cancer. *Breast Cancer Res*. 2010;12(5):R68.
 18. Hartman A-R, Kaldate RR, Sailer LM, Painter L, Grier CE, Endsley RR, et al. Prevalence of BRCA mutations in an unselected population of triple-negative breast cancer. *Cancer*. 2012;118(11):2787–95.
 19. Gonzalez-Angulo AM, Timms KM, Liu S, Chen H, Litton JK, Potter J, et al. Incidence and outcome of BRCA mutations in unselected patients with triple receptor-negative breast cancer. *Clin Cancer Res*. 2011;17(5):1082–9.
 20. Lou H, Dean M. Targeted therapy for cancer stem cells: the patched pathway and ABC transporters. *Oncogene*. 2007;26(9):1357–60.
 21. Wang Q-E. DNA damage responses in cancer stem cells: Implications for cancer therapeutic strategies. *World J Biol Chem*. 2015;6(3):57–64.
 22. Wei W, Tweardy DJ, Zhang M, Zhang X, Landua J, Petrovic I, et al. STAT3 signaling is activated preferentially in tumor-initiating cells in claudin-low models of human breast cancer. *Stem Cells*. 2014;32(10):2571–82.
 23. Collina F, Di Bonito M, Li Bergolis V, De Laurentiis M, Vitagliano C, Cerrone M, et al. Prognostic Value of Cancer Stem Cells Markers in Triple-Negative Breast Cancer. *Biomed Res Int*. 2015;2015:1–10.
 24. Beça FF de, Caetano P, Gerhard R, Alvarenga CA, Gomes M, Paredes J, et al. Cancer stem cells markers CD44, CD24 and ALDH1 in breast cancer special histological types. *J Clin Pathol*. 2013;66(3):187–91.
 25. Al-Hajj M, Wicha MS, Benito-Hernandez A, Morrison SJ, Clarke MF. Prospective identification of tumorigenic breast cancer cells. *Proc Natl Acad Sci*. 2003;100(7):3983–8.
 26. Dobbin ZC, Landen CN. Isolation and characterization of potential cancer stem cells from solid human tumors-potential applications. *Curr Protoc Pharmacol*. 2013;63:Unit 14.28.
 27. Visvader JE, Lindeman GJ. Cancer stem cells in solid tumours: accumulating evidence and unresolved questions. *Nat Rev Cancer*. 2008;8(10):755–68.
 28. Kruyt FAE, Schuringa JJ. Apoptosis and cancer stem cells: Implications for apoptosis targeted therapy. *Biochemical Pharmacology*. 2010;80(4):423-30.
 29. Dontu G, Abdallah WM, Foley JM, Jackson KW, Clarke MF, Kawamura MJ, et al. In vitro propagation and transcriptional profiling of human mammary stem/progenitor cells. *Genes Dev*. 2003;17(10):1253–70.
 30. An H, Kim JY, Oh E, Lee N, Cho Y, Seo JH. Salinomycin Promotes Anoikis and Decreases the CD44+/CD24- Stem-Like Population via Inhibition of

- STAT3 Activation in MDA-MB-231 Cells. *PLoS One*. 2015;10(11):e0141919.
31. Sieuwerts AM, Kraan J, Bolt J, van der Spoel P, Elstrodt F, Schutte M, et al. Anti-Epithelial Cell Adhesion Molecule Antibodies and the Detection of Circulating Normal-Like Breast Tumor Cells. *JNCI J Natl Cancer Inst*. 2009;101(1):61–6.
 32. Neve RM, Chin K, Fridlyand J, Yeh J, Baehner FL, Fevr T, et al. A collection of breast cancer cell lines for the study of functionally distinct cancer subtypes. *Cancer Cell*. 2006;10(6):515–27.
 33. Abraham BK, Fritz P, McClellan M, Hauptvogel P, Athelougou M, Brauch H. Prevalence of CD44+/CD24–/low Cells in Breast Cancer May Not Be Associated with Clinical Outcome but May Favor Distant Metastasis. *Clin Cancer Res*. 2005;11(3):1154–9.
 34. Bos PD, Zhang XH-F, Nadal C, Shu W, Gomis RR, Nguyen DX, et al. Genes that mediate breast cancer metastasis to the brain. *Nature*. 2009;459(7249):1005–9.
 35. Wang L, Zhang D, Zhang C, Zhang S, Wang Z, Qu C, et al. A microRNA expression signature characterizing the properties of tumor-initiating cells for breast cancer. *Oncology Letters*. 2012;3(1):119–124
 36. Sheridan C, Kishimoto H, Fuchs RK, Mehrotra S, Bhat-Nakshatri P, Turner CH, et al. CD44 + /CD24 -breast cancer cells exhibit enhanced invasive properties: an early step necessary for metastasis. *Breast Cancer Res*. 2006;8(5):1–13.
 37. Prat A, Karginova O, Parker JS, Fan C, He X, Bixby L, et al. Characterization of cell lines derived from breast cancers and normal mammary tissues for the study of the intrinsic molecular subtypes. *Breast Cancer Res Treat*. 2013;142(2):237–55.
 38. Schae D, McBride WH. Opportunities and challenges of radiotherapy for treating cancer. *Nat Rev Clin Oncol*. 2015;12(9):1–14.
 39. Shiloh Y. ATM and related protein kinases: safeguarding genome integrity. *Nat Rev Cancer*. 2003;3(3):155–68.
 40. Hoeijmakers JH. Genome maintenance mechanisms for preventing cancer. *Nature*. 2001;411(6835):366–74.
 41. Lieber MR, Wilson TE. SnapShot: Nonhomologous DNA end joining (NHEJ). *Cell*. 2010;142(3):496–496.e1.
 42. Lieber MR. NHEJ and its backup pathways in chromosomal translocations. *Nat Struct Mol Biol*. 2010;17(4):393–5.
 43. San Filippo J, Sung P, Klein H. Mechanism of eukaryotic homologous recombination. *Annu Rev Biochem*. 2008;77(1):229–57.
 44. Smith J, Mun Tho L, Xu N, A. Gillespie D. The ATM–Chk2 and ATR–Chk1 Pathways in DNA Damage Signaling and Cancer. *Advances in cancer research*. 2010;108:73–112.

45. Carruthers R, Chalmers AJ. The potential of PARP inhibitors in neuro-oncology. *CNS Oncol.* 2012;1(1):85–97.
46. NCCN Guidelines for Patients® | Breast Cancer - Stages I and II [Internet]. [cited 2017 May 3]. Available from: https://www.nccn.org/patients/guidelines/stage_i_ii_breast/index.html#66/z
47. Hoeijmakers JHJ. Genome maintenance mechanisms for preventing cancer. *Nature.* 2001;411:366–74.
48. Safa AR. Resistance to Cell Death and Its Modulation in Cancer Stem Cells. *Crit Rev Oncog.* 2016;21(3–4):203–19.
49. Bao S, Wu Q, McLendon RE, Hao Y, Shi Q, Hjelmeland AB, et al. Glioma stem cells promote radioresistance by preferential activation of the DNA damage response. *Nature.* 2006;444(7120):756–60.
50. Yin H, Glass J, Richardson C, Green S, Martin N. The Phenotypic Radiation Resistance of CD44+/CD24–or low Breast Cancer Cells Is Mediated through the Enhanced Activation of ATM Signaling. *PLoS One.* 2011;6(9):e24080.
51. Reya T, Morrison SJ, Clarke MF, Weissman IL. Stem cells, cancer, and cancer stem cells. *Nature.* 2001;414(6859):105–11.
52. Falck J, Mailand N, Syljuåsen RG, Bartek J, Lukas J. The ATM-Chk2-Cdc25A checkpoint pathway guards against radioresistant DNA synthesis. *Nature.* 2001;410(6830):842–7.
53. Shiloh Y. ATM and related protein kinases: safeguarding genome integrity. *Nat Rev Cancer.* 2003;3(3):155–68.
54. Savitsky K, Bar-Shira A, Gilad S, Rotman G, Ziv Y, Vanagaite L, et al. A single ataxia telangiectasia gene with a product similar to PI-3 kinase. *Science.* 1995;268(5218):1749–53.
55. Hopfner KP, Karcher A, Shin DS, Craig L, Arthur LM, Carney JP, et al. Structural biology of Rad50 ATPase: ATP-driven conformational control in DNA double-strand break repair and the ABC-ATPase superfamily. *Cell.* 2000;101(7):789–800.
56. Manic G, Obrist F, Sistigu A, Vitale I. Trial Watch: Targeting ATM-CHK2 and ATR-CHK1 pathways for anticancer therapy. *Mol Cell Oncol.* 2015;2(4):e1012976.
57. Wu J, Lai G, Wan F, Xiao Z, Zeng L, Wang X, et al. Knockdown of checkpoint kinase 1 is associated with the increased radiosensitivity of glioblastoma stem-like cells. *Tohoku J Exp Med.* 2012;226(4):267–74.
58. Barlow C, Hirotsune S, Paylor R, Liyanage M, Eckhaus M, Collins F, et al. *Atm*-deficient mice: a paradigm of ataxia telangiectasia. *Cell.* 1996;86(1):159–71.
59. Elson A, Wang Y, Daugherty CJ, Morton CC, Zhou F, Campos-Torres J, et al. Pleiotropic defects in ataxia-telangiectasia protein-deficient mice. *Proc Natl Acad Sci U S A.* 1996;93(23):13084–9.
60. Gueven N, Keating K, Fukao T, Loeffler H, Kondo N, Rodemann HP, et al.

- Site-directed mutagenesis of the ATM promoter: Consequences for response to proliferation and ionizing radiation. *Genes Chromosom Cancer*. 2003;38(2):157–67.
61. Bester AC, Roniger M, Oren YS, Im MM, Sarni D, Chaoat M, et al. Nucleotide Deficiency Promotes Genomic Instability in Early Stages of Cancer Development. *Cell*. 2011;145(3):435–46.
 62. Kim W, Vo QN, Shrivastav M, Lataxes TA, Brown KD. Aberrant methylation of the ATM promoter correlates with increased radiosensitivity in a human colorectal tumor cell line. *Oncogene*. 2002;21(24):3864–71.
 63. Hu H, Du L, Nagabayashi G, Seeger RC, Gatti RA. ATM is down-regulated by N-Myc-regulated microRNA-421. *Proc Natl Acad Sci*. 2010;107(4):1506–11.
 64. Berkovich E, Ginsberg D. ATM is a target for positive regulation by E2F-1. *Oncogene*. 2003;22(2):161–7.
 65. Kim S-Y, Rhee JG, Song X, Prochownik E V., Spitz DR, Lee YJ. Breast Cancer Stem Cell-Like Cells Are More Sensitive to Ionizing Radiation than Non-Stem Cells: Role of ATM. *PLoS One*. 2012;7(11):e50423.
 66. Lim YC, Roberts TL, Day BW, Harding A, Kozlov S, Kijas AW, et al. A Role for Homologous Recombination and Abnormal Cell-Cycle Progression in Radioresistance of Glioma-Initiating Cells. *Mol Cancer Ther*. 2012;11(9):1863-72.
 67. Ropolo M, Daga A, Griffiero F, Foresta M, Casartelli G, Zunino A, et al. Comparative Analysis of DNA Repair in Stem and Nonstem Glioma Cell Cultures. *Mol Cancer Res*. 2009;7(3):383–92.
 68. Sinclair WK, Morton RA. X-Ray Sensitivity during the Cell Generation Cycle of Cultured Chinese Hamster Cells. *Radiat Res*. 1966;29(3):450-74.
 69. Ahmed SU, Carruthers R, Gilmour L, Yildirim S, Watts C, Chalmers AJ. Selective Inhibition of Parallel DNA Damage Response Pathways Optimizes Radiosensitization of Glioblastoma Stem-like Cells. *Cancer Res*. 2015;75(20):4416–28.
 70. Watts TH. TNF/TNFR FAMILY MEMBERS IN COSTIMULATION OF T CELL RESPONSES. *Annu Rev Immunol*. 2005;23(1):23–68.
 71. Watts TH. Tnf/Tnfr Family Members in Costimulation of T Cell Responses. *Annu Rev Immunol*. 2005;23(1):23–68.
 72. Aggarwal BB. Signalling pathways of the TNF superfamily: a double-edged sword. *Nat Rev Immunol*. 2003;3(9):745–56.
 73. Dempsey PW, Doyle SE, He JQ, Cheng G. The signaling adaptors and pathways activated by TNF superfamily. *Cytokine Growth Factor Rev*. 2003;14(3–4):193–209.
 74. Locksley RM, Killeen N, Lenardo MJ, Kieff E, Wu H, Goddard A, et al. The TNF and TNF receptor superfamilies: integrating mammalian biology. *Cell*. 2001;104(4):487–501.


75. Park YC, Burkitt V, Villa a R, Tong L, Wu H. Structural basis for self-association and receptor recognition of human TRAF2. *Nature*. 1999;398(6727):533–8.
76. Gurney AL, Marsters SA, Huang A, Pitti RM, Mark M, Baldwin DT, et al. Identification of a new member of the tumor necrosis factor family and its receptor, a human ortholog of mouse GITR. *Current Biol*. 1999;9(4):215-18.
77. Nocentini G, Giunchi L, Ronchetti S, Tibor Krausz L, Bartoli A, Moraca R, et al. A new member of the tumor necrosis factor nerve growth factor receptor family inhibits T cell receptor-induced apoptosis. *Cell Biol*. 1997;94(12):6216–21.
78. Kim JD, Choi BK, Bae JS, Lee UH, Han IS, Lee HW, et al. Cloning and characterization of GITR ligand. *Genes Immun*. 2003;4(8):564–9.
79. Tone M, Tone Y, Adams E, Yates SF, Frewin MR, Cobbold SP, et al. Mouse glucocorticoid-induced tumor necrosis factor receptor ligand is costimulatory for T cells. *Proc Natl Acad Sci U S A*. 2003;100(25):15059–64.
80. Bossen C, Ingold K, Tardivel A, Bodmer J-L, Gaide O, Hertig S, et al. Interactions of tumor necrosis factor (TNF) and TNF receptor family members in the mouse and human. *J Biol Chem*. 2006;281(20):13964–71.
81. McHugh RS, Whitters MJ, Piccirillo CA, Young DA, Shevach EM, Collins M, et al. CD4(+)CD25(+) immunoregulatory T cells: gene expression analysis reveals a functional role for the glucocorticoid-induced TNF receptor. *Immunity*. 2002;16(2):311–23.
82. Shimizu J, Yamazaki S, Takahashi T, Ishida Y, Sakaguchi S. Stimulation of CD25+CD4+ regulatory T cells through GITR breaks immunological self-tolerance. *Nat Immunol*. 2002;3(2):135–42.
83. Khattri R, Cox T, Yasayko S-A, Ramsdell F. An essential role for Scurfin in CD4+CD25+ T regulatory cells. *Nat Immunol*. 2003;4(4):337–42.
84. Clouthier DL, Watts TH. Cell-specific and context-dependent effects of GITR in cancer, autoimmunity, and infection. *Cytokine Growth Factor Rev*. 2014;25(2):91–106.
85. Zhan Y, Gerondakis S, Coghill E, Bourges D, Xu Y, Brady JL, et al. Glucocorticoid-Induced TNF Receptor Expression by T Cells Is Reciprocally Regulated by NF- κ B and NFAT. *J Immunol*. 2008;181(8):5405-13.
86. Snell LM, Lin GHY, Watts TH. IL-15–Dependent Upregulation of GITR on CD8 Memory Phenotype T Cells in the Bone Marrow Relative to Spleen and Lymph Node Suggests the Bone Marrow as a Site of Superior Bioavailability of IL-15. *J Immunol*. 2012;188(12):5915-23.
87. Esparza EM, Arch RH. Glucocorticoid-Induced TNF Receptor Functions as a Costimulatory Receptor That Promotes Survival in Early Phases of T Cell Activation. *J Immunol*. 2005;174(12):7869-74.
88. Snell LM, McPherson AJ, Lin GHY, Sakaguchi S, Pandolfi PP, Riccardi C, et al. CD8 T Cell-Intrinsic GITR Is Required for T Cell Clonal Expansion and Mouse Survival following Severe Influenza Infection. *J Immunol*.

- 2010;185(12):7223-34.
89. Karin M, Lin A. NF- κ B at the crossroads of life and death. *Nat Immunol.* 2002;3(3):221–7.
 90. Joetham A, Ohnishi H, Okamoto M, Takeda K, Schedel M, Domenico J, et al. Loss of T Regulatory Cell Suppression following Signaling through Glucocorticoid-induced Tumor Necrosis Receptor (GITR) Is Dependent on c-Jun N-terminal Kinase Activation. *J Biol Chem.* 2012;287(21):17100–8.
 91. Spinicelli S, Nocentini G, Ronchetti S, Krausz LT, Bianchini R, Riccardi C. GITR interacts with the pro-apoptotic protein Siva and induces apoptosis. *Cell Death Differ.* 2002;9(12):1382–4.
 92. Xue L, Chu F, Cheng Y, Sun X, Borthakur A, Ramarao M, et al. Siva-1 binds to and inhibits BCL-X(L)-mediated protection against UV radiation-induced apoptosis. *Proc Natl Acad Sci U S A.* 2002;99(10):6925–30.
 93. Py B, Slomianny C, Auburger P, Petit PX, Benichou S. Siva-1 and an alternative splice form lacking the death domain, Siva-2, similarly induce apoptosis in T lymphocytes via a caspase-dependent mitochondrial pathway. *J Immunol.* 2004;172(7):4008–17.
 94. Kastan MB, Lim D. The many substrates and functions of ATM. *Nat Rev Mol Cell Biol.* 2000;1(3):179–86.
 95. Baltz KM, Krusch M, Bringmann A, Brossart P, Mayer F, Kloss M, et al. Cancer immunoediting by GITR (glucocorticoid-induced TNF-related protein) ligand in humans: NK cell/tumor cell interactions. *FASEB J.* 2007;21(10):2442–54.
 96. Hanabuchi S, Watanabe N, Wang Y-H, Wang Y-H, Ito T, Shaw J, et al. Human plasmacytoid dendritic cells activate NK cells through glucocorticoid-induced tumor necrosis factor receptor-ligand (GITRL). *Blood.* 2006;107(9):3617–23.
 97. Kim W-J, Bae E-M, Kang Y-J, Bae H-U, Hong SH, Lee JY, et al. Glucocorticoid-induced tumour necrosis factor receptor family related protein (GITR) mediates inflammatory activation of macrophages that can destabilize atherosclerotic plaques. *Immunology.* 2006;119(3):421–9.
 98. Lacal PM, Petrillo MG, Ruffini F, Muzi A, Bianchini R, Ronchetti S, et al. Glucocorticoid-Induced Tumor Necrosis Factor Receptor Family-Related Ligand Triggering Upregulates Vascular Cell Adhesion Molecule-1 and Intercellular Adhesion Molecule-1 and Promotes Leukocyte Adhesion. *J Pharmacol Exp Ther.* 2013;347(1):164-72.
 99. Liao G, van Driel B, Magelky E, O’Keeffe MS, de Waal Malefyt R, Engel P, et al. Glucocorticoid-induced TNF receptor family-related protein ligand regulates the migration of monocytes to the inflamed intestine. *FASEB J.* 2014;28(1):474–84.
 100. Grohmann U, Volpi C, Fallarino F, Bozza S, Bianchi R, Vacca C, et al. Reverse signaling through GITR ligand enables dexamethasone to activate IDO in allergy. *Nat Med.* 2007;13(5):579–86.

101. Sinik Teodorovic L, Riccardi C, Torres RM, Pelanda R, Cambier J. Murine B Cell Development and Antibody Responses to Model Antigens Are Not Impaired in the Absence of the TNF Receptor GITR. *PLoS One*. 2012;7(2):e31632.
102. Search of: gitr - List Results - ClinicalTrials.gov [Internet]. [cited 2017 Jul 12]. Available from: <https://clinicaltrials.gov/ct2/results?cond=&term=gitr&cntry1=&state1=&SearchAll=Search+all+studies&recrs=>
103. Fang ZM, Lee CS, Sarris M, Kearsley JH, Murrell D, Lavin MF, et al. Rapid radiation-induction of ATM protein levels in situ. *Pathology*. 2001;33(1):30–6.
104. Chen Y, Kamili A, Hardy JR, Groblewski GE, Khanna KK, Byrne JA. Tumor protein D52 represents a negative regulator of ATM protein levels. *Cell Cycle*. 2013;12(18):3083–97.
105. Roslan N, Bieche I, Bright RK, Lidereau R, Chen Y, Byrne JA. TPD52 represents a survival factor in ERBB2-amplified breast cancer cells. *Mol Carcinog*. 2014;53(10):807–19.
106. Azzam EI, Jay-Gerin J-P, Pain D. Ionizing radiation-induced metabolic oxidative stress and prolonged cell injury. *Cancer Lett*. 2012;327(1–2):48–60.
107. Candas D, Lu C, Fan M, Chuang F, Sweeney C, Borowsky A, et al. Mitochondrial MKP1 is a target for therapy-resistant HER2-positive breast cancer cells. *Cancer Res*. 2015;74(24):7498–509.
108. Simian virus 40 (SV40) [Internet]. [cited 2017 Jul 12]. Available from: http://www.ufrgs.br/imunovet/molecular_immunology/pathoviruses_SV40.html
109. Cancer's Achilles Heel in the Crosshairs [Internet]. 2013[cited 2017 May 7]. Available from: <https://www.currinbiotech.com/categories/20101004>
110. Signalling DNA Damage [Internet]. 2012[cited 2017 May 7] Available from: <https://www.intechopen.com/books/protein-phosphorylation-in-human-health/signalling-dna-damage>
111. GITR Pathway [Internet]. 2013[cited 2017 May 27] Available from: <https://www.qiagen.com/fr/shop/genes-and-pathways/pathway-details/?pwid=202>
112. TNFSF18 [Internet]. [cited 2017 May 27] Available from: <http://www.proteinatlas.org/search/GITRL>
113. TNFRSF18 [Internet]. [cited 2017 May 27] Available from: <http://www.proteinatlas.org/ENSG00000186891-TNFRSF18/tissue>
114. Consequences of signaling via GITR and GITRL in different cell types [Internet]. [cited 2017 May 13] Available from: <https://www.hindawi.com/journals/jir/2010/239083/fig1/>

8. APPENDICES

APPENDIX 1: Ethics Committee Approval



**T.C.
HACETTEPE ÜNİVERSİTESİ**
Girişimsel Olmayan Klinik Araştırmalar Etik Kurulu

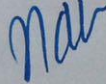
Sayı : 16969557 - 404
Konu : 14.03.2017

Doç. Dr. Güneş ESENDAĞLI
Kanser Enstitüsü
Temel Onkoloji Anabilim Dalı
Öğretim Üyesi

Sayın Doç. Dr. ESENDAĞLI,

Kurulumuza değerlendirilmek üzere sunduğunuz GO 17/227 kayıt numaralı ve "**Meme Kanseri Hücrelerinde Glukokortikoid ile İndüklenen Tümör Nekroz Faktör Reseptör (GTR)-GTR Ligand (GTRL) Etkileşiminin Ataksi-Telenjiektazi Mutasyona Uğramış (ATM) Geni Promotor Kontrolü Altında Değerlendirilmesi**" başlıklı proje Kurulumuzun 14.03.2017 tarihli toplantısında değerlendirilmiş olup, çalışma materyalinin ticari olarak satın alınmış hücrelerde yapılacağı insandan elde edilen primer kültürlerin kullanılmayacağı görülmüştür Klinik Araştırmalar Yönetmeliği gereği gönüllü insanlar üzerinde gerçekleştirilecek nitelikte olmayan bu tip çalışmalar Etik Kurulların kapsamı dışında kalmaktadır.

Bu yazı Etik Kurul kararı yerine geçmek üzere hazırlanmıştır.



Prof. Dr. Nurten AKARSU
Başkan

EK _____ :
Toplantı Katılım Tutanağı.

Girişimsel Olmayan Klinik Araştırmalar Etik Kurulu
14/03/2017 tarih ve 2017/7 no'lu toplantı
KATILIM LİSTESİ

Prof. Dr. A.Nurten AKARSU(Başkan)	
Prof. Dr. Sevda MÜFTÜOĞLU	
Prof. Dr. Yıldırım SARA	
Yrd. Doç. Dr. Özay GÖKÖZ	
Prof. Dr. Hatice Doğan BUZOĞLU	
Prof. Dr. R.Köksal ÖZGÜL	
Prof. Dr. Ayşe Lale DOĞAN	
Prof. Dr. Mintaze Kerem GÜNEL	
Prof. Dr. Oya Nuran EMİROĞLU	
Prof. Dr. Elmas Ebru YALÇIN	
Prof. Dr. Necdet SAĞLAM	
Doç. Dr. Gözde GİRGİN	
Doç. Dr. Fatma Visal OKUR	
Yrd. Doç. Dr. H. Hüseyin TURNAGÖL	
Doç. Dr. Can Ebru KURT	
Öğr. Gör. Dr. Müge DEMİR	
Öğr. Gör. Dr. Meltem ŞENGELEN	
Av. Meltem ONURLU	

9. CURRICULUM VITAE

1. PERSONAL INFORMATION

NAME, SURNAME: Bengisu Uluata-Dayanç DATE OF BIRTH and PLACE OF BIRTH: 08.01.1989, Ankara NATIONALITY: Turkish
COLLEGE ADDRESS: Hacettepe University Cancer Institute, Basic Oncology Department 06100, Sıhhiye/ANKARA TELEPHONE: 0506 975 15 76 E-MAIL: bengltbeng@gmail.com

2. EDUCATION

YEAR	DEGREE	UNIVERSITY	
2015-2017	Master of Science	Hacettepe University	Tumor Biology and Immunology
2007-2013	Undergraduate	İhsan Doğramacı Bilkent University	Molecular Biology and Genetics

POSTER PRESENTATIONS:

[P-0164] The effect of ionizing radiation and glucocorticoid induced tumor necrosis factor ligand (GITRL) expression in basal-like breast cancer cells, Bengisu Uluata Dayanç, Emre Dayanç, Güneş Esendağlı, 3rd International Molecular Immunology&Immunogenetics Congress (MIMIC-III), April 2016, Antalya.

[PP-087] Meme Kanseri Hücrelerinde Glukokortikoid ile İndüklenen Tümör Nekroz Faktör Reseptör (GITR)-GITR Ligand (GITRL) Etkileşiminin Düşük Doz İyonlaştırıcı Radyasyon Varlığında İncelenmesi, Bengisu Uluata Dayanç, Diğdem Yöyen Ermiş, Emre Dayanç, Güneş Esendağlı, XXIV. Ulusal İmmünoloji Kongresi, Nisan 2017, İstanbul.